

Our responses to review comments (repeated in *italics*) are given below in **red**.

## **Response to Reviewer 1**

*I realize that this paper concerns a multi-model effort, and that it is difficult to analyze a large number of models and find common physical threads and results. Still I feel that this manuscript is lacking discussion of some things that raise obvious questions, and it would be worth the effort for the authors to make serious revisions.*

*Hossaini and co-authors describe a multi-model intercomparison that attempts to develop a reconciled estimate of the stratospheric injection of bromine. The paper is mainly descriptive. I suggest revisions that will place results in better context and strengthen the paper.*

We thank the Reviewer for their comments on our manuscript. Many of the comments raised by the Reviewer involve clarification of points and further discussion. We have addressed these suggestions and believe the paper has been strengthened accordingly.

### **Main suggestions for revision:**

1) Rewrite the objectives. Although the paper meets the first two of the stated objectives (lines 95-100), the third and fourth objectives do not receive the attention of the first two. Objective (c) examines trends and inter-annual variability in the stratospheric loading of VSLs and (d) investigates how these relate to climate modes). The discussion of point (c) is limited to transport (mostly derived from assimilated meteorology) and point (d) is barely considered

OK, we have reworked the objectives as the Reviewer requests. The objectives now better reflect the focus of this work.

2) Include some discussion of CTM/CCM differences, and the factors that control whether or not CTMs with the same meteorological fields yield the same or similar results. Where different, the differences should be attributable to differences in CTM setup. Four of the 11 CTMs use ERA-Interim, and in addition, one version of EMAC is 'nudged' to ERA-Interim. Two CTMs use JRA-25, one uses MERRA. There are three free running models; these will give similar results to the CTMs only if free running climatology is similar to the assimilated climatology.

OK, we have added text throughout the manuscript to address these comments. Regarding model differences, we have added the convection and boundary layer parameterisation used by each model to Table 2 (as was also requested by Reviewer 2).

Specifically, regarding whether or not CTMs with the same meteorological fields yield similar results, we have added text to Section 3.1.1 discussing the cause of "outliers". We have also added text to Section 3.1.2 comparing, as an example, TOMCAT vs. B3DCTM at the surface (both models use ECMWF ERA-Interim). Note, it is not surprising that CTMs which use the same input meteorological fields can look different in terms of the simulated distribution of VSLs (or other species, as observed in previous TransCom experiments). This is because of differences in each model's parameterisation of convection and boundary layer mixing (which use the input meteorological fields in different ways and with different assumptions). As noted, details of these parameterisation are now given in Table 2. We already point to various papers in Section 3.1.2 that have shown large differences in the simulated near surface abundance of short-lived tracers due to difference in the treatment of the above transport processes.

In the revised manuscript, we have also expanded upon the discussion of convection as a large contributor to the simulated levels of CHBr<sub>3</sub> around the tropopause. For example, in Section 3.4 in discussion of Figures 14 and 15, we have added the following paragraph.

"The high altitude model-model differences in CHBr<sub>3</sub>, highlighted in Figures 14 and 15, are attributed predominately to differences in the treatment of convection. Previous studies have shown that (i) convective updraft mass fluxes, including the vertical extent of deep convection

(relevant for bromine SGI from VLS), vary significantly depending on the implementation of convection in a given model (e.g. Feng et al., 2011) and (ii) that significantly different short-lived tracer distributions are predicted from different models using different convective parameterisations (e.g. Hoyle et al., 2011). Such parameterisations are often complex, relying on assumptions regarding detrainment levels, trigger thresholds for shallow, mid-level and/or deep convection, and vary in their approach to computing updraft (and downdraft) mass fluxes. Furthermore, the vertical transport of model tracers is also sensitive to interactions of the convective parameterisation with the boundary layer mixing scheme (also parameterised) (Rybka and Tost, 2014). On the above basis and considering that the TransCom-VLS models implement these processes in different ways (Table 2), it was not possible to detangle transport effects within the scope of this project. However, no systematic similarities/differences between models according to input meteorology were apparent”.

The Reviewer asks that differences between models are attributed to “CTM setup”. The paragraph beginning “As the chemical sink of VLS...” in Section 3.1.2 has been appropriately reworked to reflect this comment (see response below). The text has also been amended in the Abstract and Conclusions so that it is clear that “implementation” of transport is important.

*Although differences are said to be ‘transport’ – does that mean real differences in meteorology (e.g., differences between assimilation or free-running), differences in implementation of a single analysis, or differences among the analyses? When 70% of the models (or 8 of 11 models) do something does that mean the 8 models that use assimilation differ from the free running models?*

We believe this is a terminology issue that simply needs clarification. As it was impossible here to isolate the exact cause of the differences between models, nor is that the focus of this work, the word “transport” is used to incorporate all the factors that the Reviewer states (considering that all models used common fluxes & chemistry). To clarify this and address the Reviewer’s comment we have:

1. Defined what we mean by “transport” early in the manuscript: “...the effects of PBL mixing, convection and advection, and the implementation of these processes” – see introduction, final paragraph.
2. Noted in the Abstract and Conclusions that the implementation of transport processes is a clear factor (as each model would say that they are simulating convection, MBL mixing, advection etc.).
3. Reworked the appropriate paragraphs in Sections 3.1.2 and 3.4, where transport is discussed, to make clear that the “implementation” of transport and “CTM setup” are contributing factors. Throughout the manuscript more discussion is now given on the reasons for model differences.

*If convection and boundary layer mixing are dealt with differently among the CTMs, and are demonstrably different from the CCMs, then there should be some mention.*

As noted, we now include the convection and boundary layer mixing scheme used by each model in Table 2.

*1) Include physical interpretation and a sense as to what we learn from ‘lack of sensitivity of the simulated seasonal cycle to the choice of inventory’ (line 615). If the mean value is sensitive to the inventory but the seasonal cycle is not, does that mean anything more compelling than that the seasonal cycle of the loss process (input to the simulations and the same in all models) is realistic?*

That is correct, we are essentially saying here that the seasonal cycle of the loss process is accurate based on the various model-measurement comparisons at the surface. There is already some discussion on this point in Section 3.1.1. However, we have now added a sentence to make the point in the 2<sup>nd</sup> paragraph of Summary and Conclusions also, where the reviewer suggests.

2) Quantify the importance of SGI of VSLS to the total stratospheric bromine budget. It would be helpful to put the difference in SGI from WMO best estimate (~1.3 vs 2.0 (this work)) in the context of the stratospheric budget. IAV is +/- 5%? Is that significant?

We have addressed these comments and added some new discussion in Section 3.5 of the revised manuscript.

The reviewer comment refers to the TransCom multi model mean SGI of bromine from  $\text{CHBr}_3$  and  $\text{CH}_2\text{Br}_2$  (2.0 ppt Br) versus WMO best estimate of the same quantity derived from observations (1.28 ppt Br). In the context of the total stratospheric  $\text{Br}_y$  budget, estimated to be ~20 ppt Br in 2011 (WMO, 2014), SGI of  $\text{CHBr}_3$  and  $\text{CH}_2\text{Br}_2$  accounts for 10% of this total (our estimate) versus 6.4% based on the current WMO best estimate.

In the context of total stratospheric  $\text{Br}_y$  (~20 ppt), the  $\pm 5\%$  IAV of modelled bromine SGI from  $\text{CHBr}_3$  and  $\text{CH}_2\text{Br}_2$  is small (sub ppt). We have made this point in the revised manuscript.

*Is uncertainty in SGI more or less important than uncertainty in product gases? How large is the uncertainty in SGI + product gases relative to the total stratospheric bromine budget?*

The uncertainty in SGI and PGI are similar. The WMO quote an uncertainty range of 0.7-3.4 ppt Br for SGI and 1.1-4.3 ppt Br for PGI (note, from all brominated VSLS). Their best estimate for SGI + PGI is therefore 2-8 ppt Br, giving an uncertainty of 6 ppt Br. Of this uncertainty PGI contributes 54% and SGI 46%.

The uncertainty in SGI + PGI (i.e. 6 ppt Br, above) corresponds to ~30% of the total stratospheric bromine budget (i.e.  $100 \times [6 \text{ ppt} / 20 \text{ ppt}]$ ).

*Is the uncertainty in SGI + product gases smaller than the uncertainty in SGI?*

No. The WMO uncertainty of SGI + PGI is 6 ppt Br. The WMO uncertainty in SGI is 2.7 ppt Br (i.e. 3.4 minus 0.7 ppt) and is therefore smaller.

We note additionally that we have amended the text in Section 3.5 to make clearer the reduction in SGI range the TransCom results suggest. In summary:

WMO SGI range ( $\text{CHBr}_3$  +  $\text{CH}_2\text{Br}_2$  only): 0.6 to 2.65 ppt Br

WMO SGI range (minor VSLS\*\* only): 0.08 to 0.71 ppt Br

WMO SGI range (total, all VSLS): 0.7 to 3.4 ppt Br

TransCom considered  $\text{CHBr}_3$  and  $\text{CH}_2\text{Br}_2$  only, which dominate the SGI uncertainty range (based on the above numbers).

TransCom SGI range ( $\text{CHBr}_3$  +  $\text{CH}_2\text{Br}_2$  only): 2.0 (1.2 to 2.5) ppt Br

Therefore, if we take the WMO SGI range for the "minor" VSLS, the total TransCom SGI range (all VSLS) would be 1.28 to 3.21 ppt Br. This range is 28% smaller than the total WMO SGI range. This result is now incorporated into the text.

\*\*including:  $\text{CHBr}_2\text{Cl}$ ,  $\text{CH}_2\text{BrCl}$ ,  $\text{CHBrCl}_2$ ,  $\text{C}_2\text{H}_5\text{Br}$ ,  $\text{C}_2\text{H}_4\text{Br}$ , and  $\text{C}_3\text{H}_7\text{Br}$

3) *How important is it that SGI does not show a transport trend? Isn't it just as likely that a trend (if any) would be due to a trend in the sources (as mentioned in penultimate paragraph)?*

There are various factors that could, in principle, cause a trend in stratospheric bromine SGI. These could potentially include a trend in sources (e.g. oceanic emissions), as the reviewer notes, or a trend in the atmospheric loss rate of VSLS (e.g. due to any oxidant changes), or a trend in transport processes (e.g. convection). To our best knowledge, there is no strong evidence that any of these factors has caused a trend in the SGI of  $\text{CHBr}_3$  and  $\text{CH}_2\text{Br}_2$  over the study period.

One aim of this work was to isolate any possible transport trend impacting SGI. Therefore, VLS emissions and the chemical loss of VLS was fixed in each year, with no inter-annual variability. The fact no SGI trend was found over the study period does not preclude future SGI changes driven by climate-driven transport changes (or other factors). We already make this point in the final paragraph of the paper but have now also included it briefly in Section 3.5.

### **Specific Comments**

*Imprecise language throughout – paper has sufficient quantitative statements and comparisons that qualified descriptions detract from overall message. These are examples: ‘reasonably well’ ‘not particularly sensitive’ ‘at most sites the amplitude of the seasonal cycle is generally consistent’ ‘to some degree likely reflects’ ‘likely’ – followed by 5 references – how many do we need to make a concrete statement?*

OK. We have been through the manuscript and addressed this by removing unnecessary qualified descriptions.

*Why ‘models are able to reproduce’? Why not ‘models reproduce’?*

OK. We have changed this throughout the manuscript.

*You don’t need to repeatedly say ‘participating models’ (unless you are also showing output from models that did not participate).*

OK. We removed ‘participating’ in virtually all instances.

*Abstract and Introduction Not clear until section 2.3 that most of the models are CTMs. Very surprising and possibly misleading that nothing is said about input meteorology. Differences among CTMs that use the same source for meteorology are differences in implementation since all of them would claim that they are trying to solve the same general equations with the same meteorological input.*

OK. We now note in the abstract that most models are CTMs. We agree that differences in CTM implementation should be commented on and have also added to the abstract: “Overall, our results do not show systematic differences between models specific to the choice of reanalysis meteorology, rather clear differences are seen related to differences in the implementation of transport processes in the models”. See earlier responses to comments also.

*Line 30 – transport driven variability in the annual mean SGI is 5% - why is that ‘however’? Isn’t that small?*

OK, we have removed ‘however’. (See above IAV discussion).

*Line 52 delete last phrase ‘in recent years’ – very long sentence already says ‘recent’*

OK, we have deleted that phrase.

*Line 55 and following: why is it important to differentiate the product gas injection from source gas injection? Is the NET impact of VSLs (PGI and SGI) better constrained than SGI or PGI separately?*

It is common to differentiate SGI from PGI in the literature concerning VLS and it has indeed been done in all recent WMO Ozone reports. It is important here because our paper deals with SGI only. More broadly, this distinction is sensible given the differences in the two processes and how they can be quantified. For example, it is easier to quantify bromine SGI, from measurements of  $\text{CHBr}_3$  and  $\text{CH}_2\text{Br}_2$  etc. in the UT, than it is to quantify PGI, which requires measurements of  $\text{Br}_y$  species (e.g.  $\text{BrO}$ ,  $\text{HBr}$ ). Observations alone cannot determine whether  $\text{Br}_y$  has come from VLS or other source gases. In addition, it is useful to consider SGI separately, as modelling work has shown that the stratospheric SGI of bromine from VLS may increase in response to climate change (Hossaini et al. 2012a). To our knowledge, this has yet to be shown for PGI.

Regarding the SGI/PGI uncertainty relative to the total (SGI + PGI), we have already answered this point (see above responses).

*Line 64 – should be ‘coincides’*

OK, this has been corrected.

*Line 83 – it seems to me that the robust evaluation of the ACTUAL SGI needs observations, not just a concerted model evaluation. All the models could give the same answer (especially if they all use the same input meteorology) and data might reveal them all to be wrong.*

As VSLS observations are limited in their space/time coverage, clearly the best approach is to consider both observations and models when evaluating SGI. That is exactly what we have done in this paper, therefore we are somewhat puzzled by this review comment. A wealth of observational data are used to evaluate the models and the model SGI results are compared to the existing measurement-derived SGI estimates from WMO.

Use of models to make predictions regarding future climate-driven changes to the stratospheric SGI of bromine from VSLS is increasing (e.g. Dessler et al. 2009; Hossaini et al. 2012a). Therefore, it is important that studies such as TransCom evaluate how these models perform in the present day. It has already been discussed above that input meteorology is not all that matters for tracer/VSLS transport in CTMs.

*Line 115 – you specify the chemistry – thereby ELIMINATING (rather the minimizing) its contribution to inter model differences. Also – since most of the models use ERAinterim, and there is no discussion of differences in its implementation, it is somewhat misleading to say that this study isolates differences due to transport processes.*

We use the work “minimising” here as it cannot be said that the chemical loss rates are *totally* identical as VSLS oxidation by OH is temperature dependent. Models use different reanalysis products (5 out of the 11 CTMs/nudged CCMs use ECMWF Era-Interim) and are expected to have similar, but not identical, temperature fields. Some differences in the chemical loss rate are therefore unavoidable, even when oxidants are prescribed in each model.

As can be seen from Figure 14, the model-model differences are quite large due to transport (mainly; only a second order effect in loss due temperature). Even the models using ERA-interim (B3DCTM, EMAC-nudge, TOMCATs) show large differences at 100 hPa. Thus the ensemble of 11 models do account for a large fraction, if not most, of the uncertainty due to model transport or implementation of such. As already noted, differences in the treatment of convection and boundary mixing can introduce significant differences in model tracer transport regardless of whether or not the models use the same reanalysis data (ECMWF or otherwise). We have been through the manuscript and made clear, where appropriate, that the treatment (or implementation) of transport processes differs between the models (though all models are attempting to simulate convection and mixing processes).

In the revised manuscript we now comment on the fact that most models use ERA-Interim (see first paragraph of Section 2.3).

*Line 136 – is aseasonal the same as ‘annual average’?*

The top-down emission inventory in question was formulated using somewhat sporadic tropospheric VSLS measurements in various years and locations. The limited availability of measurements within a given year did not allow seasonality to be derived (i.e. the inventory is aseasonal). Similarly, nor can the fluxes be considered annual averages (although this *may* be a reasonable approximation).

*Section 2.1*

*It would be useful to have some visual comparison of the emissions (perhaps supplementary material)? The words don't give a sense of how large the differences in emissions are, and without that the sensitivity to emissions or lack thereof does not make sense.*

OK. Figures comparing the surface emission fields for both  $\text{CHBr}_3$  and  $\text{CH}_2\text{Br}_2$  is now given in a new Supplementary Information.

*Line 160 the words after the semi-colon should have a verb, or the sentence should be re-written without a semi-colon.*

OK. The sentence has been re-written accordingly.

*Line 184 'diagnosed convection' – do you mean used the standard parameterization for transport? Identified convection? Not clear.*

OK. We have made this clearer now. The “diagnosed convection” in TOMCAT is the standard scheme yes.

*Section 2.3 Did the CCMs use observed sea surface temperatures (relevant for El Nino)?*

Yes and we have now noted this in the footer of Table 2.

*Section 3.1.1 Line 300 – MHD, THD, CGO, PSA - simulated seasonal cycles do not agree with data – does the simulated seasonality look like the imposed seasonality of the loss terms? (If it does, then how can the models perform differently?)*

Yes, the simulated seasonality at these sites is consistent with that expected from the seasonality of the chemical loss. We have added a sentence in Sect. 3.1.1 making this point.

The Reviewer asks “how can the models perform differently?”. On this point, first, at MHD the models in fact look very similar for both  $\text{CHBr}_3$  (see Figure 3) and  $\text{CH}_2\text{Br}_2$  (Figure 4). It is not surprising that at some sites there will be differences between the models as the models have different transport schemes. This is not limited to simply the large-scale resolved horizontal/vertical winds, for most models taken from reanalysis products (i.e. ECMWF), but also includes differences in parameterisations of both convection and boundary layer mixing. Differences in such will impact both absolute tracer mixing ratios at a given site and can also impact seasonality (see references below). We make this point in the revised paper in the following lines:

From revised Section 3.1.2:

“As the chemical sink of VSLS was consistent across all models, the inter-model differences discussed above are attributed primarily to differences in the treatment and implementation of transport processes. This includes convection and boundary layer mixing, both of which can significantly influence the near-surface abundance of VSLS in the real (Fuhlbrügge et al., 2013, 2015) and model (Zhang et al., 2008; Feng et al., 2011; Hoyle et al., 2011) atmospheres, and are parameterised in different ways (Table 2). On this basis, it is not surprising that different CTM setups lead to differences in the surface distribution of VSLS, nor that differences are apparent between CTMs that use the same meteorological input fields. Indeed, such effects have also been observed in previous model intercomparisons (Hoyle et al., 2011). Large-scale vertical advection, the native grid of a model and its horizontal/vertical resolution may also be contributing factors, though quantifying their relative influence was beyond the scope of TransCom-VSLS.”

*Line 315 – Is it important that the observed annual variation is much smaller at SMO and CGO than at many of the other sites? Disregarding SMO (some really weird behaviour), CGO and PSA amplitude greatly overestimated although shape is vaguely similar. Any commonalities among the 60% of models that do not correlate with observations > 0.5? Resolution? Meteorology? Transport scheme? Boundary Layer dynamics? Anything?*

At mid-high latitude sites, the local lifetime of these VLS is approximately 1 month or longer, and the effect of loss seasonality will be similar at sites within similar latitude bands; e.g. because of seasonality in OH following the solar insolation. Also note that the seasonal difference in OH concentration increase towards the poles. Since SMO is located in the tropics the seasonality in loss due to OH is weaker compared to CGO, MHD or PSA. Emission and transport can vary regionally and also have a local influence on concentration seasonality. The interactions of spatial distribution of emissions and transport are discussed later for the MHD case.

In the revised manuscript we have expanded the discussion of surface seasonality in Section 3.1.1. As previously noted we could not detangle individual transport components in each model within the framework of this large multi-model project (we note the Reviewer's opening sentence of his/her review). CGO and PSA, being outside of the tropics, are obviously far less relevant for bromine SGI than tropical locations. As SMO is within the tropics we have expanded the discussed in Section 3.1.1 on the possible causes of the model outliers.

*317 – virtually all do not reproduce – how about ‘almost none of the models reproduce’ or ‘virtually all of the models fail*

OK, we have changed “virtually all of the models do not reproduce” to “almost none of the models reproduce”, as requested.

*I don't understand the point of this discussion (lines 317 ff) At MHD, seasonality in the local emission flux is suggested to be the dominant factor controlling the seasonal cycle of surface CHBr<sub>3</sub> (Carpenter et al., 2005). This leads to the observed summer maximum (as shown in Figure 3) and is not represented in the models' CHBr<sub>3</sub>\_L tracer which, at the surface, is driven by the aseasonal emission inventory of Liang et al. (2010). Why did Carpenter et al. make that 'suggestion'? This sort of model can only do what you tell it, so if Carpenter et al. are correct – then you would never expect the models to do this. So then, what is the point of going to the MMM?*

Of course we agree that the seasonality in the emissions will not be captured (these are aseasonal emission inventories, as noted). However, seasonality in the emission flux (and the chemical loss) may not be the only factor contributing to the observed seasonal cycle in the CHBr<sub>3</sub> surface mixing at MHD. Our results suggest that transport processes serving the MHD site are also important. MHD is served by air masses mostly of marine origin and several studies have shown a marked seasonality in the transport of air masses arriving at the site (e.g. Cape et al., 2000).

In the revised manuscript we now include individual model-measurement correlation coefficients (in addition to the MMM) at MHD (in the new Supplementary Information, Table S1). These comparisons reveal that 7 out of the 11 models capture the MHD CHBr<sub>3</sub> seasonal cycle (with  $r > 0.65$ ) when using the Ziska et al. inventory, despite the inventory being aseasonal. (Note, this was also shown by Lennartz et al. 2015, ACP). We have also now discussed why this is seen for the Ziska inventory and not the other aseasonal emissions. Given that this is the only difference (i.e. the chemistry is the same between simulations in a given model), the only possible conclusion is that the distribution of emissions, with respect to transport processes, is causing this effect. We already make this point in the paper, but have expanded the discussion in Section 3.1.1 so that it is clearer (see response to point below).

Cape et al.: the use of trajectory cluster analysis to interpret trace gas measurements at Mace Head, Ireland, Atmos. Env., 2000.

*Why aren't you discussing whether an emission inventory that has a seasonal element does better?*

With the exception of the Ordonez et al. inventory at tropical latitudes only, where it has a small seasonal element (not relevant for MHD), the inventories are aseasonal. We are not aware of a prescribed emission inventory with global seasonality in the surface fluxes and therefore cannot

speculate. Besides, as noted above, 7 out of 11 models do not require seasonally-varying  $\text{CHBr}_3$  emissions to capture the observed seasonality in  $\text{CHBr}_3$  mixing ratios at MHD.

*It would make more sense if there was a better sense of the differences in inventories. Specifically – why would TWO aseasonal inventories give different answers at MHD, if the seasonality of the emissions is speculated to be a controlling factor?*

We have added to the new Supplementary Information figures showing surface  $\text{CHBr}_3$  and  $\text{CH}_2\text{Br}_2$  emissions for each inventory (Figure S1 and S2) to provide a better sense of the differences in the inventories, as requested. It can be clearly seen that surface  $\text{CHBr}_3$  emissions are much larger in the region of MHD, and indeed in the NH in general, for the Ziska et al. inventory. This has been previously highlighted in our recent work (Hossaini et al. 2013). In addition, we have added a supplementary figure (S3) comparing the absolute agreement between each model and measured surface  $\text{CHBr}_3$  at MHD for Liang et al. emissions and Ziska et al. emissions. The figure clearly shows that the larger emissions in the latter provide much better model-measurement absolute agreement (for the majority of models). Regarding the seasonal cycle, clearly a comprehensive trajectory analysis of air masses arriving at MHD is well beyond the scope of this work, and is not required to support our main conclusions concerning bromine SGI (mainly occurring in the tropics). However, we have extended the discussion in Section 3.1.1 so that the above points are clearer. We now suggest that the summertime transport of air that has experienced relatively large  $\text{CHBr}_3$  emissions north to north-west of MHD is the cause of the seasonal cycle seen in the Ziska et al. simulations. To further support this, animations of the seasonal evolution of surface  $\text{CHBr}_3$  have been created and have also been added to the paper as Supplementary Information.

*Section 3.1.2 338 between a model value (M) and an observation (O), why parenthesis around ‘for each model tracer’?*

OK. We have removed the parentheses.

*Figure 6 – ok these are the minimum percentages – but how does the reader know that the difference between a ‘best’ comparison and a comparison with one of the other inventories is significant?*

That is not the point of Figure 6. The point is to show which emission inventory performs best and to give the MAPE for that inventory. While it is true from Figure 6 that one cannot discern how the 2<sup>nd</sup> best inventory performs (in terms of MAPE) this is less relevant. Inclusion of that level of detail in *this* Figure would add unnecessary convolution to an already detailed figure and detract from the main message regarding the best inventory. Besides, one can see how the inventories perform against each other, within a given model, in the tropics (most important region for VSLS injection into the stratosphere) from Figure 7.

*350 I presume you don’t get MAPE for both species with the same inventory because loss processes are different time scale? Replace: ‘low  $\text{CHBr}_3$  MAPE (good agreement), at a given location using a particular inventory does not necessarily mean a corresponding low  $\text{CH}_2\text{Br}_2$  MAPE can be achieved using the same inventory, at that location’. At a given location low  $\text{CHBr}_3$  MAPE (good agreement) does not necessarily accompany a corresponding low  $\text{CH}_2\text{Br}_2$  MAPE using the same inventory*

Yes. We have reworded the sentence as the Reviewer suggests.

*355 – is this also related to how the inventories are created in the first place – i.e., how much do the inventories themselves depend on models and/or ERA-Interim?*

A brief discussion of the inventories is already given in Section 2.1. We also refer the reader to our recent paper that further describes the inventories in the following lines:



“As these inventories were recently described and compared by Hossaini et al. (2013), only a brief description of each is given below”.

The top-down inventories are derived using aircraft observations in conjunction with models. Therefore, to some degree the derived fluxes will depend on the details of the transport scheme in the model used. However, we cannot say anything quantitative regarding this and this type of analysis is well beyond the scope of this paper. It is also not required to support our conclusions. Neither of the two top-down inventories were derived in models that use ERA-Interim.

*365 – you attribute all differences to physical processes – e.g., convection and boundary layer mixing. Since most of these use assimilated meteorology, does that mean implementations differ among CTMs. Also, there are some pretty large differences between a free running simulation and a nudged simulation, so differences among ‘variants’ should not be surprising.*

Yes, the differences are attributed to both the convection and boundary layer schemes in these models. Implementation of ERA-Interim is not necessarily the key or only point here, rather the fact that these models use different parameterisations of the above sub-grid processes is important. In other words, simply because a number of the models read ERA-Interim fields (horizontal/vertical winds, temperature and humidity), tracer transport will be different because of the way the above sub-grid scale processes are treated. We already include several citations to modelling work which has shown large differences in the simulated near-surface abundance of short-lived tracers, depending on the choice of convection and boundary layer transport schemes.

In addition, as noted earlier, we have now (i) defined what we mean by “transport” in the Introduction, (ii) amended the text in numerous places to clarify that implementation of transport processes is important and (iii) added the boundary layer and convection scheme used by each model to Table 2.

Regarding the variants, we removed the word “even” from the following sentence so that it sounds less surprising.

“At some sites, differences among emission inventory performance are ~~even~~ apparent between model variants that, besides transport, are otherwise identical.”

*Finally, in the prior modelling studies that had best agreement with different inventories, the loss terms were presumably different.*

Yes, that is correct. We now make that point in Section 3.12.

*370 – why are differences in model variants surprising? In one case, this is the difference between free-running and nudged, and it is more likely than not that convection differs between these two in both intensity and location. In the second case, the chief difference that is discussed in convection, so again, performance is more likely to be different than it is to be the same.*

As already answered above, regarding the variants, we removed the word “even” so that the sentence sounds less like the result is surprising.

*395 It would be better to say ‘For the N (fill in number) models that submitted hourly output . .*

OK. We have done this.

*After that, paper says “Generally, the models reproduce the observed mixing ratios from SHIVA well, with a MMM campaign MAPE of 25% or less for both VSLS.” This good agreement clearly depends on who is looking, and whether it makes sense to compute MAPE for the multimodel mean when the spread indicated by shading can be as much as 1 ppt (lowest value) and about 2 ppt (MMM) (top panel).*

It is not clear what the Reviewer is asking for. It is common practice in large multi-model assessments to include multi-model mean (MMM) values and to indicate the model spread. We have done both of these things in Figure 8 (and 9). For CHBr<sub>3</sub>, we believe a MAPE of <25% on the multi-model mean is good. Inclusion of more (unnecessary) data on these figures would distract from the main point that the models perform reasonably well at the surface in the tropical West Pacific, giving confidence in the corresponding modelled bromine SGI.

*It is also confusing since each model is using its 'preferred' inventory, and seriously in the real world there is only one actually set of emissions. In the best of circumstances, I think the MMM conceals physical differences and/or deficiencies in a subgroup of models. Here, with each model using its 'preferred' inventory, I think it is nearly impossible to understand the significance of good or poor agreement with the MMM.*

As noted, it is common practice in large multi-model assessments to include MMM values. Naturally it will be the case that some models look better than others and that the MMM does not provide that information. However, we already provide the model spread (as is also common practice) and most comparisons throughout the paper show results from individual model profiles. The point on "preferred" inventory is dealt with below.

*Section 3.2 412 – by using the model 'preferred' inventory, what you are testing here is given surface values, how similar is the transport to higher levels to that inferred from observations in the real atmosphere. There are other ways to do this of course – in fact, looking at EACH tracer profile as a fraction of its near surface value might be even more instructive. Nonetheless – the discussion is convoluted and should be re-written to state the main (physical) point clearly. I presume 'parameterized transport schemes' later in this paragraph refers mainly to convection?*

Yes. A major goal of this work was to provide the first multi-model estimate of the climatological SGI of bromine from VLSR reaching the stratosphere. To accomplish this, the preferred tracer approach was needed. It would not be correct to make predictions of how much CHBr<sub>3</sub>/CH<sub>2</sub>Br<sub>2</sub> enters the stratosphere, from a given model, using an emission inventory that does not provide that model with good or reasonable agreement to measured surface CHBr<sub>3</sub>/CH<sub>2</sub>Br<sub>2</sub>. Use of the optimal/preferred inventory in this regard is essential. We note, a major and novel finding of this work is that the models do not necessarily agree as to which inventory performs the best in many locations.

We have reworded the sentence beginning "This approach ensures.." in Section 3.2 for clarity. Directly after this we have now stated what we are testing, as suggested by the Reviewer.

Yes, we are referring to sub-grid scale transport schemes, such as convection. We have now added "sub-grid scale" for clarity.

*447 Only the number of flights controls the variability comparing Pre-AVE to CR-AVE? Nothing seasonal or spatial? Are the models sampled like the aircraft to produce average profiles? Is the error bar the range of values, the standard deviation? Would standard error of the mean be better? The correlation coefficient – is that the correlation for the whole profile? Isn't that guaranteed to be large since observed and simulated profiles general decrease with altitude?*

Pre-AVE and CR-AVE were broadly in the same region and in the same months (already clear from Figure 2 and from the campaign descriptions in Section 2.4.2). We therefore anticipate that the sample size is a significant contributor to the variability.

Yes. The models are sampled like the aircraft and then averaged.

The error bars on Figure 11 are the standard deviation as indicated in the caption. For consistency we have used standard deviation throughout the paper.

Yes, the correlation coefficient is over the whole profile. It is not guaranteed to be large since variability can be significant (see e.g. panel c of Figure 11). It is a good indicator of model skill that the models reproduce the decrease with altitude and that correlation coefficients are large.

*ATTREX higher values at higher altitude ‘possibly reflects the location’? Isn’t this true (and backed by other observations?) If it is only ‘possible’, what are the other causes?*

Yes, OK, we have removed “possibly”.

*grammar - CR-AVE had nearly twice the number of flights AS Pre-Ave and . . .*

OK, we have changed “than” to “as”.

### Section 3.3

*470 ‘likely reflects the location at which the measurements were made’ Why so many words, why ‘likely’ (what else could it be) and why no direct statement about zonal asymmetry? Would the model zonal means compare better with Carpenter and Reimann? Or should it be model mean in a different region compared with Carpenter and Reimann?*

OK. We have removed “likely”. We do not follow the 2<sup>nd</sup> part of the Reviewer’s comment. The last paragraph of Section 3.3 discusses measurements of CHBr<sub>3</sub> and CH<sub>2</sub>Br<sub>2</sub> from ATTREX (not models) versus those from the WMO compilation.

### Section 3.4

*515 If most of the models are using assimilated fields, how can they fail to locate the areas of deep convection and the seasonal dependence therein? It is all right to describe this behaviour, but I would hardly call it a prediction. Too much discussion, especially since the result is not novel.*

Perhaps the Reviewer is asking a rhetorical question here. As noted earlier, the treatment of convection in models can vary significantly. Use of meteorological fields from reanalysis data (e.g. ECMWF) does not guarantee a “good” simulation of deep convection, though clearly accurate fields of temperature, pressure, humidity and wind fields (from the reanalysis), which feed into convective parameterisation, are desirable. Such parameterisations are often complex (with many tuneable parameters) and make assumptions, for example, on whether shallow, mid-level or deep convection takes place in a column and the trigger threshold for such. Clearly, the point of this paper is not to provide a comprehensive critique of the parameterisation of convection in 11 models. We already make the point in the introduction that “While global models generally simulate broadly similar features in the spatial distribution of convection, large inter-model differences in the amount of tracers transported to the tropopause have been reported...”. It is unclear where the Reviewer is referring when he/she says there is too much discussion. On line 515, where he/she states, there is only a very brief description that the models show the largest CHBr<sub>3</sub> mixing ratios at the tropopause over the West Pacific in DJF.

*525 – variations in the importance of Monsoon – any connection to the input data or model type? I don’t think this is evidence that UKCA-HI has a more faithful representation of convection – you would need some other information about HI vs LOW to make this statement.*

No clear relationship between the importance of the Monsoon and the input data/model type could be discerned from this analysis (this is not required to support our main conclusions). This would require a more detailed and dedicated examination of the Monsoon region, outside the scope of the TransCom-VSLS framework. We now make this point in Section 3.4 of the revised manuscript.

Regarding UKCA-HI vs LOW, we agree that the statement was too strong and have reworded.

### Section 4

605 previously when you talked about variability it was physical (e.g., seasonal etc. –something real). Here you are talking about differences among models for different inventories. It is confusing to call this ‘variability’.

We agree and have changed “inter-model variability to “inter-model differences”.

622 – model variants are identical except for tropospheric transport schemes. Based on everything else written, I don’t think this statement is correct. E.g, the tropospheric transport of ‘nudged’ vs ‘free-running’ will differ for physical reasons, not just ‘transport schemes’.

Yes, we agree that is the case for EMAC\_N vs free-running EMAC\_F. However, for TOMCAT and TOMCAT\_CONV (offline CTMs), the models are identical apart from the convective transport schemes. Therefore, we have replaced:

“This effect was even observed between model variants which, other than tropospheric transport schemes, are identical”.

With:

“This effect was also observed between CTM variants which, other than tropospheric transport schemes, are identical”.

The problem with single model studies of inventories or deriving inventories is that they don’t typically include model error. If they did then the inventories would be more robust – or the differences among studies would likely fall within the errors.

We agree.

625 – For both CHBr<sub>3</sub> and CH<sub>2</sub>Br<sub>2</sub> the ‘best’ inventory for the tropics is the lowest – but at the same time agreement here is ‘less sensitive to choice of inventory’. What point are you trying to make? I don’t see how the statements about seasonally resolved air-to-sea fluxes follow from anything in this paragraph (noting this is the ‘discussion and conclusions’ section).

OK, this was not clear. The “less sensitive to choice of inventory” refers to CH<sub>2</sub>Br<sub>2</sub> not the tropics. We have reworded this sentence to clarify.

The inventories we currently use are aseasonal. We feel it is good to make the point that a move towards seasonally-resolved VSLs emissions in models would be a good direction to go in. We feel as though this fits in following the discussion of surface emission inventories.

665 – the very long sentence beginning ‘Although . . . ’ should be clarified.

OK, we have shortened this sentence and removed unnecessary words to improve clarity.

Picky comment Example: Do you really need to include so many references – e.g., five references to say that Bromine + chlorine destroys ozone more than chlorine by itself?

OK, we removed one of the references on this point from the introductory paragraph.

Our responses to review comments (repeated in *italics*) are given below in **red**.

## **Response to Reviewer 2**

*This paper presents a comprehensive model intercomparison of the impact of bromine containing VSLs on the stratospheric bromine loading. This is a good initiative and the outcome of this intercomparison will be important of assessing the impact of bromine on stratospheric ozone. It is in particular noteworthy that a lot of observations are employed to assess the quality of the model results.*

We thank the Reviewer for his/her comments on our manuscript. We are pleased that he/she finds the work important and acknowledges the large body of atmospheric observations used throughout.

*I have some points (see below), where I think the discussion in the paper can be clarified and improved. The impact of particular model features (e.g., the convective schemes employed) on the different results could be brought out more clearly. The reader ultimately will be interested in what the problematic model features are, because these are the features that need improvement in the further developments of such models. This point could be brought across in the paper in a better way. In summary, I think that a revised version of the paper, taking into account the points raised in the reviews will be a valuable contribution to ACP.*

We have addressed the review comments and believe the paper has been strengthened accordingly. We are pleased the Reviewer thinks this work will make a valuable contribution to ACP.

### **Detailed comments**

*Five out of the 11 participating models are nudged to or driven by ERA-Interim. While ERA-Interim is a good choice, this fact will lead to the multi-model mean being biased to an ERA-Interim world. I suggest to bring this point across more clearly. Does this fact have any implications for the conclusions of this model intercomparison?*

It is indeed the case that most models use ERA-Interim met fields, but as you can see other models (ACTM, NIES or the free running models) do not produce MAPE very different from those produced by the ERA-interim driven model. In fact there is quite good agreement between the major reanalysis products from ECMWF, JMA and NCEP. This was very recently highlighted by Harada et al., (2016) and is clearly shown in Figure 4 of that paper: see: <http://jmsj.metsoc.jp/EOR/2016-015.pdf>. Thus we do not believe at this stage that our model spread is hugely biased towards ERA-interim. In the revised manuscript we have commented on this, as requested, in the first paragraph of Section 2.3.

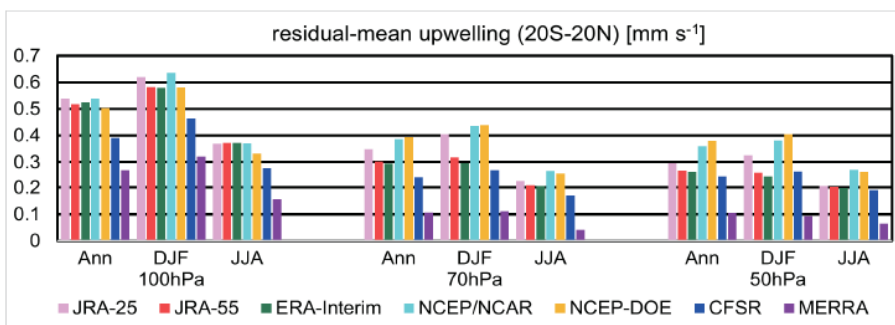


Figure 4. Annual and seasonal mean residual-mean upwelling within 20° of the equator, averaged from 1979 to 2012.

Figure from Harada et al., JMSJ, 2016

*Another model feature, which is important for tropospheric transport of VSLs is the convective parametrisation used in the model (see for example Rybka, H. and Tost, H.: Uncertainties in future climate predictions due to convection parameterisations, Atmos. Chem. Phys., 14, 5561-5576, doi:10.5194/acp-14-5561-2014, 2014, and references therein). I suggest more discussion of this point in the paper. Also, the information of the convective scheme used in the different models should be included in Table 2. Perhaps some of the model differences and some of the model similarities can be attributed to using a particular convective parametrisation or a particular meteorology?*

As per the Reviewer's suggestion, we have extended Table 2 to include the convection and boundary layer mixing schemes used by each model. We did not find any systematic differences in our results related to the choice of convection scheme or input meteorology. We have now made this point in the abstract:

"Overall, our results do not show systematic differences between models specific to the choice of reanalysis meteorology, rather clear differences are seen related to differences in the implementation of transport processes in models".

Related to the above, and following comments from Reviewer #1, we have made clear that differences between CTM setup and the implementation of transport processes is important, as all models would claim to be simulating the above physical processes. Further, we now define what we mean when referring to "transport" differences early on in the manuscript (last paragraph of Introduction):

"... we define *transport* differences between models as the effects of boundary layer mixing, convection and advection, and the implementation of these processes. Note, the project was not designed to separate clearly the contributions of each transport component in the large model ensemble, but can be inferred as the boundary layer mixing affects tracer concentrations mainly near the surface, convection controls tracer transport to the upper troposphere and advection mainly distributes tracers horizontally (e.g. Patra et al. 2009)"

Finally, we have expanded the discussion of the role of convection in the manuscript. In addition to new text placed in Section 3.1.2 (suggested by Reviewer #1), we have added discussion in Section 3.4 relating to model differences shown in Figures 14 and 15. We also cite the *Rybka and Tost* paper.

"The high altitude model-model differences in CHBr<sub>3</sub>, highlighted in Figures 14 and 15, are attributed predominately to differences in the treatment of convection. Previous studies have shown that (i) convective updraft mass fluxes, including the vertical extent of deep convection (relevant for bromine SGI from VSLs), vary significantly depending on the implementation of convection in a given model (e.g. Feng et al., 2011) and (ii) that significantly different short-lived tracer distributions are predicted from different models using different convective parameterisations (e.g. Hoyle et al., 2011). Such parameterisations are often complex, relying on assumptions regarding detrainment levels, trigger thresholds for shallow, mid-level and/or deep convection, and vary in their approach to computing updraft (and downdraft) mass fluxes. Furthermore, the vertical transport of model tracers is also sensitive to interactions of the convective parameterisation with the boundary layer mixing scheme (also parameterised) (Rybka and Tost, 2014). On the above basis and considering that the TransCom-VSLs models implement these processes in different ways (Table 2), it was not possible to detangle transport effects within the scope of this project. However, no systematic similarities/differences between models according to input meteorology were apparent".

*I also have reservations about the concept of a "preferred" tracer. I think this means that the emission inventory somehow interacts with the transport scheme of the model to produce reasonable results at higher altitudes. But this means that the higher altitude agreement could be right for the wrong reason. I know it is demanding a lot from models, but of course one would*

*expect to design independently the best emission inventory and the best (vertical) transport to obtain the best agreement with measurements. Obviously this model intercomparison cannot achieve this goal, but I think the discussion of these issues could be improved.*

The overarching goal of the work was to calculate a climatological multi-model best estimate of stratospheric bromine SGI from  $\text{CHBr}_3$  and  $\text{CH}_2\text{Br}_2$ . It was essential, of course, for this estimate to be based on simulations that provide the best possible model-measurement agreement at the surface. Given good surface agreement, the models' transport of  $\text{CHBr}_3/\text{CH}_2\text{Br}_2$  from the surface to higher altitudes, against that observed, has been tested. The fact that models do not necessarily agree as to which emission inventory "performs best" at all surface sites (against measurements) we believe is an important finding of this work. It has implications for model studies attempting to quantify the global flux of VLSL to the atmosphere and, in particular, for studies attempting to reconcile such estimates obtained from different models. We have added a sentence to the revised manuscript in Section 3.1.2 (end of 3<sup>rd</sup> paragraph), where the above is discussed, to make the latter point more clear:

*"Ultimately, attempts to reconcile estimates of global VLSL emissions, obtained from different modelling studies, need to consider the influence of inter-model differences, as discussed above."*

The discussion of "preferred tracer" has also been clarified in Section 3.2 in response to a comment from Reviewer #1.

*Finally, the impact of ENSO activity on the stratospheric bromine loading is unclear. What is the message of the paper here? The paper states that there is a strong correlation of SGI with ENSO (e.g. abstract), but that there is no correlation of ENSO (MEI) with the bromine loading in the LS (e.g. conclusions). But SGI is important for the bromine loading in the LS. This points needs to be clarified and better discussed in the paper.*

OK, we have clarified this. Our results show that (i) SGI is enhanced over the East Pacific during strong El Niño conditions (e.g. in 1997/1998 as can be seen in Figure 17). Related to this (ii) SGI is strongly correlated to MEI over the East Pacific (where significant SST warming occurs under El Niño conditions) but (iii) averaged over the whole tropical domain, there is little correlation between SGI and ENSO. The latter point is because of the zonal structure in SST anomalies (and therefore convective activity) associated with ENSO activity. Essentially, the effect of warming and intensified convection in some areas (i.e. East Pacific) on stratospheric Br SGI can be cancelled out by the cooler SSTs in other tropical regions. Aschmann et al. (2011) performed a detailed analysis of how bromine SGI is affected by ENSO and indeed reported this complex zonal structure. We have now clarified these points at the end of Section 3.5 of the revised manuscript.

### **Minor issues**

• *Title: I am not sure if "TransCom-VLSL" should be in the title; the name of the project will not be relevant on a timescale of years, when the paper will still be read.*

Since the concept and experimental method are chosen from previous TransCom experiments, it gives a link to the paper's evolution. Thus we would prefer to keep this term in the title.

• *l. 7: I do not think that model estimates should be used to "constrain" measurements.*

We are referring here to using models to help constrain the current SGI range.

• *line 20: change 'optimal' to 'best'*

OK. We have done this.

• *l. 36: Isn't 6 month a bit long for very short lived?*

We agree that intuitively it does seem long for a “very short-lived” compound. However, this is the definition used in previous WMO Ozone reports. VSLs local lifetimes at the surface can vary substantially in space and time, though the <6 months rule is broadly accurate.

• I 51: ‘recent’ twice in this sentence

OK. A “recent” has been removed.

• I. 52: try  $\mathrm{VSLs}$  to avoid italics in VSLs. (Similar for MAPE (l. 345) below).

We thank the Reviewer for this suggestion. The italics have been removed from “VSLs” in  $\mathrm{Br}_y^{\mathrm{VSLs}}$  throughout the manuscript.

• I. 59: ‘owing to’ instead of ‘due to’

OK, we have replaced this.

• I. 76: I think you mean Tissier and Legras here

Yes, that has been corrected.

• I. 78: do you mean “broadly similar” here?

Yes, we have corrected this.

• I. 100: what do you mean by “climate modes” – more explanation here.

We are referring to modes of climate variability, specifically ENSO in this case. We have been more explicit in the revised manuscript and refer directly to ENSO rather than “climate modes”.

• Figure 1: This figure is not really discussed in the paper. Which message does it communicate? I suggest removing the figure from the paper.

We feel that Figure 1 provides a visual overview of the experimental design for the reader. Otherwise it is extremely difficult to show the flow of work and the design of experiments, with several emission scenarios, to a new reader. In this figure we also show how the model output is used for calculating SGI. Some of these concepts are new to the TransCom initiative, thus we would prefer to keep it.

• I. 144: is a bottom-up . . .

We have changed “bottom-up” to “a bottom-up”.

• line 179: this means that the multi-model mean is highly influenced by CTMs driven by ERA-Interim data – correct?

Yes. We have now commented on this in the manuscript. Please see our above response to the first detailed review comment on page 1 of this document.

• I. 211: instead of ‘see also’ you could perhaps state for which information which paper should be consulted.

We have removed the reference following “see also” as this was not needed.

• I 301: what is the reason that ‘clear outliers’ are found? Are these models with obvious errors?



The text here is discussing Figure 3. Generally there are few outliers and these outliers are limited to specific sites (for example, B3DCTM and STAG at SMO). We have added some text directly following the sentence containing “clear outliers” in Section 3.1.1 commenting on potential causes.

“The cause of the outliers at a given site are likely in part related to the model sampling error, including distance of a model grid from the measurement site and resolution (as was shown for CO<sub>2</sub> in Patra et al., 2008). These instances are rare for VSLS but can be seen in B3DCTM’s output in Figure 3 for CHBr<sub>3</sub> at SMO. B3DCTM ran at a relatively coarse horizontal resolution (3.75°) and with less (40) vertical layers compared to most other models. Note, it also has the simplest implementation of boundary layer mixing (Table 2). This above behaviour is also seen at SMO but to a lesser extent for CH<sub>2</sub>Br<sub>2</sub>, for which the seasonal cycle is smaller (see below). The STAG model also produces distinctly different features in the seasonal cycle of both species at some sites (prominently at CGO, SMO and HFM). We attribute these deviations to STAG’s parameterisation of boundary layer mixing, noting that differences for CHBr<sub>3</sub> are greater at KUM than at MLO – two sites in very close proximity but with the latter elevated at ~3000 metres above sea level (i.e. above the boundary layer).”

Later in the paragraph: “The NIES-TM model does not show major differences from other models for CHBr<sub>3</sub>, but outliers for CH<sub>2</sub>Cl<sub>2</sub> at Southern Hemispheric sites (SMO to SPO) are apparent. We are unable to assign any specific reason for the inter-species differences seen for this model”.

- I. 329: *use r for the correlation coefficient*

OK, we have italicized “r” throughout the text.

- I. 366: *why does convection influence “near-surface” abundances of VSLS?*

Convection lofts tracer mass away from the boundary layer. We already point to several references which show this to be the case. For example, see plot of convective updraft mass fluxes in Figure 3 of Feng et al. (2011) which shows the vertical extent of convection.

- I. 414: *I think it is problematic that models have a preferred tracer: doesn’t this imply that results could be right for the wrong reason?*

This comment is addressed in the detailed comments section above.

- I. 425: *Where is the reproduction of the c-shape shown? This seems an important issue.*

It is clearly visible for SHIVA and HIPPO-1. We have now been explicit as to where we are referring: panel (a), 2<sup>nd</sup> and 3<sup>rd</sup> row of Figure 10.

- I. 435: *The concept of a ‘preferred’ tracer means that the emission inventory somehow interacts with the models transport scheme to produce reasonable results at higher altitudes – correct? Can you describe in more detail here, what ‘worse agreement’ means?*

The models, with good agreement at the surface (by way of their preferred tracer), produce a sound simulation of the transport of CHBr<sub>3</sub>/CH<sub>2</sub>Br<sub>2</sub> from the surface to higher altitudes (as evidenced in Figures 10 and 11). The point we are making is that if the model-measurement agreement at the surface is degraded (e.g. in the simulations using the non-preferred tracer), then the absolute model-measurement agreement at higher altitudes is also worsened. We have reworded the text here for clarity. The sentence now reads:

“For a given model, simulations using the non-preferred tracers (i.e. with different CHBr<sub>3</sub>/CH<sub>2</sub>Br<sub>2</sub> emission inventories, not shown), generally lead to worse model-measurement agreement in the TTL. This is not surprising as model-measurement agreement at the surface is poorer in those simulations.”

- I. 485: *is CO really short-lived?*

CO has a global lifetime of several months and therefore is similar to some VSLS. In order that CO and VSLS are not confused, we have reworked this sentence.

- I. 492: *state the lifetime in months/weeks*

OK, we now state that CH<sub>2</sub>Cl<sub>2</sub> has a local lifetime > 1 year in the TTL.

- I. 527: *you might want to add here also Tissier and Legras 2015; Vogel et al. 2014*

OK. We have done this.

- I 560: *Clarify which best estimate is meant here, TransCom or WMO.*

WMO. We have added the citation to Carpenter and Reimann to clarify.

- I. 593-595: *The last sentence states that the VSLS loading in the LS is not correlated to MEI. But the sentences above state that bromine SGI is sensitive to modes such as MEI. Isn't this a contradiction? I think more discussion is require here.*

See earlier and also later comment. We have clarified this section of text and we are saying that the correlation is related to a particular region (the tropical E Pacific).

- I. 598: *change to: these processes*

OK, we have added "processes".

- I. 599: *change 'a range' to 'a number'*

OK, we have done this.

- I. 614-618: *Is the point here that the seasonal cycle is not dependent on the emission inventory, but the absolute model-measurement agreement is? How can this be the case. Please clarify. (See also abstract).*

Yes, that is correct and is the case because at most sites the seasonal CHBr<sub>3</sub>/CH<sub>2</sub>Br<sub>2</sub> abundance is determined from seasonality in the chemical loss rate (same for all models and same between model simulations with different emissions). We have clarified this point. The sentence now reads:

"At most sites, (i) the simulated seasonal cycle of these VSLS is not particularly sensitive to the choice of emission inventory, and (ii) the observed cycle is reproduced well simply from seasonality in the chemical loss (a notable exception is at Mace Head, Ireland)."

Of course the absolute model-measurement agreement will be sensitive to the emission fluxes as they vary in strength.

- I. 626: *change optimal to best*

OK, we have done this.

- I. 634: *what exactly is meant by 'online calculations'?*

An "online" emission calculation here refers to one in which emissions are calculated by taking into account the interaction between the atmospheric state and the ocean. Online calculations consider the actual seawater concentration of VSLS to derive air-sea concentration gradients and calculate

fluxes. This is different to the approach mostly used to date whereby climatological emissions are prescribed. We have clarified this in the text.

- I. 648: *But the 'higher altitudes' are most relevant for the transport of VSLS into the stratosphere – correct?*

Yes. The model-measurement agreement during ATTREX is discussed in Section 3.3. We have added a sentence in the Summary and Conclusions noting that most models fall within 1 standard deviation of the observed mean at the tropopause.

- I. 663: *You mean the SGI range by Carpenter and Reiman, add the citation for clarification.*

OK, we have done this.

- I. 670-672: *This is astonishing, isn't it? I suggest somewhat more discussion on this point.*

This comment was answered earlier. Essentially, it may not be too surprising as changes to SSTs (and convective activity) associated with ENSO is zonally very asymmetric, with warming in some regions and cooling in others. The warming of East Pacific SSTs under El Niño conditions leads to enhanced SGI over this region, but when SGI is averaged over the whole of the tropics, this effect is dampened/cancelled. We have clarified these points at the end of Section 3.5

- I. 676: *change 'changes to' to 'changes of'*

We feel that “changes to emissions” reads better than “changes of emissions”.

- I. 678: *change 'increased' to 'increase of the'*

OK, we have done this.

- I. 679: *distinguished from what?*

From the present day loading. To clarify we have changed “distinguished” to “determined”.

- I. 689: *why is R Hommel not abbreviated?*

*We did not abbreviate R Hommel because the abbreviation would be the same as the earlier, but different “RH”.*

- Fig. 1: *not sure if this figure is necessary*

We feel that Figure 1 provides a visual overview of the experimental design for the reader. We would prefer to keep it. Perhaps the Editor can comment on this.

- Fig. 2: *Continents in light grey would look better than in black.*

OK, we will update.

- References: *There are some references that need to be updated; ACP vs ACPD, Werner et al., 2016 etc.*

We have updated the reference list.

# **A multi-model intercomparison of halogenated very short-lived substances (TransCom-VSLS): linking oceanic emissions and tropospheric transport for a reconciled estimate of the stratospheric source gas injection of bromine**

R. Hossaini<sup>1,a</sup>, P. K. Patra<sup>2</sup>, A. A. Leeson<sup>1,b</sup>, G. Krysztofiak<sup>3,c</sup>, N. L. Abraham<sup>4,5</sup>, S. J. Andrews<sup>6</sup>, A. T. Archibald<sup>4</sup>, J. Aschmann<sup>7</sup>, E. L. Atlas<sup>8</sup>, D. A. Belikov<sup>9,10,11</sup>, H. Bönisch<sup>12</sup>, R. Butler<sup>13</sup>, L. J. Carpenter<sup>6</sup>, S. Dhomse<sup>1</sup>, M. Dorf<sup>14</sup>, A. Engel<sup>12</sup>, L. Feng<sup>13</sup>, W. Feng<sup>1,4</sup>, S. Fuhlbrügge<sup>15</sup>, P. T. Griffiths<sup>5</sup>, N. R. P. Harris<sup>5</sup>, R. Hommel<sup>7</sup>, T. Keber<sup>12</sup>, K. Krüger<sup>15,16</sup>, S. T. Lennartz<sup>15</sup>, S. Maksyutov<sup>9</sup>, H. Mantle<sup>1</sup>, G. P. Mills<sup>17</sup>, B. Miller<sup>18</sup>, S. A. Montzka<sup>18</sup>, F. Moore<sup>18</sup>, M. A. Navarro<sup>8</sup>, D. E. Oram<sup>17</sup>, P. I. Palmer<sup>13</sup>, K. Pfeilsticker<sup>19</sup>, J. A. Pyle<sup>4,5</sup>, B. Quack<sup>15</sup>, A. D. Robinson<sup>5</sup>, E. Saikawa<sup>20,21</sup>, A. Saiz-Lopez<sup>22</sup>, S. Sala<sup>12</sup>, B.-M. Sinnhuber<sup>3</sup>, S. Taguchi<sup>23</sup>, S. Tegtmeier<sup>15</sup>, R. T. Lidster<sup>6</sup>, C. Wilson<sup>1,24</sup>, and F. Ziska<sup>15</sup>

<sup>1</sup>School of Earth and Environment, University of Leeds, Leeds, UK.

<sup>2</sup>Department of Environmental Geochemical Cycle Research, JAMSTEC, Yokohama, Japan.

<sup>3</sup>Institute for Meteorology and Climate Research, Karlsruhe Institute of Technology, Karlsruhe, Germany.

<sup>4</sup>National Centre for Atmospheric Science, UK.

<sup>5</sup>Department of Chemistry, University of Cambridge, Cambridge, UK.

<sup>6</sup>Department of Chemistry, University of York, Heslington, York, UK.

<sup>7</sup>Institute of Environmental Physics, University of Bremen, Bremen, Germany.

<sup>8</sup>Rosenstiel School of Marine and Atmospheric Science, University of Miami, USA.

<sup>9</sup>Center for Global Environmental Research, National Institute for Environmental Studies, Tsukuba, Japan.

<sup>10</sup>National Institute of Polar Research, Tokyo, Japan.

<sup>11</sup>Tomsk State University, Tomsk, Russia.

<sup>12</sup>Institute for Atmospheric and Environmental Sciences, Universität Frankfurt/Main, Germany.

<sup>13</sup>School of GeoSciences, The University of Edinburgh, Edinburgh, UK.

<sup>14</sup>Max-Planck-Institute for Chemistry, Mainz, Germany.

<sup>15</sup>GEOMAR Helmholtz Centre for Ocean Research Kiel, Kiel, Germany.

<sup>16</sup>University of Oslo, Department of Geosciences, Oslo, Norway.

<sup>17</sup>School of Environmental Sciences, University of East Anglia, Norwich, UK.

<sup>18</sup>National Oceanic and Atmospheric Administration, Boulder, USA.

<sup>19</sup>Institute for Environmental Physics, University of Heidelberg, Heidelberg, Germany.

<sup>20</sup>Department of Environmental Sciences, Emory University, Atlanta, USA.

<sup>21</sup>Department of Environmental Health, Rollins School of Public Health, Emory University, Atlanta, USA.

<sup>22</sup>Atmospheric Chemistry and Climate Group, Institute of Physical Chemistry Rocasolano, CSIC, Madrid, Spain.

<sup>23</sup>National Institute of Advanced Industrial Science and Technology, Japan.

<sup>24</sup>National Centre for Earth Observation, Leeds, UK.

<sup>a</sup>now at: Department of Chemistry, University of Cambridge, Cambridge, UK.

<sup>b</sup>now at: Lancaster Environment Centre, University of Lancaster, Lancaster, UK.

<sup>c</sup>now at: Laboratoire de Physique et Chimie de l'Environnement et de l'Espace, CNRS-Université d'Orléans, Orléans, France.

*Correspondence to:* Ryan Hossaini

(r.hossaini@leeds.ac.uk)

**Abstract.** The first concerted multi-model intercomparison of halogenated very short-lived substances (VSLS) has been performed, within the framework of the ongoing Atmospheric Tracer Transport Model Intercomparison Project (TransCom). Eleven global models or model variants participated (**nine chemical transport models and two chemistry-climate models**) by simulating the major natural bromine VSLS, bromoform ( $\text{CHBr}_3$ ) and dibromomethane ( $\text{CH}_2\text{Br}_2$ ), over a 20-year period (1993-2012). **Except for 3 model simulations, all others were driven offline by (or nudged to) re-analysed meteorology.** The overarching goal of TransCom-VSLS was to provide a reconciled model estimate of the stratospheric source gas injection (SGI) of bromine from these gases, to constrain the current measurement-derived range, and to investigate inter-model differences due to emissions and transport processes. Models ran with standardised idealised chemistry, to isolate differences due to transport, and we investigated the sensitivity of results to a range of VSLS emission inventories. Models were tested in their ability to reproduce the observed seasonal and spatial distribution of VSLS at the surface, using measurements from NOAA's long-term global monitoring network, and in the tropical troposphere, using recent aircraft measurements - including high altitude observations from the NASA Global Hawk platform.

The models generally capture the **observed** seasonal cycle of surface  $\text{CHBr}_3$  and  $\text{CH}_2\text{Br}_2$  well, with a strong model-measurement correlation ( $r \geq 0.7$ ) **and a low sensitivity to the choice of emission inventory**, at most sites. In a given model, the absolute model-measurement agreement **at the surface** is highly sensitive to the choice of emissions. **and Large** inter-model differences are **also** apparent when using the same **emission** inventory, highlighting the challenges faced in evaluating such inventories at the global scale. Across the ensemble, most consistency is found within the tropics where most of the models (8 out of 11) achieve **optimal best** agreement to surface  $\text{CHBr}_3$  observations using the lowest of the three  $\text{CHBr}_3$  emission inventories tested (similarly, 8 out of 11 models for  $\text{CH}_2\text{Br}_2$ ). In general, the models **are able to** reproduce well observations of  $\text{CHBr}_3$  and  $\text{CH}_2\text{Br}_2$  obtained in the tropical tropopause layer (TTL) at various locations throughout the Pacific. Zonal variability in VSLS loading in the TTL is generally consistent among models, with  $\text{CHBr}_3$  (and to a lesser extent  $\text{CH}_2\text{Br}_2$ ) most elevated over the tropical West Pacific during boreal winter. The models also indicate the Asian Monsoon during boreal summer to be an important pathway for VSLS reaching the stratosphere, though the strength of this signal varies considerably among models.

We derive an ensemble climatological mean estimate of the stratospheric bromine SGI from  $\text{CHBr}_3$  and  $\text{CH}_2\text{Br}_2$  of 2.0 (1.2-2.5) ppt,  $\sim 57\%$  larger than the best estimate from the most recent World Meteorological Organization (WMO) Ozone Assessment Report. We find no evidence for a long-term, transport-driven trend in the stratospheric SGI of bromine over the simulation period. **However,** The transport-driven inter-annual variability in the annual mean bromine SGI is of the order of  $\pm 5\%$ , with SGI exhibiting a strong positive correlation with ENSO in the East Pacific. **Overall, our results do not show systematic differences between models specific to the choice of**

reanalysis meteorology, rather clear differences are seen related to differences in the implementation of transport processes in the models.

## 40 1 Introduction

Halogenated very short-lived substances (VSLS) are gases with atmospheric lifetimes shorter than, or comparable to, tropospheric transport timescales ( $\sim 6$  months or less at the surface). Naturally-emitted VSLS, such as bromoform ( $\text{CHBr}_3$ ), have marine sources and are produced by phytoplankton (e.g. Quack and Wallace, 2003) and various species of seaweed (e.g. Carpenter and Liss, 2000) - a number of which are farmed for commercial application (Leedham et al., 2013). Once in the atmosphere, VSLS (and their degradation products) may ascend to the lower stratosphere (LS), where they contribute to the inorganic bromine ( $\text{Br}_y$ ) budget (e.g. Pfeilsticker et al., 2000; Sturges et al., 2000) and thereby enhance halogen-driven ozone ( $\text{O}_3$ ) loss (Salawitch et al., 2005; Feng et al., 2007; Sinnhuber et al., 2009; Sinnhuber and Meul, 2015). On a per molecule basis,  $\text{O}_3$  perturbations near the tropopause exert the largest radiative effect (e.g. Lacis et al., 1990; Forster and Shine, 1997; Riese et al., 2012) and recent work has highlighted the climate relevance of VSLS-driven  $\text{O}_3$  loss in this region (Hossaini et al., 2015a).

Quantifying the contribution of VSLS to stratospheric  $\text{Br}_y$  ( $\text{Br}_y^{\text{VSLS}}$ ) has been a major objective of numerous recent observational studies (e.g. Dorf et al., 2008; Laube et al., 2008; Brinckmann et al., 2012; Sala et al., 2014; Wisher et al., 2014) and modelling efforts (e.g. Warwick et al., 2006; Hossaini et al., 2010; Liang et al., 2010; Aschmann et al., 2011; Tegtmeier et al., 2012; Hossaini et al., 2012b, 2013; Aschmann and Sinnhuber, 2013; Fernandez et al., 2014) ~~in recent years~~. However, despite a wealth of research,  $\text{Br}_y^{\text{VSLS}}$  remains poorly constrained, with a current best-estimate range of 2-8 ppt reported in the most recent World Meteorological Organization (WMO) Ozone Assessment Report (Carpenter and Reimann, 2014). Between 15% and 76% of this supply comes from the stratospheric *source gas injection* (SGI) of VSLS; i.e. the transport of a source gas (e.g.  $\text{CHBr}_3$ ) across the tropopause, followed by its breakdown and in-situ release of  $\text{Br}_y^{\text{VSLS}}$  in the LS. The remainder comes from the troposphere-to-stratosphere transport of both organic and inorganic product gases, formed following the breakdown of VSLS below the tropopause; termed *product gas injection* (PGI).

~~Due to~~ **Owing to** their short tropospheric lifetimes, combined with significant spatial and temporal inhomogeneity in their emissions (e.g. Carpenter et al., 2005; Archer et al., 2007; Orlikowska and Schulz-Bull, 2009; Ziska et al., 2013; Stemmler et al., 2015), the atmospheric abundance of VSLS can exhibit sharp tropospheric gradients. The stratospheric SGI of VSLS is expected to be most efficient in regions where strong uplift, such as convectively active regions, coincides with regions of elevated surface mixing ratios (e.g. Tegtmeier et al., 2012, 2013; Liang et al., 2014), driven by strong localised emissions or “hot spots”. Both the magnitude and distribution of emissions, with respect to transport processes, could be, therefore, an important determining factor for SGI. However, current

global-scale emission inventories of  $\text{CHBr}_3$  and  $\text{CH}_2\text{Br}_2$  are poorly constrained, owing to a paucity of observations used to derive their surface fluxes (Ashfold et al., 2014), contributing significant  
75 uncertainty to model estimates of  $\text{Br}_y^{\text{VLSL}}$  (Hossaini et al., 2013). Given the uncertainties outlined above, it is unclear how well preferential transport pathways of VLSL to the LS are represented in global scale models.

Strong convective source regions, such as the tropical West Pacific during boreal winter, are likely important for the troposphere-to-stratosphere transport of VLSL (e.g. Levine et al., 2007;  
80 Aschmann et al., 2009; Pisso et al., 2010; Hossaini et al., 2012b; Liang et al., 2014). The Asian Monsoon also represents an effective pathway for boundary layer air to be rapidly transported to the LS (e.g. Randel et al., 2010; Vogel et al., 2014; Orbe et al., 2015; Tissier and Legras, 2016), though its importance for the troposphere-to-stratosphere transport of VLSL is largely unknown, owing to a lack of observations in the region. While global models **generally** simulate **broad and similar broadly**  
85 **similar** features in the spatial distribution of convection, large inter-model differences in the amount of tracers transported to the tropopause have been reported by Hoyle et al. (2011), who performed a model intercomparison of idealised (“VLSL-like”) tracers with a uniform surface distribution. In order for a robust estimate of the stratospheric SGI of bromine, it is necessary to consider spatial variations in VLSL emissions, and how such variations couple with transport processes. However, a  
90 concerted model evaluation of this type has yet to be performed.

Over a series of two papers, we present results from the first VLSL multi-model intercomparison project (TransCom-VLSL). The TransCom initiative was setup in the 1990s to examine the performance of chemical transport models. Previous TransCom studies have examined non-reactive tropospheric species, such as sulphur hexafluoride ( $\text{SF}_6$ ) (Denning et al., 1999) and carbon dioxide ( $\text{CO}_2$ ) (Law et al., 1996, 2008). Most recently, TransCom projects have examined the influence of emissions, transport and chemical loss on atmospheric  $\text{CH}_4$  (Patra et al., 2011) and  $\text{N}_2\text{O}$  (Thompson et al., 2014). The overarching goal of TransCom-VLSL was to constrain estimates of  $\text{Br}_y^{\text{VLSL}}$ , towards closure of the stratospheric bromine budget, by (i) providing a reconciled climatological model estimate of bromine SGI, to reduce uncertainty on the measurement-derived range  
100 (0.7-3.4 ppt Br) - currently uncertain by a factor of  $\sim 5$  (Carpenter and Reimann, 2014) - and (ii) quantify the influence of emissions and transport processes on inter-model differences in SGI. **In this regard, we define *transport* differences between models as the effects of boundary layer mixing, convection and advection, and the implementation of these processes. The project was not designed to separate clearly the contributions of each transport component in the large model ensemble, but can be inferred as the boundary layer mixing affects tracer concentrations mainly near the surface, convection controls tracer transport to the upper troposphere and advection mainly distributes tracers horizontally (e.g. Patra et al., 2009).** Specific objectives were to (a) evaluate models against measurements from the surface to the tropical tropopause layer (TTL) **and** (b) examine zonal and seasonal variations in VLSL loading in the TTL. ~~(c) examine trends and inter-annual variability in the strato-~~



110 spheric loading of VSLS and (d) investigate how these relate to climate modes. We also show inter-  
annual variability in the stratospheric loading of VSLS (limited to transport) and briefly discuss  
possible trends related to the El Niño Southern Oscillation (ENSO). Section 2 gives a description of  
the experimental design and an overview of participating models. Model-measurement comparisons  
are given in Sections 3.1 to 3.3. Section 3.4 examines zonal/seasonal variations in the troposphere-  
115 stratosphere transport of VSLS and Section 3.5 provides our reconciled estimate of bromine SGI and  
discusses inter-annual variability.

## 2 Methods, Models and Observations

Eleven models, or their variants, took part in TransCom-VSLS. Each model simulated the major  
bromine VSLS, bromoform ( $\text{CHBr}_3$ ) and dibromomethane ( $\text{CH}_2\text{Br}_2$ ), which together account for  
120 77-86% of the total bromine SGI from VSLS reaching the stratosphere (Carpenter and Reimann,  
2014). Participating models also simulated the major iodine VSLS, methyl iodide ( $\text{CH}_3\text{I}$ ), though  
results from the iodine simulations will feature in a forthcoming, stand-alone paper (Hossaini et al.  
2016, in prep). Each model ran with multiple  $\text{CHBr}_3$  and  $\text{CH}_2\text{Br}_2$  emission inventories (see Section  
2.1) in order to (i) investigate the performance of each inventory, in a given model, against observa-  
125 tions and (ii) identify potential inter-model differences whilst using the same inventory. Analogous  
to previous TransCom experiments (e.g. Patra et al., 2011), a standardised treatment of tropospheric  
chemistry was employed, through use of prescribed oxidants and photolysis rates (see Section 2.2).  
This approach (i) ensured a consistent chemical sink of VSLS among models, minimising the in-  
fluence of inter-model differences in tropospheric chemistry on the results, and thereby (ii) isolated  
130 differences due to transport processes. Long-term simulations, over a 20 year period (1993-2012),  
were performed by each model in order to examine trends and transport-driven inter-annual vari-  
ability in the stratospheric SGI of  $\text{CHBr}_3$  and  $\text{CH}_2\text{Br}_2$ . Global monthly mean model output over the  
full simulation period, along with output at a higher temporal resolution (typically hourly) over mea-  
surement campaign periods, was requested from each group. A brief description of the participating  
135 models is given in Section 2.3 and a description of the observational data used in this work is given  
in Section 2.4. Figure 1 summarises the approach of TransCom-VSLS and its broad objectives.

### 2.1 Tracers and oceanic emission fluxes

Owing to significant differences in the magnitude and spatial distribution of VSLS emission fluxes,  
among previously published inventories (Hossaini et al., 2013), all participating models ran with  
140 multiple  $\text{CHBr}_3$  and  $\text{CH}_2\text{Br}_2$  tracers. Each of these tracers used a different set of prescribed sur-  
face emissions. Tracers named “ $\text{CHBr}_3_{\text{L}}$ ”, “ $\text{CHBr}_3_{\text{O}}$ ” and “ $\text{CHBr}_3_{\text{Z}}$ ” used the inventories of  
Liang et al. (2010), Ordóñez et al. (2012) and Ziska et al. (2013), respectively. These three stud-  
ies also reported emission fluxes for  $\text{CH}_2\text{Br}_2$ , and thus the same (L/O/Z) notation applies to the

model CH<sub>2</sub>Br<sub>2</sub> tracers, as summarised in Table 1. As these inventories were recently described  
145 and compared by Hossaini et al. (2013), only a brief description of each is given below. **Surface  
CHBr<sub>3</sub>/CH<sub>2</sub>Br<sub>2</sub> emission maps for each inventory are given in the Supplementary Information (Fig-  
ures S1 and S2).**

The Liang et al. (2010) inventory is a top-down estimate of VSLS emissions based on aircraft  
observations, mostly concentrated around the Pacific and North America between 1996 and 2008.  
150 Measurements of CHBr<sub>3</sub> and CH<sub>2</sub>Br<sub>2</sub> from the following National Aeronautics and Space Admin-  
istration (NASA) aircraft campaigns were used to derive the ocean fluxes: PEM-Tropics, TRACE-P,  
INTEX, TC4, ARCTAS, STRAT, Pre-AVE and AVE. This inventory is aseasonal and assumes the  
same spatial distribution of emissions for CHBr<sub>3</sub> and CH<sub>2</sub>Br<sub>2</sub>. The Ordóñez et al. (2012) inventory  
is also a top-down estimate based on the same set of aircraft measurements with the addition of the  
155 NASA POLARIS and SOLVE campaigns. This inventory weights tropical ( $\pm 20^\circ$  latitude) CHBr<sub>3</sub>  
and CH<sub>2</sub>Br<sub>2</sub> emissions according to a monthly-varying satellite climatology of chlorophyll a (chl  
a), a proxy for oceanic bio-productivity, providing some seasonality to the emission fluxes. The  
Ziska et al. (2013) inventory is a bottom-up estimate of VSLS emissions, based on a compilation of  
seawater and ambient air measurements of CHBr<sub>3</sub> and CH<sub>2</sub>Br<sub>2</sub>. Climatological, aseasonal emission  
160 maps of these VSLS were calculated using the derived sea-air concentration gradients and a com-  
monly used sea-to-air flux parameterisation; considering wind speed, sea surface temperature and  
salinity (Nightingale et al., 2000).

## 2.2 Tropospheric chemistry

Participating models considered chemical loss of CHBr<sub>3</sub> and CH<sub>2</sub>Br<sub>2</sub> through oxidation by the hy-  
droxyl radical (OH) and by photolysis. These loss processes are comparable for CHBr<sub>3</sub>, with pho-  
165 tolysis contributing  $\sim 60\%$  of the CHBr<sub>3</sub> chemical sink at the surface (Hossaini et al., 2010). For  
CH<sub>2</sub>Br<sub>2</sub>, photolysis is a minor tropospheric sink, with its loss dominated by OH-initiated oxidation.  
The overall local lifetimes of CHBr<sub>3</sub> and CH<sub>2</sub>Br<sub>2</sub> in the tropical marine boundary layer have recently  
been evaluated to be 15 (13-17) and 94 (84-114) days, respectively (Carpenter and Reimann, 2014).  
170 These values are calculated based on  $[\text{OH}] = 1 \times 10^6 \text{ molecules cm}^{-3}$ ,  $T = 275 \text{ K}$  and with a global  
annual mean photolysis rate. For completeness, **participating** models also considered loss of CHBr<sub>3</sub>  
and CH<sub>2</sub>Br<sub>2</sub> by reaction with atomic oxygen (O(<sup>1</sup>D)) and chlorine (Cl) radicals. However, these  
are generally very minor loss pathways owing to the far larger relative abundance of tropospheric  
OH and the respective rate constants for these reactions. **Kinetic data (Table 1) was** taken from the  
175 most recent Jet Propulsion Laboratory (JPL) data evaluation (Sander et al., 2011). Note, the focus  
and design of TransCom-VSLS was to constrain the stratospheric SGI of VSLS, thus product gases  
- formed following the breakdown of CHBr<sub>3</sub> and CH<sub>2</sub>Br<sub>2</sub> in the TTL (Werner et al. 2016, in prep) -  
and the stratospheric PGI of bromine was not considered.

Participating models ran with the same global monthly-mean oxidant fields. For OH, O(<sup>1</sup>D) and Cl, these fields were the same as those used in the previous TransCom-CH<sub>4</sub> model inter-comparison (Patra et al., 2011). Within the TransCom framework, these fields have been extensively used and evaluated and shown to give a realistic simulation of the tropospheric burden and lifetime of methane and also methyl chloroform. Models also ran with the same monthly-mean CHBr<sub>3</sub> and CH<sub>2</sub>Br<sub>2</sub> photolysis rates, calculated offline from the TOMCAT chemical transport model (Chipperfield, 2006). TOMCAT has been used extensively to study the tropospheric chemistry of VLS (e.g. Hossaini et al., 2010, 2012b, 2015b) and photolysis rates from the model were used to evaluate the lifetime of VLS for the recent WMO Ozone Assessment Report (Carpenter and Reimann, 2014).

### 2.3 Participating models and output

Eight global models (ACTM, B3DCTM, EMAC, MOZART, NIES-TM, STAG, TOMCAT and UKCA) and 3 of their variants (see Table 2) participated in TransCom-VLS. All the models are offline chemical transport models (CTMs), forced with analysed meteorology (e.g. winds and temperature fields), with the exception of EMAC and UKCA which are free-running chemistry-climate models (CCMs), calculating winds and temperature online. The horizontal resolution of participating models ranged from  $\sim 1^\circ \times 1^\circ$  (longitude  $\times$  latitude) to  $3.75^\circ \times 2.5^\circ$ . In the vertical, the number of levels varied from 32 to 85, with various coordinate systems. A summary of the participating models and their salient features is given in Table 2. Note, these features do not necessarily link to model performance as evaluated in this work. Note also, approximately half of the models used ECMWF ERA-Interim meteorological data. In terms of mean upwelling in the tropics, where stratospheric bromine SGI takes place, there is generally good agreement between the most recent major reanalysis products from ECMWF, JMA and NCEP (e.g. Harada et al., 2015). Therefore, we do not expect a particular bias in our results from use of ERA-Interim.

Three groups, the Karlsruhe Institute of Technology (KIT), the University of Leeds (UoL) and the University of Cambridge (UoC), submitted output from an additional set of simulations using variants of their models. KIT ran the EMAC model twice, as a free running model (here termed “EMAC\_F”) and also in *nudged* mode (EMAC\_N). The UoL performed two TOMCAT simulations, the first of which ~~diagnosed convection~~ used the model’s *standard* convection parameterisation, based on the mass flux scheme of Tiedtke (1989). The second TOMCAT simulation (“TOMCAT\_conv”) used archived convective mass fluxes, taken from the ECMWF ERA-Interim reanalysis. A description and evaluation of these TOMCAT variants is given in Feng et al. (2011). In order to investigate the influence of resolution, the UoC ran two UKCA model simulations with different horizontal/vertical resolutions. The horizontal resolution in the “UKCA\_high” simulation was a factor of 4 (2 in 2 dimensions) greater than that of the *standard* UKCA run (Table 2).

All [participating](#) models simulated the 6 CHBr<sub>3</sub> and CH<sub>2</sub>Br<sub>2</sub> tracers (see Section 2.1) over a 20  
215 year period; 01/01/1993 to 31/12/2012. This period was chosen as it (i) encompasses a range of field  
campaigns during which VLS measurements were taken and (ii) allows the strong El Niño event of  
1997/1998 to be investigated in the analysis of SGI trends. The monthly mean volume mixing ratio  
(vmr) of each tracer was archived by each model on the same 17 pressure levels, extending from  
220 the surface to 10 hPa over the full simulation period. The models were also sampled hourly at 15  
surface sites over the full simulation period and during periods of recent ship/aircraft measurement  
campaigns, described in Section 2.4 below. Note, the first two years of simulation were treated as  
spin up and output was analysed post 1995.

## 2.4 Observational data and processing

### 2.4.1 Surface

225 Model output was compared to and evaluated against a range of observational data. At the surface,  
VLS measurements at 15 sites were considered (Table 3). All sites except one form part of the on-  
going global monitoring program (see <http://www.esrl.noaa.gov/gmd>) of the National Oceanic and  
Atmospheric Administration’s Earth System Research Laboratory (NOAA/ESRL). Further details  
related to the sampling network are given in Montzka et al. (2011) ([see also](#)). Briefly, NOAA/ESRL  
230 measurements of CHBr<sub>3</sub> and CH<sub>2</sub>Br<sub>2</sub> are obtained from whole air samples, collected approximately  
weekly into paired steel or glass flasks, prior to being analysed using gas chromatography/mass spec-  
trometry (GC/MS) in their central Boulder laboratory. Here, the climatological monthly mean mole  
fractions of these VLS were calculated at each site based on monthly mean surface measurements  
over the 01/01/98 to 31/12/2012 period (except SUM, THD and SPO which have shorter records).  
235 Similar climatological fields of CHBr<sub>3</sub>, CH<sub>2</sub>Br<sub>2</sub> were calculated from each model’s hourly output  
sampled at each location.

Surface measurements of CHBr<sub>3</sub> and CH<sub>2</sub>Br<sub>2</sub>, obtained by the University of Cambridge in Malaysian  
Borneo (Tawau, site “TAW”, Table 3), were also considered. A description of these data is given in  
Robinson et al. (2014). Briefly, in-situ measurements were made using the  $\mu$ -Dirac gas chromato-  
240 graph instrument with electron capture detection (GC-ECD) (e.g. Pyle et al., 2011). Measurements  
at TAW are for a single year (2009) only, making the observed record at this site far shorter than that  
at NOAA/ESRL stations discussed above.

A subset of [participating](#) models also provided hourly output over the period of the TransBrom  
and SHIVA (Stratospheric Ozone: Halogen Impacts in a Varying Atmosphere) ship cruises. During  
245 both campaigns, surface CHBr<sub>3</sub> and CH<sub>2</sub>Br<sub>2</sub> measurements were obtained on-board the Research  
Vessel (R/V) *Sonne*. TransBrom sampled along a meridional transect of the West Pacific, from Japan  
to Australia, during October 2009 (Krüger and Quack, 2013). SHIVA was a European Union (EU)-  
funded project to investigate the emissions, chemistry and transport of VLS ([9](http://shiva.iup.uni-</a></p></div><div data-bbox=)

heidelberg.de/). Ship-borne measurements of surface  $\text{CHBr}_3$  and  $\text{CH}_2\text{Br}_2$  were obtained in November 2011, with sampling extending from Singapore to the Philippines, within the South China Sea and along the northern coast of Borneo (Fuhlbrügge et al., 2015). The ship track is shown in Figure 2.

#### 2.4.2 Aircraft

Observations of  $\text{CHBr}_3$  and  $\text{CH}_2\text{Br}_2$  from a range of aircraft campaigns were also used (Figure 2). As (i) the troposphere-to-stratosphere transport of air (and VSLs) primarily occurs in the tropics, and (ii) because VSLs emitted in the extratropics have a negligible impact on stratospheric ozone (Tegtmeier et al., 2015), TransCom-VSLs focused on aircraft measurements obtained in the latitude range  $30^\circ\text{N}$  to  $30^\circ\text{S}$ . Hourly model output was interpolated to the relevant aircraft sampling location, allowing for point-by-point model-measurement comparisons. A brief description of the aircraft campaigns follows.

The HIAPER Pole-to-Pole Observations (HIPPO) project (<http://www.eol.ucar.edu/projects/hippo>) comprised a series of aircraft campaigns between 2009 and 2011 (Wofsy et al., 2011), supported by the National Science Foundation (NSF). Five campaigns were conducted; HIPPO-1 (January 2009), HIPPO-2 (November 2009), HIPPO-3 (March/April 2010), HIPPO-4 (June 2011) and HIPPO-5 (August/September 2011). Sampling spanned a range of latitudes, from near the North Pole to coastal Antarctica, on board the NSF Gulfstream V aircraft, and from the surface to  $\sim 14$  km over the Pacific Basin. Whole air samples, collected in stainless steel and glass flasks, were analysed by two different laboratories using GC/MS; NOAA/ESRL and the University of Miami. HIPPO results from both laboratories are provided on a scale consistent with NOAA/ESRL.

The SHIVA aircraft campaign, based in Miri (Malaysian Borneo), was conducted during November–December 2011. Measurements of  $\text{CHBr}_3$  and  $\text{CH}_2\text{Br}_2$  were obtained during 14 flights of the DLR Falcon aircraft, with sampling over much of the northern coast of Borneo, within the South China and Sulu seas, up to an altitude of  $\sim 12$  km (Sala et al., 2014; Fuhlbrügge et al., 2015). VSLs measurements were obtained by two groups; the University of Frankfurt (UoF) and the University of East Anglia (UEA). UoF measurements were made using an in-situ GC/MS system (Sala et al., 2014), while UEA analysed collected whole air samples, using GC/MS.

CAST (Coordinated Airborne Studies in the Tropics) is an ongoing research project funded by the UK Natural Environment Research Council (NERC) and is a collaborative initiative with the NASA ATTREX programme (see below). The CAST aircraft campaign, based in Guam, was conducted in January-February 2014 with VSLs measurements made by the University of York on-board the FAAM (Facility for Airborne Atmospheric Measurements) BAe-146 aircraft, up to an altitude of  $\sim 8$  km. These observations were made by GC/MS collected from whole air samples as described in Andrews et al. (2016).

Observations of  $\text{CHBr}_3$  and  $\text{CH}_2\text{Br}_2$  within the TTL and lower stratosphere (up to  $\sim 20$  km) were  
285 obtained during the NASA (i) Pre-Aura Validation Experiment (Pre-AVE), (ii) Costa Rica Aura  
Validation Experiment (CR-AVE) and (iii) Airborne Tropical Tropopause Experiment (ATTREX)  
missions. The Pre-AVE mission was conducted in 2004 (January-February), with measurements  
obtained over the equatorial eastern Pacific during 8 flights of the high altitude WB-57 aircraft.  
The CR-AVE mission took place in 2006 (January-February) and sampled a similar region around  
290 Costa Rica (Figure 2), also with the WB-57 aircraft (15 flights). The ATTREX mission consists of  
an ongoing series of aircraft campaigns using the unmanned Global Hawk aircraft. Here,  $\text{CHBr}_3$   
and  $\text{CH}_2\text{Br}_2$  measurements from 10 flights of the Global Hawk, over two ATTREX campaigns,  
were used. The first campaign (February-March, 2013) sampled large stretches of the north east and  
central Pacific ocean, while the second campaign (January-March, 2014) sampled predominantly the  
295 West Pacific, around Guam. During Pre-AVE, CR-AVE and ATTREX, VLS measurements were  
obtained by the University of Miami following GC/MS analysis of collected whole air samples.

### 3 Results and Discussion

#### 3.1 Model-observation comparisons: surface

In this section, we evaluate the models in terms of (i) their ability to capture the observed seasonal  
300 cycle of  $\text{CHBr}_3$  and  $\text{CH}_2\text{Br}_2$  at the surface and (ii) the absolute agreement to the observations. We  
focus on investigating the relative performance of each of the tested emission inventories, within a  
given model, and the performance of the inventories across the ensemble.

##### 3.1.1 Seasonality

We first consider the seasonal cycle of  $\text{CHBr}_3$  and  $\text{CH}_2\text{Br}_2$  at the locations given in Table 3. Fig-  
305 ure 3 compares observed and simulated ( $\text{CHBr}_3$ \_L tracer) monthly mean anomalies, calculated by  
subtracting the climatological monthly mean  $\text{CHBr}_3$  surface mole fraction from the climatological  
annual mean (to focus on the seasonal variability). Based on photochemistry alone, in the north-  
ern hemisphere (NH) one would expect a  $\text{CHBr}_3$  winter (Dec-Feb) maximum owing to a reduced  
chemical sink (e.g. slower photolysis rates and lower  $[\text{OH}]$ ) and thereby a relatively longer  $\text{CHBr}_3$   
310 lifetime. This seasonality, apparent at most NH sites shown in Figure 3, is particularly pronounced  
at high-latitudes ( $>60^\circ\text{N}$ , e.g. ALT, BRW and SUM), where the amplitude of the observed seasonal  
cycle is greatest. A number of features are apparent from these comparisons. First, in general most  
models reproduce the observed phase of the  $\text{CHBr}_3$  seasonal cycle well, even with emissions that  
do not vary seasonally, suggesting that seasonal variations in the  $\text{CHBr}_3$  chemical sink are generally  
315 well represented. For example, model-measurement correlation coefficients ( $r$ ), summarised in Ta-  
ble 4, are  $>0.7$  for at least 80% of the models at 7 of 11 NH sites. Second, at some sites, notably  
MHD, THD, CGO and PSA, the observed seasonal cycle of  $\text{CHBr}_3$  is not captured well by virtually

all of the models (see discussion below). Third, at most sites the amplitude of the seasonal cycle is generally consistent across the models (within a few percent, excluding clear outliers). The cause of outliers at a given site are likely in part related to the model sampling error, including distance of a model grid from the measurement site and resolution (as was shown for CO<sub>2</sub> in Patra et al. (2008)). These instances are rare for VSLS but can be seen in B3DCTM's output in Figure 3 for CHBr<sub>3</sub> at SMO. B3DCTM ran at a relatively coarse horizontal resolution (3.75°) and with less vertical layers (40) compared to most other models. Note, it also has the simplest implementation of boundary layer mixing (Table 2). The above behaviour is also seen at SMO but to a lesser extent for CH<sub>2</sub>Br<sub>2</sub>, for which the seasonal cycle is smaller (see below). The STAG model also produces distinctly different features in the seasonal cycle of both species at some sites (prominently at CGO, SMO and HFM). We attribute these deviations to STAG's parameterisation of boundary layer mixing, noting that differences for CHBr<sub>3</sub> are greater at KUM than at MLO – two sites in very close proximity but with the latter elevated at ~3000 metres above sea level (i.e. above the boundary layer). With respect to the observations, the amplitude of the seasonal cycle is either under- (e.g. BRW) or over-estimated (e.g. KUM) at some locations, by all of the models. This possibly reflects a more systematic bias in the prescribed CHBr<sub>3</sub> loss rate and/or relates to emissions, though this effect is generally small and localised.

A similar analysis has been performed to examine the seasonal cycle of surface CH<sub>2</sub>Br<sub>2</sub>. Observed and simulated monthly mean anomalies, calculated in the same fashion as those for CHBr<sub>3</sub> above, are shown in Figure 4 and correlation coefficients are given in Table 5. The dominant chemical sink of CH<sub>2</sub>Br<sub>2</sub> is through OH-initiated oxidation and thus its seasonal cycle at most stations reflects seasonal variation in [OH] and temperature. At most sites, this gives rise to a minimum in the surface mole fraction of CH<sub>2</sub>Br<sub>2</sub> during summer months, owing to greater [OH] and temperature, and thereby a faster chemical sink. Relative to CHBr<sub>3</sub>, CH<sub>2</sub>Br<sub>2</sub> is considerably longer-lived (and thus well mixed) near the surface, meaning the amplitude of the seasonal cycle is far smaller. At most sites, most models capture the observed phase and amplitude of the CH<sub>2</sub>Br<sub>2</sub> seasonal cycle well, though as was the case for CHBr<sub>3</sub>, agreement in the southern hemisphere (SH, e.g. SMO, CGO, PSA) seems poorest. For example, at SMO and CGO only 40% of the models are positively correlated to the observations with  $r > 0.5$  (Table 5). The NIES-TM model does not show major differences from other models for CHBr<sub>3</sub>, but outliers for CH<sub>2</sub>Cl<sub>2</sub> at SH sites (SMO to SPO) are apparent. We were unable to assign any specific reason for the inter-species differences seen for this model.

At two sites (MHD and THD) ~~virtually all of the models do not reproduce~~ almost none of the models reproduce the observed CHBr<sub>3</sub> seasonal cycle, exhibiting an anti-correlation with the observed cycle (see bold entries in Table 4). Here, the simulated cycle follows that expected from seasonality in the chemical sink. At MHD, seasonality in the local emission flux is suggested to be the dominant factor controlling the seasonal cycle of surface CHBr<sub>3</sub> (Carpenter et al., 2005). This

355 leads to the observed summer maximum (as shown in Figure 3) and is not represented in the models' CHBr<sub>3</sub>\_L tracer which, at the surface, is driven by the aseasonal emission inventory of Liang et al. (2010). A similar summer maximum seasonal cycle is observed for CH<sub>2</sub>Br<sub>2</sub>, also not captured by the models' CH<sub>2</sub>Br<sub>2</sub>\_L tracer. To investigate the sensitivity of the model-measurement correlation to the prescribed surface fluxes, multi-model mean (MMM) surface CHBr<sub>3</sub> and CH<sub>2</sub>Br<sub>2</sub> fields were  
 360 calculated for each tracer (i.e. for each emission inventory considered) and each site. Figure 5 shows calculated MMM *r* values at each site for CHBr<sub>3</sub> and CH<sub>2</sub>Br<sub>2</sub>. For CHBr<sub>3</sub>, *r* generally has a low sensitivity to the choice of emission fluxes at most sites (e.g. ALT, SUM, BRW, LEF, NWR, KUM, MLO, SPO), though notably at MHD, use of the Ziska et al. (2013) inventory (which is aseasonal) reverses the sign of *r* to give a strong positive correlation (MMM *r* > 0.70) against the observations.  
 365 Individual model *r* values for MHD are given in Table S1 of the Supplementary Information. With the exception of TOMCAT, TOMCAT\_CONV and UKCA\_HI, the remaining 7 models each reproduce the MHD CHBr<sub>3</sub> seasonality well (with *r* > 0.65). That good agreement is obtained with the Ziska aseasonal inventory, compared to the other aseasonal inventories considered, highlights the importance of the CHBr<sub>3</sub> emission distribution, with respect to transport processes, serving this lo-  
 370 cation. We suggest that the summertime transport of air that has experienced relatively large CHBr<sub>3</sub> emissions north/north-west of MHD is the cause of the apparent seasonal cycle seen in most models using the Ziska inventory (example animations of the seasonal evolution of surface CHBr<sub>3</sub> are given in the Supplementary Information to visualise this). Note also, the far better absolute model-measurement agreement obtained at MHD for models using this inventory (Supplementary Figure  
 375 S3). At other sites, such as TAW, no clear seasonality is apparent in the observed background mixing ratios of CHBr<sub>3</sub> and CH<sub>2</sub>Br<sub>2</sub> (Robinson et al., 2014). Here, the models exhibit little or no significant correlation to measured values and are unlikely to capture small-scale features in the emission distribution (e.g the contribution from local aquaculture) that conceivably contribute to observed levels of CHBr<sub>3</sub> and CH<sub>2</sub>Br<sub>2</sub> in this region (Robinson et al., 2014).

### 380 3.1.2 Absolute agreement

To compare the absolute agreement between a model (M) and an observation (O) value, for each monthly mean surface model-measurement comparison, the mean absolute percentage error (MAPE, equation 1) was calculated (for each model tracer). Figure 6 shows the CHBr<sub>3</sub> and CH<sub>2</sub>Br<sub>2</sub> tracer that provides the lowest MAPE (i.e. best agreement) for each model (indicated by the fill colour of  
 385 cells). The numbers within the cells give the MAPE value itself, and therefore correspond to the “best agreement” that can be obtained from the various tracers with the emission inventories that were tested.

$$\text{MAPE} = \frac{100}{n} \sum_{t=1}^n \left| \frac{M_t - O_t}{O_t} \right| \quad (1)$$



For both  $\text{CHBr}_3$  and  $\text{CH}_2\text{Br}_2$ , within any given model, no single emission inventory is able to provide the best agreement at all surface locations (i.e. from the columns in Figure 6). This was previously noted by Hossaini et al. (2013) using the TOMCAT model, and to some degree likely reflects the geographical coverage of the observations used to create the emission inventories. Hossaini et al. (2013) also noted significant differences between simulated and observed  $\text{CHBr}_3$  and  $\text{CH}_2\text{Br}_2$ , using the same inventory; i.e. **at a given location, low  $\text{CHBr}_3$  MAPE (good agreement) does not necessarily accompany a corresponding low  $\text{CH}_2\text{Br}_2$  MAPE using the same inventory. a low  $\text{CHBr}_3$  MAPE (good agreement), at a given location using a particular inventory, does not necessarily mean a corresponding low  $\text{CH}_2\text{Br}_2$  MAPE can be achieved using the same inventory, at that location.**

A key finding of this study is that significant inter-model differences are also apparent (i.e. see rows in Figure 6 grid). For example, for  $\text{CHBr}_3$ , no single inventory performs best across the full range of models at any given surface site. **TOMCAT and B3DCTM - both of which are driven by ERA-Interim - agree on the best  $\text{CHBr}_3$  inventory (lowest MAPE) at approximately half of the 17 sites considered.** This analysis implies that, on a global scale, the “performance” of emission inventories is somewhat model-specific and highlights the challenges of evaluating such inventories. Previous conclusions as to the *best* performing VLSL inventories, based on single model simulations (Hossaini et al., 2013), must therefore be treated with caution. When one considers that previous modelling studies (Warwick et al., 2006; Liang et al., 2010; Ordóñez et al., 2012), each having derived different VLSL emissions based on aircraft observations, **and having different tropospheric chemistry**, report generally good agreement between their respective model and observations, our findings are perhaps not unexpected. However, we note also that few VLSL modelling studies have used long-term surface observations to evaluate their models, as performed here. **This suggests any attempts to reconcile estimates of global VLSL emissions, obtained from different modelling studies, need to consider the influence of inter-model differences.**

As the chemical sink of VLSL was consistent across all models, the inter-model differences discussed above are attributed primarily to differences in **the treatment and implementation** of transport processes ~~, including (i)~~. **This includes** convection and ~~(ii)~~ boundary layer mixing, both of which can significantly influence the near-surface abundance of VLSL in the real (Fuhlbrügge et al., 2013, 2015) and model (Zhang et al., 2008; Feng et al., 2011; Hoyle et al., 2011) atmospheres, **and are parameterised in different ways (Table 2). On this basis, it is not surprising that different CTM setups lead to differences in the surface distribution of VLSL, nor that differences are apparent between CTMs that use the same meteorological input fields. Indeed, such effects have also been observed in previous model intercomparisons (Hoyle et al., 2011).** Large-scale vertical advection, the native grid of a model and its horizontal/vertical resolution may also be contributing factors, though quantifying their relative influence was beyond the scope of TransCom-VLSL. At some sites, differences among emission inventory performance are **even** apparent between model variants that, besides transport,

425 are otherwise identical; [i.e. for example, see EMAC\\_F and EMAC\\_N model entries, and also the TOMCAT and TOMCAT\\_CONV entries of Figure 6.](#)

Despite the inter-model differences in the performance of emission inventories, some generally consistent features are found across the ensemble. First, for  $\text{CHBr}_3$  the tropical MAPE (see Figure 7), based on the model-measurement comparisons in the latitude range  $\pm 20^\circ$ , is lowest when using the emission inventory of Ziska et al. (2013), for most (8 out of 11,  $\sim 70\%$ ) of the [participating](#) models. This is significant as troposphere-to-stratosphere transport primarily occurs in the tropics and the Ziska et al. (2013) inventory has the lowest  $\text{CHBr}_3$  emission flux in this region (and globally, Table 1). Second, for  $\text{CH}_2\text{Br}_2$ , the tropical MAPE is lowest for most (also  $\sim 70\%$ ) of the models when using the Liang et al. (2010) inventory, which also has the lowest global flux of the three inventories tested. For a number of models, a similar agreement is also obtained with Ordóñez et al. (2012) inventory, as the two are broadly similar in magnitude/distribution (Hossaini et al., 2013). For  $\text{CH}_2\text{Br}_2$ , the Ziska et al. (2013) inventory performs poorest across the ensemble (models generally overestimate  $\text{CH}_2\text{Br}_2$  with this inventory). Overall, the tropical MAPE for a given model is more sensitive to choice of emission inventory for  $\text{CHBr}_3$  than  $\text{CH}_2\text{Br}_2$  (Figure 7). Based on each model's *preferred* inventory (i.e. from Figure 7), the tropical MAPE is generally  $\sim 40\%$  for  $\text{CHBr}_3$  and  $< 20\%$  for  $\text{CH}_2\text{Br}_2$  (in most models). One model (STAG) exhibited a MAPE of  $> 50\%$  for both species, regardless of the choice of emission inventory, and was therefore omitted from the subsequent model-measurement comparisons to aircraft data and also from the multi-model mean SGI estimate derived in Section 3.5.

445 For the [subset of 5](#) models that submitted hourly output over the period of the SHIVA (2011) and TransBrom (2009) ship cruises, Figures 8 and 9 compare the multi-model mean (MMM)  $\text{CHBr}_3$  and  $\text{CH}_2\text{Br}_2$  mixing ratio (and the model spread) to the observed values. Note, the MMM was calculated based on each model's preferred tracer (i.e. preferred emissions inventory). Generally, the models reproduce the observed mixing ratios from SHIVA well, with a MMM campaign MAPE of 450 25% or less for both VSLs. This is encouraging as SHIVA sampled in the tropical West Pacific region, where rapid troposphere-to-stratosphere transport of VSLs likely occurs (e.g. Aschmann et al., 2009; Liang et al., 2014) and where VSLs emissions, weighted by their ozone depletion potential, are largest (Tegtmeier et al., 2015). Model-measurement comparisons during TransBrom are varied with models generally underestimating observed  $\text{CHBr}_3$  and  $\text{CH}_2\text{Br}_2$  during significant portions of 455 the cruise. The underestimate is most pronounced close to the start and end of the cruise during which observed mixing ratios were more likely influenced by coastal emissions, potentially underestimated in global-scale models. Note, TransBrom also sampled sub-tropical latitudes (see Figure 2).

Overall, our results show that most [participating](#) models capture the observed seasonal cycle and 460 the magnitude of surface  $\text{CHBr}_3$  and  $\text{CH}_2\text{Br}_2$  reasonably well, using a combination of emission inventories. Generally, this leads to a realistic surface distribution at most locations, and thereby

provides good agreement between models and aircraft observations above the boundary layer; see Section 3.2 below.

### 3.2 Model-observation comparisons: free troposphere

465 We now evaluate modelled profiles of  $\text{CHBr}_3$  and  $\text{CH}_2\text{Br}_2$  using observations from a range of recent aircraft campaigns (see Section 2.4). Note, for these comparisons, and from herein unless noted, all analysis is performed using ~~each models the preferred~~  $\text{CHBr}_3$  and  $\text{CH}_2\text{Br}_2$  tracer ~~for each model~~ (i.e. preferred emissions inventory), as was diagnosed in the previous discussion (i.e. from Figure 7, see also Section 3.1.2). ~~This approach ensures that an estimate of stratospheric bromine SGI, from a given model, is based on a simulation in which the optimal  $\text{CHBr}_3/\text{CH}_2\text{Br}_2$  model-measurement agreement at the surface was achieved. This approach ensures consistent model estimates of stratospheric bromine SGI, based on simulations with optimal model-measurement agreement at the surface.~~ The objective of ~~the comparisons below here~~ is to show that the ~~participating models produce a realistic simulation of  $\text{CHBr}_3$  and  $\text{CH}_2\text{Br}_2$  in the tropical free troposphere and to test model transport~~ of  $\text{CHBr}_3$  and  $\text{CH}_2\text{Br}_2$  from the surface to high altitudes, against that from atmospheric measurements. Intricacies of individual model-measurement comparison are not discussed. Rather, Figure 10 compares MMM profiles (and the model spread) of  $\text{CHBr}_3$  and  $\text{CH}_2\text{Br}_2$  mixing ratio to observed campaign means within the tropics ( $\pm 20^\circ$  latitude). Generally model-measurement agreement, diagnosed by both the campaign-averaged MAPE and the correlation coefficient ( $r$ ) is excellent during most campaigns. For all of the 7 campaigns considered, the modelled MAPE for  $\text{CHBr}_3$  is  $\leq 35\%$  ( $\leq 20\%$  for  $\text{CH}_2\text{Br}_2$ ). The models also capture much of the observed variability throughout the observed profiles, including, for example, the signature “c-shape” of convection in the measured  $\text{CHBr}_3$  profile from SHIVA and HIPPO-1 (panel (a), 2nd and 3rd rows of Figure 10). Correlation coefficients between modelled and observed  $\text{CHBr}_3$  are  $\geq 0.8$  for 5 of the 7 campaigns and for  $\text{CH}_2\text{Br}_2$  are generally  $> 0.5$ .

It is unclear why model-measurement agreement (particularly the  $\text{CHBr}_3$  MAPE) is poorest for the HIPPO-4 and HIPPO-5 campaigns. However, we note that at most levels MMM  $\text{CHBr}_3$  and  $\text{CH}_2\text{Br}_2$  falls within  $\pm 1$  standard deviation ( $\sigma$ ) of the observed mean. Note, an underestimate of surface  $\text{CHBr}_3$  does not generally translate to a consistent underestimate of measured  $\text{CHBr}_3$  at higher altitude. Critically, for the most part, the models are able to reproduce observed values of both gases well at  $\sim 12$ - $14$  km, within the lower TTL. Recall that the TTL is defined as the layer between the level of main convective outflow ( $\sim 200$  hPa,  $\sim 12$  km) and the tropical tropopause ( $\sim 100$  hPa,  $\sim 17$  km) (Gettelman and Forster, 2002). ~~For a given model, simulations using the non-preferred tracers (i.e. with different  $\text{CHBr}_3/\text{CH}_2\text{Br}_2$  emission inventories, not shown), generally lead to worse model-measurement agreement in the TTL. This is not surprising as model-measurement agreement at the surface is poorer in those simulations (as discussed in Section 3.1.2.)~~

Overall, given the large spatial/temporal variability in observed VLS mixing ratios, in part due to the influence of transport processes, global-scale models driven by aseasonal emissions and using parameterised **sub-grid scale** transport schemes face challenges in reproducing VLS observations  
500 in the tropical atmosphere. Yet despite this, we find that the TransCom-VLS models generally provide a very good simulation of the tropospheric abundance of  $\text{CHBr}_3$  and  $\text{CH}_2\text{Br}_2$ , particularly in the important tropical West Pacific region (e.g. SHIVA comparisons).

### 3.3 Model-observation comparisons: TTL and lower stratosphere

Figure 11 compares model profiles of  $\text{CHBr}_3$  and  $\text{CH}_2\text{Br}_2$  with high altitude measurements obtained  
505 in the TTL, extending into the tropical lower stratosphere. Across the ensemble, model-measurement agreement is varied but generally the models capture observed  $\text{CHBr}_3$  from the Pre-AVE and CR-AVE campaigns, in the Eastern Pacific, well. It should be noted that the number of observations varies significantly between these two campaigns; CR-AVE had almost twice the number of flights **than as** Pre-AVE and this is reflected in the larger variability in the observed profile, particularly in  
510 the lower TTL. For both campaigns, the models capture the observed gradients in  $\text{CHBr}_3$  and variability throughout the profiles; model-measurement correlation coefficients ( $r$ ) for all of the models are  $>0.93$  and  $>0.88$  for Pre-AVE and CR-AVE, respectively. In terms of absolute agreement, 100% of the models fall within  $\pm 1\sigma$  of the observed  $\text{CHBr}_3$  mean at the tropopause during Pre-AVE (and  $\pm 2\sigma$  for CR-AVE). For both campaigns, virtually all models are within the measured (min-max)  
515 range (not shown) around the tropopause.

During both ATTREX campaigns, larger  $\text{CHBr}_3$  mixing ratios were observed in the TTL (panels c and d of Figure 11). This reflects the location of the ATTREX campaigns compared to Pre-AVE and CR-AVE; over the tropical West Pacific, the level of main convective outflow extends deeper into the TTL compared to the East Pacific (Gettelman and Forster, 2002), allowing a larger portion of the  
520 surface  $\text{CHBr}_3$  mixing ratio to detrain at higher altitudes. Overall, model-measurement agreement of  $\text{CHBr}_3$  in the TTL is poorer during the ATTREX campaigns, with most models exhibiting a low bias between 14-16 km altitude. MOZART and UKCA simulations (which prefer the Liang  $\text{CHBr}_3$  inventory) exhibit larger mixing ratios in the TTL, though are generally consistent with other models around the tropopause. Most ( $\geq 70\%$ ) of the models reproduce  $\text{CHBr}_3$  at the tropopause to within  
525  $\pm 1\sigma$  of the observed mean and all the models are within the measured range (not shown) during both ATTREX campaigns. Model-measurement  $\text{CHBr}_3$  correlation is  $>0.8$  for each ATTREX campaign, showing that again much of the observed variability throughout the  $\text{CHBr}_3$  profiles is captured. The same is true for  $\text{CH}_2\text{Br}_2$ , with  $r > 0.84$  for all but one of the models during Pre-AVE and  $r > 0.88$  for all of the models in each of the other campaigns.

530 Overall, mean  $\text{CHBr}_3$  and  $\text{CH}_2\text{Br}_2$  mixing ratios around the tropopause, observed during the 2013/2014 ATTREX missions, are larger than the mean mixing ratios (from previous aircraft campaigns) reported in the latest WMO Ozone Assessment Report (Table 1-7 of Carpenter and Reimann

(2014)). As noted, this **likely** reflects the location at which the measurements were made; ATTREX 2013/2014 sampled in the tropical West and Central Pacific, whereas the WMO estimate is based on a compilation of measurements with a paucity in that region. From Figure 11, observed  $\text{CHBr}_3$  and  $\text{CH}_2\text{Br}_2$  at the tropopause was (on average)  $\sim 0.35$  ppt and  $\sim 0.8$  ppt, respectively, during ATTREX 2013/2014, compared to the 0.08 (0.00–0.31) ppt  $\text{CHBr}_3$  and 0.52 (0.3–0.86) ppt  $\text{CH}_2\text{Br}_2$  ranges reported by Carpenter and Reimann (2014).

### 3.4 Seasonal and zonal variations in the troposphere-to-stratosphere transport of VSLS

In this section we examine seasonal and zonal variability in the loading of  $\text{CHBr}_3$  and  $\text{CH}_2\text{Br}_2$  in the TTL and lower stratosphere, indicative of transport processes. In the tropics, a number of previous studies have shown a marked seasonality in convective outflow around the tropopause, owing to seasonal variations in convective cloud top heights (e.g. Folkins et al., 2006; Hosking et al., 2010; Bergman et al., 2012). **Such variations influence the near-tropopause abundance of brominated VSLS** (Hoyle et al., 2011; Liang et al., 2014) **and other tracers, such as CO** (Folkins et al., 2006).

Figures 12 and 13 show the simulated seasonal cycle of  $\text{CHBr}_3$  and  $\text{CH}_2\text{Br}_2$ , respectively, at the base of the TTL and the cold point tropopause (CPT).  $\text{CHBr}_3$  exhibits a pronounced seasonal cycle at the CPT, with virtually all models showing the same phase; with respect to the annual mean and integrated over the tropics,  $\text{CHBr}_3$  is most elevated during boreal winter (DJF). The amplitude of the cycle varies considerably between models, with departures from the annual mean ranging from around  $\pm 10\%$  to  $\pm 40\%$ , in a given month (panel b of Figure 12). Owing to its relatively long tropospheric lifetime, particularly in the TTL (**>1 year**) (Hossaini et al., 2010),  $\text{CH}_2\text{Br}_2$  exhibits a weak seasonal cycle at the CPT as it is less influenced by seasonal variations in transport.

Panels (c) and (d) of Figures 12 and 13, also show the modelled absolute mixing ratios of  $\text{CHBr}_3$  and  $\text{CH}_2\text{Br}_2$  at the TTL base and CPT. Annually averaged, for  $\text{CHBr}_3$ , the model spread results in a factor of  $\sim 3$  difference in simulated  $\text{CHBr}_3$  at both levels (similarly, for  $\text{CH}_2\text{Br}_2$  a factor of 1.5). The modelled mixing ratios fall within the measurement-derived range reported by Carpenter and Reimann (2014). The MMM  $\text{CHBr}_3$  mixing ratio at the TTL base is 0.51 ppt, within the 0.2–1.1 ppt measurement-derived range. At the CPT, the MMM  $\text{CHBr}_3$  mixing ratio is 0.20 ppt, also within the measured range of 0.0–0.31 ppt. On average, the models suggest a  $\sim 60\%$  gradient in  $\text{CHBr}_3$  between the TTL base and tropopause. Similarly, the annual MMM  $\text{CH}_2\text{Br}_2$  mixing ratio is 0.82 ppt at the TTL base, within the measured range of 0.6–1.2 ppt, and at the CPT is 0.73 ppt, within the measured range of 0.3–0.86 ppt. On average, the models show a  $\text{CH}_2\text{Br}_2$  gradient of 10% between the two levels. These model absolute values are annual means over the whole tropical domain. However, zonal variability in VSLS loading within the TTL is expected to be large (e.g. Aschmann et al., 2009; Liang et al., 2014), owing to inhomogeneity in the spatial distribution of convection and oceanic emissions. The Indian Ocean, the Maritime Continent (incorporating Malaysia, Indonesia, and the surrounding islands and ocean), central America, and central Africa are all convectively-active regions, shown to

experience particularly deep convective events with the potential, therefore, to rapidly loft VSLS  
570 from the surface into the TTL (e.g. Gettelman et al., 2002, 2009; Hosking et al., 2010). As previ-  
ously noted, the absolute values can vary, though generally the TransCom-VSLS models agree on  
the locations with the highest VSLS mixing ratios, as seen from the zonal  $\text{CHBr}_3$  anomalies at the  
CPT shown in Figure 14. These regions are consistent with the convective source regions discussed  
above. The largest  $\text{CHBr}_3$  mixing ratios at the CPT are predicted over the tropical West Pacific  
575 (20°S-20°N, 100°E-180°E), particularly during DJF. Integrated over the tropical domain, this signal  
exerts the largest influence on the  $\text{CHBr}_3$  seasonal cycle at the CPT. This result is consistent with  
the model intercomparison of Hoyle et al. (2011), who examined the seasonal cycle of idealised  
VSLS-like tracers around the tropopause, and reported a similar seasonality.

While meridionally, the width of elevated  $\text{CHBr}_3$  mixing ratios during DJF is similar across the  
580 models, differences during boreal summer (JJA) are apparent, particularly in the vicinity of the Asian  
Monsoon (5°N-35°N, 60°E-120°E). Note, the  $\text{CHBr}_3$  anomalies shown in Figure 14 correspond  
to departures from the mean calculated in the latitude range of  $\pm 30^\circ$ , and therefore encompass  
most of the Monsoon region. A number of studies have highlighted (i) the role of the Monsoon  
in transporting pollution from east Asia into the stratosphere (e.g. Randel et al., 2010) and (ii) its  
585 potential role in the troposphere-to-stratosphere transport of aerosol precursors, such as volcanic  
 $\text{SO}_2$  (e.g. Bourassa et al., 2012; Fromm et al., 2014). For VSLS, and other short-lived tracers, the  
Monsoon may also represent a significant pathway for transport to the stratosphere (e.g. Vogel et al.,  
2014; Orbe et al., 2015; Tissier and Legras, 2016). Here, a number of models show elevated  $\text{CHBr}_3$   
in the lower stratosphere over the Monsoon region, though the importance of the Monsoon with  
590 respect to the tropics as a whole varies substantially between the models. For example, from Figure  
14, models such as ACTM and UKCA show far greater enhancement in  $\text{CHBr}_3$  associated with  
the Monsoon during JJA, compared to others (e.g. MOZART, TOMCAT). A comparison of  $\text{CHBr}_3$   
anomalies at 100 hPa but confined to the Monsoon region, as shown in Figure 15, reveals a Monsoon  
signal in most of the models, but as noted above the strength of this signal varies considerably.

595 **The STAG model, which does not include a treatment of *deep* convection and has been shown to  
have weak ventilation through the boundary layer (Law et al., 2008), exhibits virtually no  $\text{CHBr}_3$   
enhancement over the Monsoon region.**

**The high altitude model-model differences in  $\text{CHBr}_3$ , highlighted in Figures 14 and 15, are at-  
tributed predominately to differences in the treatment of convection. Previous studies have shown  
600 that (i) convective updraft mass fluxes, including the vertical extent of deep convection (relevant for  
bromine SGI from VSLS), vary significantly depending on the implementation of convection in a  
given model (e.g. Feng et al., 2011) and (ii) that significantly different short-lived tracer distributions  
are predicted from different models using different convective parameterisations (e.g. Hoyle et al.,  
2011). Such parameterisations are often complex, relying on assumptions regarding detrainment lev-  
605 els, trigger thresholds for shallow, mid-level and/or deep convection, and vary in their approach to**

610 computing updraft (and downdraft) mass fluxes. Furthermore, the vertical transport of model tracers is also sensitive to interactions of the convective parameterisation with the boundary layer mixing scheme (also parameterised) (Rybka and Tost, 2014). On the above basis and considering that the TransCom-VSLS models implement these processes in different ways (Table 2), it was not possible to detangle transport effects within the scope of this project. However, no systematic similarities/differences between models according to input meteorology were apparent. Examining the difference between UKCA\_HI and UKCA\_LO reveals that horizontal resolution is a significant factor. The UKCA\_HI simulation shows a greater role of the Monsoon region, ~~likely due to a more faithful representation of convection (including its occurrence related to surface emissions)~~ likely due to differences in the distribution of surface emissions (e.g. along longer coastlines in the higher resolution model) with respect to the occurrence of convection ~~in higher resolution model simulations~~ as shown by Russo et al. (2015). Overall, aircraft VSLS observations within this poorly sampled region are required in order to elucidate further the role of the Monsoon in the troposphere-to-stratosphere transport of brominated VSLS.

### 620 3.5 Stratospheric source gas injection of bromine and trends

In this section we quantify the climatological SGI of bromine from  $\text{CHBr}_3$  and  $\text{CH}_2\text{Br}_2$  to the tropical LS and examine inter-annual variability. The current measurement-derived range of bromine SGI ( $[3 \times \text{CHBr}_3] + [2 \times \text{CH}_2\text{Br}_2]$  at the tropical tropopause) from these two VSLS is 1.28 (0.6-2.65) ppt Br, i.e. uncertain by a factor of  $\sim 4.5$  (Carpenter and Reimann, 2014). This uncertainty dominates the overall uncertainty on the *total* stratospheric bromine SGI range (0.7-3.4 ppt Br), which includes relatively minor contributions from other VSLS (e.g.  $\text{CHBr}_2\text{Cl}$ ,  $\text{CH}_2\text{BrCl}$  and  $\text{CHBrCl}_2$ ). Given that SGI may account for up to 76% of stratospheric  $\text{Br}_y^{\text{VSLS}}$  (Carpenter and Reimann, 2014) (note,  $\text{Br}_y^{\text{VSLS}}$  also includes the contribution of product gas injection), constraining the contribution from  $\text{CHBr}_3$  and  $\text{CH}_2\text{Br}_2$  is, therefore, desirable.

630 The TransCom-VSLS climatological MMM estimate of Br SGI from  $\text{CHBr}_3$  and  $\text{CH}_2\text{Br}_2$  is 2.0 (1.2-2.5) ppt Br, with the reported uncertainty from the model spread.  $\text{CH}_2\text{Br}_2$  accounts for  $\sim 72\%$  of this total, in good agreement with the  $\sim 80\%$  reported by Carpenter and Reimann (2014). The model spread encompasses the best estimate reported by Carpenter and Reimann (2014), though our best estimate is 0.72 ppt (57%) larger. The spread in the TransCom-VSLS models is also 37% lower than the Carpenter and Reimann (2014) range, suggesting that their measurement-derived range in bromine SGI from  $\text{CHBr}_3$  and  $\text{CH}_2\text{Br}_2$  is possibly too conservative, particularly at the lower limit (Figure 16), and from a climatological perspective. We note that (i) the TransCom-VSLS estimate is based on models, shown here, to simulate the surface to tropopause abundance of  $\text{CHBr}_3$  and  $\text{CH}_2\text{Br}_2$  well and (ii) represents a climatological estimate over the simulation period, 1995-2012.

640 The measurement-derived best estimate and range (i.e. that from Carpenter and Reimann (2014)) ~~at present~~, does not include the high altitude observations over the tropical West Pacific obtained

during the most recent NASA ATTREX missions. As noted in Section 3.3, mean  $\text{CHBr}_3$  and  $\text{CH}_2\text{Br}_2$  measured around the tropopause during ATTREX (2013/2014 missions), is at the upper end of the compilation of observed values given in the recent WMO Ozone Assessment Report (Table 1-7 of Carpenter and Reimann (2014)). Inclusion of these data would bring the WMO SGI estimate from  $\text{CHBr}_3$  and  $\text{CH}_2\text{Br}_2$  closer to the TransCom-VSLS estimate reported here. For context, the TransCom-VSLS MMM estimate of Br SGI from  $\text{CHBr}_3$  and  $\text{CH}_2\text{Br}_2$  (2.0 ppt Br) represents 10% of total stratospheric  $\text{Br}_y$  (i.e. considering long-lived sources gases also) - estimated at  $\sim 20$  ppt in 2011 (Carpenter and Reimann, 2014).

The TransCom-VSLS MMM SGI range discussed above is from  $\text{CHBr}_3$  and  $\text{CH}_2\text{Br}_2$  only. Minor VSLS, including  $\text{CHBr}_2\text{Cl}$ ,  $\text{CH}_2\text{BrCl}$ ,  $\text{CHBrCl}_2$ ,  $\text{C}_2\text{H}_5\text{Br}$ ,  $\text{C}_2\text{H}_4\text{Br}$  and  $\text{C}_3\text{H}_7\text{Br}$ , are estimated to contribute a further 0.08 to 0.71 ppt Br through SGI (Carpenter and Reimann, 2014). If we add this contribution on to our MMM estimate of bromine SGI from  $\text{CHBr}_3$  and  $\text{CH}_2\text{Br}_2$ , a reasonable estimate of 1.28 to 3.21 ppt Br is derived from our results for the total SGI range. This range is 28% smaller than the equivalent estimate of total SGI reported by Carpenter and Reimann (2014), because of the constraint on the contribution from  $\text{CHBr}_3$  and  $\text{CH}_2\text{Br}_2$ , as discussed above.

Our uncertainty estimate on simulated bromine SGI (from the model spread) reflects inter-model variability, primarily due to differences in transport, but does not account for uncertainty on the chemical factors influencing the loss rate and lifetime of VSLS (e.g. tropospheric  $[\text{OH}]$ ) - as all of the models used the same prescribed oxidants. However, Aschmann and Sinnhuber (2013) found that the stratospheric SGI of Br exhibited a low sensitivity to large perturbations to the chemical loss rate of  $\text{CHBr}_3$  and  $\text{CH}_2\text{Br}_2$ ; a  $\pm 50\%$  perturbation to the loss rate changed bromine SGI by 2% at most in their model sensitivity experiments. Furthermore, our SGI range is compatible with recent model SGI estimates that used different  $[\text{OH}]$  fields; for example, Fernandez et al. (2014) simulated a stratospheric SGI of 1.7 ppt Br from  $\text{CHBr}_3$  and  $\text{CH}_2\text{Br}_2$ .

We found no clear long-term transport-driven trend in the stratospheric SGI of bromine. Clearly, this result is limited to the study period examined and does not preclude potential future changes due to climate change, as suggested by some studies (e.g. Hossaini et al., 2012b). However, In terms of inter-annual variability, the simulated annual mean bromine SGI varied by  $\pm 5\%$  around the climatological mean (panel (b) of Figure 16) over the simulation period (small in the context of total stratospheric  $\text{Br}_y$ , see above). Naturally, this encompasses inter-annual variability of both  $\text{CHBr}_3$  and  $\text{CH}_2\text{Br}_2$  reaching the tropical LS. The latter of which is far smaller and given that  $\text{CH}_2\text{Br}_2$  is the larger contributor to SGI, dampens the overall inter-annual variability. Note, inter-annual changes in emissions,  $[\text{OH}]$  or photolysis rates were not quantified here (only transport). On a monthly basis, the amount of  $\text{CHBr}_3$  reaching the tropical LS can clearly exhibit larger variability.  $\text{CHBr}_3$  anomalies (calculated as monthly departures from the climatological monthly mean mixing ratio) at the tropical tropopause are shown in Figure 17. Also shown in Figure 17 is the Multivariate El Niño Southern Oscillation ENSO Index (MEI) - a time-series which characterises ENSO intensity based



on a range of meteorological and oceanographic components (Wolter and Timlin, 1998). See also:  
680 <http://www.esrl.noaa.gov/psd/enso/mei/>. The transport of  $\text{CHBr}_3$  (and  $\text{CH}_2\text{Br}_2$ , not shown) to the  
tropical LS is strongly correlated ( $r$  values ranging from 0.6 to 0.75 across the ensemble) to ENSO  
activity over the Eastern Pacific (owing to the influence of sea surface temperature on convection).  
For example, a clear signal of the very strong El Niño event of 1997/1998 is apparent in the models  
(i.e. with enhanced  $\text{CHBr}_3$  at the tropopause), ~~for that region~~, supporting the notion that bromine  
685 SGI is sensitive to such climate modes, *in this region* (Aschmann et al., 2011). However, *integrated*  
*when averaged* over the tropics no strong correlation between VLS loading in the LS and the MEI  
(or just sea surface temperature) was found across the ensemble. *We suggest that zonal variations in*  
*SST anomalies (and convective activity) associated with ENSO, with warming in some regions and*  
*cooling in others, has a cancelling effect on the tropical mean bromine SGI. Indeed, previous model*  
690 *studies have showed a marked zonal structure in  $\text{CHBr}_3/\text{CH}_2\text{Br}_2$  loading in the LS in strong ENSO*  
*years, with relative increases and decreases with respect to climatological averages depending on*  
*region (Aschmann et al., 2011). Further investigation, beyond the scope of this work, is needed to*  
*determine the sensitivity of total stratospheric  $\text{Br}_y^{\text{VLS}}$  (i.e. including the contribution from product*  
*gas injection), to this and other modes of climate variability.*

#### 695 4 Summary and Conclusions

Understanding the chemical and dynamical processes which influence the atmospheric loading of  
VLS in the present, and how these *processes* may change in the future, is important to understand  
the role of VLS in a *range number* of issues. In the context of the stratosphere, it is important to  
(i) determine the relevance of VLS for assessments of  $\text{O}_3$  layer recovery timescales (Yang et al.,  
700 2014), (ii) assess the full impact of proposed stratospheric geoengineering strategies (Tilmes et al.,  
2012) and (iii) accurately quantify the ozone-driven radiative forcing (RF) of climate (Hossaini et al.,  
2015a). Here we performed the first concerted multi-model intercomparison of halogenated VLS.  
The overarching objective of TransCom-VLS was to provide a reconciled model estimate of the  
SGI of bromine from  $\text{CHBr}_3$  and  $\text{CH}_2\text{Br}_2$  to the lower stratosphere and to investigate inter-model  
705 *variability differences* due to emissions and transport processes. Participating models performed sim-  
ulations over a 20-year period, using a standardised chemistry setup (prescribed oxidants/photolysis  
rates) to isolate, predominantly, transport-driven variability between models. We examined the sen-  
sitivity of results to the choice of  $\text{CHBr}_3/\text{CH}_2\text{Br}_2$  emission inventory within individual models, and  
also quantified the performance of emission inventories across the ensemble. The main findings of  
710 TransCom-VLS are summarised below.

- The TransCom-VLS models ~~are able to~~ reproduce the observed surface abundance, distribution  
and seasonal cycle of  $\text{CHBr}_3$  and  $\text{CH}_2\text{Br}_2$ , at most locations where long-term measurements are  
available, reasonably well. At most sites, (i) the simulated seasonal cycle of these VLS is not par-

ticularly sensitive to the choice of emission inventory, and (ii) the observed cycle is reproduced well simply from seasonality in the chemical loss (a notable exception is at Mace Head, Ireland). Within a given model, absolute model-measurement agreement at the surface is highly dependent on the choice of VSLs emission inventory, particularly for  $\text{CHBr}_3$  for which the global emission distribution and magnitude is somewhat poorly constrained. We find that at a number of locations, no consensus among participating models as to which emission inventory performs best can be reached.

This is due to differences in the representation /implementation of transport processes between models which can significantly influence the boundary layer abundance of short-lived tracers. This effect was also observed between model CTM variants which, other than tropospheric transport schemes, are identical. A major implication of this finding is that care must be taken when assessing the performance of emission inventories in order to constrain global VSLs emissions, based on single model studies alone. However, we also find that within the tropics - where the troposphere-to-stratosphere transport of VSLs takes place - most participating models ( $\sim 70\%$ ) achieve optimal best agreement with measured surface  $\text{CHBr}_3$  when using a bottom-up derived inventory, with the lowest  $\text{CHBr}_3$  emission flux (Ziska et al., 2013). Similarly for  $\text{CH}_2\text{Br}_2$  most (also  $\sim 70\%$ ) of the models achieve optimal agreement using the  $\text{CH}_2\text{Br}_2$  inventory with the lowest tropical emissions flux-in-the-tropics (Liang et al., 2010), though agreement is generally less sensitive to the choice of emission inventory (compared to  $\text{CHBr}_3$ ). Recent studies have questioned the effectiveness of using aircraft observations and global-scale models (i.e. the top-down approach) in order to constrain regional VSLs emissions (Russo et al., 2015). For this reason and given growing interest as to possible climate-driven changes in VSLs emissions (e.g. Hughes et al., 2012), online calculations (e.g. Lennartz et al., 2015) which (i) consider interactions between the ocean/atmosphere state (based on observed seawater concentrations) and (ii) produce seasonally-resolved sea-to-air fluxes may prove a more insightful approach, over use of prescribed emission climatologies, in future modelling work.

The TransCom-VSLs models generally agree on the locations where  $\text{CHBr}_3$  and  $\text{CH}_2\text{Br}_2$  are most elevated around the tropopause. These locations are consistent with known convectively active regions and include the Indian Ocean, the Maritime Continent and wider tropical West Pacific and the tropical Eastern Pacific, in agreement with a number of previous VSLs-focused modelling studies (e.g. Aschmann et al., 2009; Pisso et al., 2010; Hossaini et al., 2012b; Liang et al., 2014). Owing to significant inter-model differences in transport processes, both the absolute tracer amount transported to the stratosphere and the amplitude of the seasonal cycle varies among models. However, of the above regions, the tropical West Pacific is the most important in all of the models (regardless of the emission inventory), due to rapid vertical ascent of VSLs simulated during boreal winter. In the free troposphere, the models were able to reproduce observed  $\text{CHBr}_3$  and  $\text{CH}_2\text{Br}_2$  from the recent SHIVA and CAST campaigns in this region to within  $\leq 16\%$  and  $\leq 32\%$ , respectively. However, at higher altitudes in the TTL the models generally (i) underestimated  $\text{CHBr}_3$  between 14-16 km observed during the 2014 NASA ATTREX mission in this region but (ii) fell within  $\pm 1 \sigma$  of

the observed mean around the tropical tropopause ( $\sim 17$  km). Generally good agreement was also obtained to high altitude aircraft measurements of VSLS around the tropopause in the Eastern Pacific. During boreal summer, most models show elevated  $\text{CHBr}_3$  around the tropopause above the Asian Monsoon region. However, the strength of this signal varies considerably among the models with a spread that encompasses virtually no  $\text{CHBr}_3$  enhancement over the Monsoon region to strong (85%)  $\text{CHBr}_3$  enhancements at the tropopause, with respect to the zonal average. Measurements of VSLS in the poorly sampled Monsoon region from the upcoming StratoClim campaign (<http://www.stratoclim.org/>) will prove useful in determining the importance of this region for the troposphere-to-stratosphere transport of VSLS.

760– Climatologically, we estimate that  $\text{CHBr}_3$  and  $\text{CH}_2\text{Br}_2$  contribute 2.0 (1.2-2.5) ppt Br to the lower stratosphere through SGI, with the reported uncertainty due to the model spread. The TransCom-VSLS best estimate of 2.0 ppt Br is (i)  $\sim 57\%$  larger than the measurement-derived best estimate of 1.28 ppt Br reported by Carpenter and Reimann (2014), and (ii) the TransCom-VSLS range (1.2-2.5 ppt Br) is  $\sim 37\%$  smaller than the 0.6-2.65 ppt Br range reported by Carpenter and Reimann (2014).  
765 From this we suggest that, climatologically, the Carpenter and Reimann (2014) measurement-derived SGI range, based on a limited number of aircraft observations (with a particular paucity in the tropical West Pacific), is potentially too conservative at the lower limit. Although we acknowledge that ~~(i) our uncertainty estimate (the model spread) accounts for uncertainty within the constraints of the TransCom experimental design and therefore~~ (ii) does not account for a number of intrinsic uncertainties within global models, for example, tropospheric  $[\text{OH}]$  (as the participating models used the same set of prescribed oxidants). No significant transport-driven trend in stratospheric bromine SGI was found over the simulation period, though inter-annual variability was of the order of  $\pm 5\%$ . Loading of both  $\text{CHBr}_3$  and  $\text{CH}_2\text{Br}_2$  around the tropopause over the East Pacific is strongly coupled to ENSO activity but no strong correlation to ENSO or sea surface temperature was found when  
775 averaged across the wider tropical domain.

Overall, results from the TransCom-VSLS model intercomparison support the large body of evidence that natural VSLS contribute significantly to stratospheric bromine. Given suggestions that VSLS emissions from the growing aquaculture sector will likely increase in the future (WMO, 2014; Phang et al., 2015) and that climate-driven changes to ocean emissions (Tegtmeier et al., 2015), tropospheric transport and/or oxidising capacity (Dessens et al., 2009; Hossaini et al., 2012a) could lead to an increased increase in the stratospheric loading of VSLS, it is paramount to constrain the present day  $\text{Br}_y^{\text{VSLS}}$  contribution to allow any possible future trends to be distinguished determined. In addition to SGI, this will require constraint on the stratospheric product gas injection of bromine which conceptually presents a number of challenges for global models given its inherent complexity.

785 *Acknowledgements.* RH thanks M. Chipperfield for comments and the Natural Environment Research Council (NERC) for funding through the TropHAL project (NE/J02449X/1). PKP was supported by JSPS/MEXT

KAKENHI-A (grant 22241008). GK, B-MS and PK acknowledge funding by the Deutsche Forschungsgemeinschaft (DFG) through the Research Unit SHARP (SI 1400/1-2 and PF 384/9-1 and in addition through grant PF 384/12-1) and by the Helmholtz Association through the Research Programme ATMO. NRPH and JAP ac-  
790 knowledge support of this work through the ERC ACCI project (project no. 267760), and by NERC through grant nos. NE/J006246/1 and NE/F1016012/1. NRPH was supported by a NERC Advanced Research Fellowship (NE/G014655/1). PTG was also support through ERC ACCI. Contribution of JA and R Hommel has been funded in part by the DFG Research Unit 1095 SHARP, and by the German Ministry of Education and Research (BMBF) within the project ROMIC-ROSA (grant 01LG1212A).

795 **References**

- Andrews, S. J., Carpenter, L. J., Apel, E. C., Atlas, E., Donets, V., Hopkins, J. F., Hornbrook, R. S., Lewis, A. C., Lidster, R. T., Lueb, R., Minaeian, J., Navarro, M., Punjabi, S., Riemer, D., and Schauffler, S.: A comparison of very short-lived halocarbon (VSLS) and DMS aircraft measurements in the Tropical West Pacific from CAST, ATTREX and CONTRAST, *Atmos. Meas. Tech. Discuss.*, doi:10.5194/amt-2016-94, in review, 2016.
- 800
- Arakawa, A. and Shubert, W. H.: Interaction of a cumulus ensemble with the large-scale environment, Part I, *J. Atmos. Sci.*, 31, 674–704, 1974.**
- Archer, S. D., Goldson, L. E., Liddicoat, M. I., Cummings, D. G., and Nightingale, P. D.: Marked seasonality in the concentrations and sea-to-air flux of volatile iodocarbon compounds in the western English Channel, *J. Geophys. Res.*, 112, C08009, doi:10.1029/2006JC003963, 2007.
- 805
- Aschmann, J. and Sinnhuber, B.-M.: Contribution of very short-lived substances to stratospheric bromine loading: uncertainties and constraints, *Atmos. Chem. Phys.*, 13, 1203–1219, doi:10.5194/acp-13-1203-2013, 2013.
- 810
- Aschmann, J., Sinnhuber, B.-M., Atlas, E. L., and Schauffler, S. M.: Modeling the transport of very short-lived substances into the tropical upper troposphere and lower stratosphere, *Atmos. Chem. Phys.*, 9, 9237–9247, 2009.
- Aschmann, J., Sinnhuber, B.-M., Chipperfield, M. P., and Hossaini, R.: Impact of deep convection and dehydration on bromine loading in the upper troposphere and lower stratosphere, *Atmos. Chem. Phys.*, 11, 2671–2687, doi:10.5194/acp-11-2671-2011, 2011.
- 815
- Aschmann, J., Burrows, J. P., Gebhardt, C., Rozanov, A., Hommel, R., Weber, M., and Thompson, A. M.: On the hiatus in the acceleration of tropical upwelling since the beginning of the 21st century, *Atmos. Chem. Phys.*, 14, 12803–12814, doi:10.5194/acp-14-12803-2014, 2014.
- Ashfold, M. J., Harris, N. R. P., Manning, A. J., Robinson, A. D., Warwick, N. J., and Pyle, J. A.: Estimates of tropical bromoform emissions using an inversion method, *Atmos. Chem. Phys.*, 14, 979–994, doi:10.5194/acp-14-979-2014, 2014.
- 820
- Belikov, D., Maksyutov, S., Miyasaka, T., Saeki, T., Zhuravlev, R., and Kiryushov, B.: Mass-conserving tracer transport modelling on a reduced latitude-longitude grid with NIES-TM, *Geosci. Model Dev.*, 4, 207–222, doi:10.5194/gmd-4-207-2011, 2011.
- 825
- Belikov, D. A., Maksyutov, S., Sherlock, V., Aoki, S., Deutscher, N. M., Dohe, S., Griffith, D., Kyro, E., Morino, I., Nakazawa, T., Notholt, J., Rettinger, M., Schneider, M., Sussmann, R., Toon, G. C., Wennberg, P. O., and Wunch, D.: Simulations of column-averaged CO<sub>2</sub> and CH<sub>4</sub> using the NIES TM with a hybrid sigma- $\theta$  vertical coordinate, *Atmos. Chem. Phys.*, 13, 1713–1732, doi:10.5194/acp-13-1713-2013, 2013.
- 830
- Bergman, J. W., Jensen, E. J., Pfister, L., and Yang, Q.: Seasonal differences of vertical-transport efficiency in the tropical tropopause layer: On the interplay between tropical deep convection, large-scale vertical ascent, and horizontal circulations, *J. Geophys. Res.*, 117, D05302, doi:10.1029/2011JD016992, 2012.

- Bourassa, A. E., Robock, A., Randel, W. J., Deshler, T., Rieger, L. A., Lloyd, N. D., Llewellyn, E. J. T., and Degenstein, D. A.: Large volcanic aerosol load in the stratosphere linked to asian monsoon transport, *Science*, 337, 78–81, doi:10.1126/science.1219371, 2012.
- 835
- Brinckmann, S., Engel, A., Bönisch, H., Quack, B., and Atlas, E.: Short-lived brominated hydrocarbons – observations in the source regions and the tropical tropopause layer, *Atmos. Chem. Phys.*, 12, 1213–1228, doi:10.5194/acp-12-1213-2012, 2012.
- Carpenter, L. and Liss, P.: On temperate sources of bromoform and other reactive organic bromine gases, *J. Geophys. Res.*, 105, 20 539–20 547, doi:10.1029/2000JD900242, 2000.
- 840
- Carpenter, L., Wevill, D., O’Doherty, S., Spain, G., and Simmonds, P.: Atmospheric bromoform at Mace Head, Ireland: seasonality and evidence for a peatland source, *Atmos. Chem. Phys.*, 5, 2927–2934, 2005.
- Carpenter, L. J., Reimann, S., Burkholder, J. B., Clerbaux, C., Hall, B. D., Hossaini, R., Laube, J. C., and Yvon-Lewis, S. A.: Ozone-Depleting Substances (ODSs) and Other Gases of Interest to the Montreal Protocol, in: Scientific Assessment of Ozone Depletion: 2014, Global Ozone Research and Monitoring Project, Report No. 55, Chapt. 1, World Meteorological Organization, Geneva, 2014.
- 845
- Chipperfield, M. P.: New version of the TOMCAT/SLIMCAT off-line chemical transport model: intercomparison of stratospheric tracer experiments, *Q. J. Roy. Meteor. Soc.*, 132, 1179–1203, doi:10.1256/qj.05.51, 2006.
- 850
- Chipperfield, M.: Nitrous oxide delays ozone recovery, *Nat. Geosci.*, 2, 742–743, doi:10.1038/ngeo678, 2009.
- Denning, A. S., Holzer, M., Gurney, K. R., Heimann, M., Law, R. M., Rayner, P. J., Fung, I. Y., Fan, S.-M., Taguchi, S., Freidlingstein, P., Balkanski, Y., Taylor, J., Maiss, M., and Levin, I.: Three-dimensional transport and concentration of SF<sub>6</sub>: A model intercomparison study (TransCom 2), *Tellus*, 51B, 266–297, 1999.
- Dessens, O., Zeng, G., Warwick, N., and Pyle, J.: Short-lived bromine compounds in the lower stratosphere; impact of climate change on ozone, *Atmos. Sci. Lett.*, 10, 201–206, doi:10.1002/asl.236, 2009.
- 855
- Dorf, M., Butz, A., Camy-Peyret, C., Chipperfield, M. P., Kritten, L., and Pfeilsticker, K.: Bromine in the tropical troposphere and stratosphere as derived from balloon-borne BrO observations, *Atmos. Chem. Phys.*, 8, 7265–7271, 2008.
- Emmons, L. K., Walters, S., Hess, P. G., Lamarque, J.-F., Pfister, G. G., Fillmore, D., Granier, C., Guenther, A., Kinnison, D., Laepple, T., Orlando, J., Tie, X., Tyndall, G., Wiedinmyer, C., Baughcum, S. L., and Kloster, S.: Description and evaluation of the Model for Ozone and Related chemical Tracers, version 4 (MOZART-4), *Geosci. Model Dev.*, 3, 43–67, doi:10.5194/gmd-3-43-2010, 2010.
- 860
- Feng, W., Chipperfield, M. P., Dorf, M., Pfeilsticker, K., and Ricaud, P.: Mid-latitude ozone changes: studies with a 3-D CTM forced by ERA-40 analyses, *Atmos. Chem. Phys.*, 7, 2357–2369, 2007.
- 865
- Feng, W., Chipperfield, M. P., Dhomse, S., Monge-Sanz, B. M., Yang, X., Zhang, K., and Ramonet, M.: Evaluation of cloud convection and tracer transport in a three-dimensional chemical transport model, *Atmos. Chem. Phys.*, 11, 5783–5803, doi:10.5194/acp-11-5783-2011, 2011.
- Fernandez, R. P., Salawitch, R. J., Kinnison, D. E., Lamarque, J.-F., and Saiz-Lopez, A.: Bromine partitioning in the tropical tropopause layer: implications for stratospheric injection, *Atmos. Chem. Phys.*, 14, 13 391–13 410, doi:10.5194/acp-14-13391-2014, 2014.
- 870

- Folkens, I., Bernath, P., Boone, C., Lesins, G., Livesey, N., Thompson, A. M., Walker, K., and Witte, J. C.: Seasonal cycles of O<sub>3</sub>, CO, and convective outflow at the tropical tropopause, *Geophys. Res. Lett.*, 33, doi:10.1029/2006GL026602, 2006.
- Forster, P. M. and Shine, K. P.: Radiative forcing and temperature trends from stratospheric ozone changes, *J. Geophys. Res.*, 102, 10841-10855, doi:10.1029/96JD03510, 1997.
- 875 Fromm, M., Kablick, G., Nedoluha, G., Carboni, E., Grainger, R., Campbell, J., and Lewis, J.: Correcting the record of volcanic stratospheric aerosol impact: Nabro and Sarychev Peak, *J. Geophys. Res.*, 119, 10,343–10,364, doi:10.1002/2014JD021507, 2014.
- Fuhlbrügge, S., Krüger, K., Quack, B., Atlas, E., Hepach, H., and Ziska, F.: Impact of the marine atmospheric boundary layer conditions on VLS abundances in the eastern tropical and subtropical North Atlantic Ocean, *Atmos. Chem. Phys.*, 13, 6345–6357, doi:10.5194/acp-13-6345-2013, 2013.
- 880 Fuhlbrügge, S., Quack, B., Tegtmeier, S., Atlas, E., Hepach, H., Shi, Q., Raimund, S., and Krüger, K.: The contribution of oceanic halocarbons to marine and free troposphere air over the tropical West Pacific, *Atmos. Chem. Phys. Discuss.*, 15, 17 887–17 943, doi:10.5194/acpd-15-17887-2015, 2015.
- 885 **Gregory, D. and Rowntree, P. R.: A mass flux convection scheme with representation of cloud ensemble characteristics and stability-dependent closure, *Mon. Weather Rev.*, 118, 1483–1506, 1990.**
- Gottelman, A. and Forster, P. M.: A Climatology of the Tropical Tropopause Layer, *J. Meteor. Soc. Japan.*, 80, 911–924, 2002.
- 890 Gottelman, A., Seidel, D. J., Wheeler, M. C., and Ross, R. J.: Multidecadal trends in tropical convective available potential energy, *J. Geophys. Res.*, 107, 4606, doi:10.1029/2001JD001082, 2002.
- Gottelman, A., Lauritzen, P. H., Park, M., and Kay, J. E.: Processes regulating short-lived species in the tropical tropopause layer, *J. Geophys. Res.*, 114, doi:10.1029/2009JD011785, 2009.
- 895 **Hack, J. J.: Parameterization of moist convection in the NCAR community climate model (CCM2), *J. Geophys. Res.*, 99, 5551—5568, 1994.**
- Harada, Y., Kamahori, H., Kobayashi, C., Endo, H., Kobayashi, S., Ota, Y., Onoda, H., Onogi, K., Miyaoka, K., and Takahashi, K.: The JRA-55 Reanalysis: Representation of atmospheric circulation and climate variability, *J. Meteor. Soc. Japan*, in press, 2015.**
- 900 **Holtlag, A. and Boville, B.: Local versus nonlocal boundary-layer diffusion in a global climate model, *Journal of Climate*, 6, 1825–1842, 1993.**
- Hosking, J. S., Russo, M. R., Braesicke, P., and Pyle, J. A.: Modelling deep convection and its impacts on the tropical tropopause layer, *Atmos. Chem. Phys.*, 10, 11 175–11 188, doi:10.5194/acp-10-11175-2010, 2010.
- 905 Hossaini, R., Chipperfield, M. P., Monge-Sanz, B. M., Richards, N. A. D., Atlas, E., and Blake, D. R.: Bromoform and dibromomethane in the tropics: a 3-D model study of chemistry and transport, *Atmos. Chem. Phys.*, 10, 719–735, doi:10.5194/acp-10-719-2010, 2010.
- Hossaini, R., Chipperfield, M. P., Dhomse, S., Ordonez, C., Saiz-Lopez, A., Abraham, N. L., Archibald, A., Braesicke, P., Telford, P., Warwick, N., Yang, X., and Pyle, J.: Modelling future changes to
- 910

- the stratospheric source gas injection of biogenic bromocarbons, *Geophys. Res. Lett.*, 39, L20813, doi:10.1029/2012GL053401, 2012a.
- Hossaini, R., Chipperfield, M. P., Feng, W., Breider, T. J., Atlas, E., Montzka, S. A., Miller, B. R., Moore, F., and Elkins, J.: The contribution of natural and anthropogenic very short-lived species to stratospheric bromine, *Atmos. Chem. Phys.*, 12, 371–380, doi:10.5194/acp-12-371-2012, 2012b.
- Hossaini, R., Mantle, H., Chipperfield, M. P., Montzka, S. A., Hamer, P., Ziska, F., Quack, B., Krüger, K., Tegtmeier, S., Atlas, E., Sala, S., Engel, A., Bönisch, H., Keber, T., Oram, D., Mills, G., Ordóñez, C., Saiz-Lopez, A., Warwick, N., Liang, Q., Feng, W., Moore, F., Miller, B. R., Marécal, V., Richards, N. A. D., Dorf, M., and Pfeilsticker, K.: Evaluating global emission inventories of biogenic bromocarbons, *Atmos. Chem. Phys.*, 13, 11 819–11 838, doi:10.5194/acp-13-11819-2013, 2013.
- Hossaini, R., Chipperfield, M. P., Montzka, S. A., Rap, A., Dhomse, S., and Feng, W.: Efficiency of short-lived halogens at influencing climate through depletion of stratospheric ozone, *Nat. Geosci.*, 8, 186–190, doi:10.1038/ngeo2363, 2015a.
- Hossaini, R., Chipperfield, M. P., Saiz-Lopez, A., Harrison, J. J., von Glasow, R., Sommariva, R., Atlas, E., Navarro, M., Montzka, S. A., Feng, W., Dhomse, S., Harth, C., Mühle, J., Lunder, C., O’Doherty, S., Young, D., Reimann, S., Vollmer, M. K., Krummel, P. B., and Bernath, P. F.: Growth in stratospheric chlorine from short-lived chemicals not controlled by the Montreal Protocol, *Geophys. Res. Lett.*, 42, 4573–4580, doi:10.1002/2015GL063783, 2015b.
- Hoyle, C. R., Marecal, V., Russo, M. R., Allen, G., Arteta, J., Chemel, C., Chipperfield, M. P., D’Amato, F., Dessens, O., Feng, W., Hamilton, J. F., Harris, N. R. P., Hosking, J. S., Lewis, A. C., Morgenstern, O., Peter, T., Pyle, J. A., Reddman, T., Richards, N. A. D., Telford, P. J., Tian, W., Viciani, S., Volz-Thomas, A., Wild, O., Yang, X., and Zeng, G.: Representation of tropical deep convection in atmospheric models - Part 2: Tracer transport, *Atmos. Chem. Phys.*, 11, 8103–8131, doi:10.5194/acp-11-8103-2011, 2011.
- Hughes, C., Johnson, M., von Glasow, R., Chance, R., Atkinson, H., Souster, T., Lee, G. A., Clarke, A., Meredith, M., Venables, H. J., Turner, S. M., Malin, G., and Liss, P. S.: Climate-induced change in biogenic bromine emissions from the Antarctic marine biosphere, *Global Biogeochem. Cycles*, 26, GB3019, doi:10.1029/2012GB004295, 2012.
- Jöckel, P., Tost, H., Pozzer, A., Brühl, C., Buchholz, J., Ganzeveld, L., Hoor, P., Kerkweg, A., Lawrence, M. G., Sander, R., Steil, B., Stiller, G., Tanarhte, M., Taraborrelli, D., van Aardenne, J., and Lelieveld, J.: The atmospheric chemistry general circulation model ECHAM5/MESSy1: consistent simulation of ozone from the surface to the mesosphere, *Atmos. Chem. Phys.*, 6, 5067–5104, doi:10.5194/acp-6-5067-2006, 2006.
- Jöckel, P., Kerkweg, A., Pozzer, A., Sander, R., Tost, H., Riede, H., Baumgaertner, A., Gromov, S., and Kern, B.: Development cycle 2 of the Modular Earth Submodel System (MESSy2), *Geosci. Model Dev.*, 3, 717–752, doi:10.5194/gmd-3-717-2010, 2010.
- Krüger, K. and Quack, B.: Introduction to special issue: the TransBrom Sonne expedition in the tropical West Pacific, *Atmos. Chem. Phys.*, 13, 9439–9446, doi:10.5194/acp-13-9439-2013, 2013.
- Lacis, A. A., Wuebbles, D. J., and Logan, J. A.: Radiative forcing of climate by changes in the vertical distribution of ozone, *J. Geophys. Res.*, 95, 9971–9981, doi:10.1029/JD095iD07p09971, 1990.



- Laube, J. C., Engel, A., Boenisch, H., Moebius, T., Worton, D. R., Sturges, W. T., Grunow, K., and Schmidt,  
950 U.: Contribution of very short-lived organic substances to stratospheric chlorine and bromine in the tropics -  
a case study, *Atmos. Chem. Phys.*, 8, 7325–7334, 2008.
- Law, R. M., Rayner, P. J., Denning, A. S., Erickson, D., Fung, I. Y., Heimann, M., Piper, S. C., Ramonet,  
M., Taguchi, S., Taylor, J. A., Trudinger, C. M., and Watterson, I. G.: Variations in modelled atmospheric  
transport of carbon dioxide and the consequences for CO<sub>2</sub> inversions, *Global Biogeochem. Cy.*, 10, 783–796,  
955 1996.
- Law, R. M., Peters, W., Rödenbeck, C., Aulagnier, C., Baker, I., Bergmann, D. J., Bousquet, P., Brandt, J., Bruh-  
wiler, L., Cameron-Smith, P. J., Christensen, J. H., Delage, F., Denning, A. S., Fan, S., Geels, C., Houweling,  
S., Imasu, R., Karstens, U., Kawa, S. R., Kleist, J., Krol, M. C., Lin, S. J., Lokupitiya, R., Maki, T., Maksyu-  
tov, S., Niwa, Y., Onishi, R., Parazoo, N., Patra, P. K., Pieterse, G., Rivier, L., Satoh, M., Serrar, S., Taguchi,  
960 S., Takigawa, M., Vautard, R., Vermeulen, A. T., and Zhu, Z.: TransCom model simulations of hourly at-  
mospheric CO<sub>2</sub>: Experimental overview and diurnal cycle results for 2002, *Global Biogeochem. Cy.*, 22,  
GB3009, doi:10.1029/2007gb003050, 2008.
- Leedham, E. C., Hughes, C., Keng, F. S. L., Phang, S.-M., Malin, G., and Sturges, W. T.: Emission of atmo-  
spherically significant halocarbons by naturally occurring and farmed tropical macroalgae, *Biogeosciences*,  
965 10, 3615–3633, doi:10.5194/bg-10-3615-2013, 2013.
- Lennartz, S. T., Krysztofiak, G., Marandino, C. A., Sinnhuber, B.-M., Tegtmeier, S., Ziska, F., Hossaini, R.,  
Krüger, K., Montzka, S. A., Atlas, E., Oram, D. E., Keber, T., Bönnisch, H., and Quack, B.: Modelling marine  
emissions and atmospheric distributions of halocarbons and dimethyl sulfide: the influence of prescribed  
water concentration vs. prescribed emissions, *Atmos. Chem. Phys.*, 15, 11753-11772, doi:10.5194/acp-15-  
970 11753-2015, 2015.
- Levine, J. G., Braesicke, P., Harris, N. R. P., Savage, N. H., and Pyle, J. A.: Pathways and timescales for  
troposphere-to-stratosphere transport via the tropical tropopause layer and their relevance for very short  
lived substances, *J. Geophys. Res.*, 112, doi:10.1029/2005JD006940, 2007.
- Liang, Q., Atlas, E., Blake, D., Dorf, M., Pfeilsticker, K., and Schauffler, S.: Convective trans-  
975 port of very short lived bromocarbons to the stratosphere, *Atmos. Chem. Phys.*, 14, 5781–5792,  
doi:10.5194/acp-14-5781-2014, 2014.
- Liang, Q., Stolarski, R. S., Kawa, S. R., Nielsen, J. E., Douglass, A. R., Rodriguez, J. M., Blake, D. R., Atlas,  
E. L., and Ott, L. E.: Finding the missing stratospheric Br<sub>y</sub>: a global modeling study of CHBr<sub>3</sub> and CH<sub>2</sub>Br<sub>2</sub>,  
*Atmos. Chem. Phys.*, 10, 2269–2286, 2010.
- 980 Lock, A., Brown, A., Bush, M., Martin, G., and Smith, R.: A new boundary layer mixing scheme. Part I: Scheme  
description and single-column model tests, *Mon. Weather Rev.*, 128, 3187–3199, 2000.
- Mellor, G. L. and Yamada, A.: A hierarchy of turbulence closure models for planetary boundary layers, *J.*  
*Atmos. Sci.*, 31, 1791– 1806, 1974.
- 985 Montzka, S. A., Krol, M., Dlugokencky, E., Hall, B., Jöckel, P., and Lelieveld, J.: Small Interannual Variability  
of Global Atmospheric Hydroxyl, *Science*, 331, 67–69, doi:10.1126/science.1197640, 2011.

- Morgenstern, O., Braesicke, P., O'Connor, F. M., Bushell, A. C., Johnson, C. E., Osprey, S. M., and Pyle, J. A.: Evaluation of the new UKCA climate-composition model - Part 1: The stratosphere, *Geosci. Model Dev.*, 2, 43–57, doi:10.5194/gmd-2-43-2009, 2009.
- 990 Nightingale, P. D., Malin, G., Law, C. S., Watson, A. J., Liss, P. S., Liddicoat, M. I., Boutin, J., and Upstill-Goddard, R. C.: In situ evaluation of air-sea gas exchange parameterizations using novel conservative and volatile tracers, *Glob. Biogeochem. Cy.*, 14, 373–387, 2000.
- Nordeng, T. E.: Extended versions of the convective parametrization scheme at ECMWF and their impact on the mean and transient activity of the model in the tropics. Technical Memorandum 206, ECMWF Research Department, European Centre for Medium Range Weather Forecasts, Reading, UK, 1994.
- 995 Nordeng, T. E.: Extended versions of the convective parametrization scheme at ECMWF and their impact on the mean and transient activity of the model in the tropics. Technical Memorandum 206, ECMWF Research Department, European Centre for Medium Range Weather Forecasts, Reading, UK, 1994.
- Orbe, C., Waugh, D. W., and Newman, P. A.: Air-mass origin in the tropical lower stratosphere: The influence of Asian boundary layer air, *Geophys. Res. Lett.*, 42, 4240–4248, doi:10.1002/2015GL063937, 2015.
- Ordóñez, C., Lamarque, J.-F., Tilmes, S., Kinnison, D. E., Atlas, E. L., Blake, D. R., Santos, G. S., Brasseur, G., and Saiz-Lopez, A.: Bromine and iodine chemistry in a global chemistry-climate model: description and evaluation of very short-lived oceanic sources, *Atmos. Chem. Phys.*, 12, 1423–1447, doi:10.5194/acp-12-1423-2012, 2012.
- 1000 Orlikowska, A. and Schulz-Bull, D.: Seasonal variations of volatile organic compounds in the coastal Baltic Sea, *Envir. Chem.*, 6, doi:10.1071/EN09107, 2009.
- 1005 Patra, P. K., Law, R. M., Peters, W., Rodenbeck, C., Takigawa, M., Aulagnier, C., Baker, I., Bergmann, D. J., Bousquet, P., Brandt, J., Bruhwiler, L., Cameron-Smith, P. J., Christensen, J. H., Delage, F., Denning, A. S., Fan, S., Geels, C., Houweling, S., Imasu, R., Karstens, U., Kawa, S. R., Kleist, J., Krol, M. C., Lin, S.-J., Lokupitiya, R., Maki, T., Maksyutov, S., Niwa, Y., Onishi, R., Parazoo, N., Pieterse, G., Rivier, L., Satoh, M., Serrar, S., Taguchi, S., Vautard, R., Vermeulen, A. T., and Zhu, Z.: TransCom model simulations of hourly atmospheric CO<sub>2</sub>: analysis of synoptic-scale variations for the period 2002–2003, *Global Biogeochem. Cy.*, 22, GB4013, doi:10.1029/2007GB003081, 2008.
- 1010 Patra, P. K., Takigawa, M., Dutton, G. S., Uhse, K., Ishijima, K., Lintner, B. R., Miyazaki, K., and Elkins, J. W.: Transport mechanisms for synoptic, seasonal and interannual SF<sub>6</sub> variations and "age" of air in troposphere, *Atmos. Chem. Phys.*, 9, 1209–1225, doi:10.5194/acp-9-1209-2009, 2009.
- 1015 Patra, P. K., Houweling, S., Krol, M., Bousquet, P., Belikov, D., Bergmann, D., Bian, H., Cameron-Smith, P., Chipperfield, M. P., Corbin, K., Fortems-Cheiney, A., Fraser, A., Gloor, E., Hess, P., Ito, A., Kawa, S. R., Law, R. M., Loh, Z., Maksyutov, S., Meng, L., Palmer, P. I., Prinn, R. G., Rigby, M., Saito, R., and Wilson, C.: TransCom model simulations of CH<sub>4</sub> and related species: linking transport, surface flux and chemical loss with CH<sub>4</sub> variability in the troposphere and lower stratosphere, *Atmos. Chem. Phys.*, 11, 12 813–12 837, doi:10.5194/acp-11-12813-2011, 2011.
- 1020 Phang, S.-M., Keng, F.S.-L., Paramjeet-Kaur, M. S., Lim, Y.-K., Rahman, N. A., Leedham, E. C., Robinson, A. D., Harris, N. R. P., Pyle, J. A., and Sturges, W. T.: Can seaweed farming in the tropics contribute to climate change through emissions of short-lived halocarbons, *Malaysian Journal of Science*, 34, 8–19, 2015.

- 1025 Pfeilsticker, K., Sturges, W. T., Bösch, H., Camy-Peyret, C., Chipperfield, M. P., Engel, A., Fitzenberger, R., Müller, M., Payan, S., and Sinnhuber, B.-M.: Lower stratospheric organic and inorganic bromine budget for the Arctic winter 1998/99, *Geophys. Res. Lett.*, 27, 20, 3305-3308, 2000.
- Pisso, I., Haynes, P. H., and Law, K. S.: Emission location dependent ozone depletion potentials for very short-lived halogenated species, *Atmos. Chem. Phys.*, 10, 12 025–12 036, doi:10.5194/acp-10-12025-2010, 2010.
- 1030 Pyle, J. A., Ashfold, M. J., Harris, N. R. P., Robinson, A. D., Warwick, N. J., Carver, G. D., Gostlow, B., O'Brien, L. M., Manning, A. J., Phang, S. M., Yong, S. E., Leong, K. P., Ung, E. H., and Ong, S.: Bromoform in the tropical boundary layer of the Maritime Continent during OP3, *Atmos. Chem. Phys.*, 11, 529–542, doi:10.5194/acp-11-529-2011, 2011.
- Quack, B. and Wallace, D.: Air-sea flux of bromoform: Controls, rates, and implications, *Global Biogeochem. Cycles*, 17, doi:10.1029/2002GB001890, 2003.
- 1035 Randel, W. J., Park, M., Emmons, L., Kinnison, D., Bernath, P., Walker, K. A., Boone, C., and Pumphrey, H.: Asian Monsoon Transport of Pollution to the Stratosphere, *Science*, 328, 611–613, doi:10.1126/science.1182274, 2010.
- Riese, M., Ploeger, F., Rap, A., Vogel, B., Konopka, P., Dameris, M., and Forster, P.: Impact of uncertainties in atmospheric mixing on simulated UTLS composition and related radiative effects, *J. Geophys. Res.*, 117, D16305, doi:10.1029/2012JD017751, 2012.
- 1040 Robinson, A. D., Harris, N. R. P., Ashfold, M. J., Gostlow, B., Warwick, N. J., O'Brien, L. M., Beardmore, E. J., Nadzir, M. S. M., Phang, S. M., Samah, A. A., Ong, S., Ung, H. E., Peng, L. K., Yong, S. E., Mohamad, M., and Pyle, J. A.: Long-term halocarbon observations from a coastal and an inland site in Sabah, Malaysian Borneo, *Atmos. Chem. Phys.*, 14, 8369–8388, doi:10.5194/acp-14-8369-2014, 2014.
- 1045 Roeckner, E., Brokopf, R., Esch, M., Giorgetta, M., Hagemann, S., Kornbluh, L., Manzini, E., Schlese, U., and Schulzweida, U.: Sensitivity of simulated climate to horizontal and vertical resolution in the ECHAM5 atmosphere model, *J. Climate*, 19, 3771–3791, doi:10.1175/JCLI3824.1, 2006.
- Russo, M. R., Ashfold, M. J., Harris, N. R. P., and Pyle, J. A.: On the emissions and transport of bromoform: sensitivity to model resolution and emission location, *Atmos. Chem. Phys.*, 15, 14031–14040, doi:10.5194/acp-15-14031-2015, 2015.
- 1050 Rybka, H. and Tost, H.: Uncertainties in future climate predictions due to convection parameterisations, *Atmos. Chem. Phys.*, 14, 5561–5576, doi:10.5194/acp-14-5561-2014, 2014.
- Sala, S., Bönisch, H., Keber, T., Oram, D. E., Mills, G., and Engel, A.: Deriving an atmospheric budget of total organic bromine using airborne in situ measurements from the western Pacific area during SHIVA, *Atmospheric Chemistry and Physics*, 14, 6903–6923, doi:10.5194/acp-14-6903-2014, 2014.
- 1055 Salawitch, R., Weisenstein, D., Kovalenko, L., Sioris, C., Wennberg, P., Chance, K., Ko, M., and McLinden, C.: Sensitivity of ozone to bromine in the lower stratosphere, *Geophys. Res. Lett.*, 32, L05811, doi:10.1029/2004GL021504, 2005.
- 1060 Sander, S., Friedl, R., Barker, J., Golden, D., Kurylo, M., Wine, P., Abbatt, J., Burkholder, J., Kolb, C., Moortgat, G., Huie, R., and Orkin, V.: *Chemical Kinetics and Photochemical Data for Use in Atmospheric Studies*, Evaluation Number 17, JPL Publication 10-6, Jet Propulsion Laboratory, 2011.
- Sinnhuber, B.-M. and Meul, S.: Simulating the impact of emissions of brominated very short lived substances on past stratospheric ozone trends, *Geophys. Res. Lett.*, 42, 2449–2456, doi:10.1002/2014GL062975, 2015.

- 1065 Sinnhuber, B.-M., Sheode, N., Sinnhuber, M., Chipperfield, M. P., and Feng, W.: The contribution of anthropogenic bromine emissions to past stratospheric ozone trends: a modelling study, *Atmos. Chem. Phys.*, 9, 2863–2871, 2009.
- Stemmler, I., Hense, I., and Quack, B.: Marine sources of bromoform in the global open ocean – global patterns and emissions, *Biogeosciences*, 12, 1967–1981, doi:10.5194/bg-12-1967-2015, 2015.
- 1070 Sturges, W., Oram, D., Carpenter, L., Penkett, S., and Engel, A.: Bromoform as a source of stratospheric bromine, *Geophys. Res. Lett.*, 27, 2081–2084, doi:10.1029/2000GL011444, 2000.
- Taguchi, S.: A three-dimensional model of atmospheric CO<sub>2</sub> transport based on analyzed winds: Model description and simulation results for TRANSCOM, *J. Geophys. Res.*, 101, 15099–15109, doi:10.1029/96JD00504, 1996.
- 1075 Taguchi, S., Tasaka, S., Matsubara, M., Osada, K., Yokoi, T., and Yamanouchi, T.: Air-sea gas transfer rate for the Southern Ocean inferred from 222Rn concentrations in maritime air and a global atmospheric transport model, *J. Geophys. Res.*, 118, 7606–7616, doi:10.1002/jgrd.50594, 2013.
- Tegtmeier, S., Krüger, K., Quack, B., Atlas, E. L., Pisso, I., Stohl, A., and Yang, X.: Emission and transport of bromocarbons: from the West Pacific ocean into the stratosphere, *Atmos. Chem. Phys.*, 12, 10633–10648, doi:10.5194/acp-12-10633-2012, 2012.
- 1080 Tegtmeier, S., Krüger, K., Quack, B., Atlas, E., Blake, D. R., Boenisch, H., Engel, A., Hepach, H., Hossaini, R., Navarro, M. A., Raimund, S., Sala, S., Shi, Q., and Ziska, F.: The contribution of oceanic methyl iodide to stratospheric iodine, *Atmos. Chem. Phys.*, 13, 11869–11886, doi:10.5194/acp-13-11869-2013, 2013.
- Tegtmeier, S., Ziska, F., Pisso, I., Quack, B., Velders, G. J. M., Yang, X., and Krüger, K.: Oceanic bromine emissions weighted by their ozone depletion potential, *Atmos. Chem. Phys.*, 15, 13647–13663, doi:10.5194/acp-15-13647-201, 2015.
- 1085 Tiedtke, M.: A comprehensive mass flux scheme for cumulus parameterization in large-scale models, *Mon. Weather Rev.*, 117, 1779–1800, doi:10.1175/1520-0493, 1989.
- Tilmes, S., Kinnison, D. E., Garcia, R. R., Salawitch, R., Canty, T., Lee-Taylor, J., Madronich, S., and Chance, K.: Impact of very short-lived halogens on stratospheric ozone abundance and UV radiation in a geo-engineered atmosphere, *Atmos. Chem. Phys.*, 12, 10945–10955, doi:10.5194/acp-12-10945-2012, 2012.
- 1090 Tissier, A.-S. and Legras, B.: Transport across the tropical tropopause layer and convection, *Atmos. Chem. Phys.*, 16, 3383–3398, doi:10.5194/acp-16-3383-2016, 2016.
- Thompson, R. L., Patra, P. K., Ishijima, K., Saikawa, E., Corazza, M., Karstens, U., Wilson, C., Bergamaschi, P., Dlugokencky, E., Sweeney, C., Prinn, R. G., Weiss, R. F., O’Doherty, S., Fraser, P. J., Steele, L. P., Krummel, P. B., Saunio, M., Chipperfield, M., and Bousquet, P.: TransCom N<sub>2</sub>O model inter-comparison – Part 1: Assessing the influence of transport and surface fluxes on tropospheric N<sub>2</sub>O variability, *Atmos. Chem. Phys.*, 14, 4349–4368, doi:10.5194/acp-14-4349-2014, 2014.
- 1095 Vogel, B., Günther, G., Müller, R., Groß, J.-U., Hoor, P., Krämer, M., Müller, S., Zahn, A., and Riese, M.: Fast transport from Southeast Asia boundary layer sources to northern Europe: rapid uplift in typhoons and eastward eddy shedding of the Asian monsoon anticyclone, *Atmos. Chem. Phys.*, 14, 12745–12762, doi:10.5194/acp-14-12745-2014, 2014.
- 1100 Warwick, N. J., Pyle, J. A., Carver, G. D., Yang, X., Savage, N. H., O’Connor, F. M., and Cox, R. A.: Global modeling of biogenic bromocarbons, *J. Geophys. Res.*, 111, doi:10.1029/2006JD007264, 2006.

- 1105 Werner, B., Atlas, E., Cheung, R., Chipperfield, M. P., Colosimo, F., Daube, B., Deutschmann, T., Elkins, J. W., Fahey, D. W., Feng, W., Festa, J., Gao, R-S., Hints, E. J., Hossaini, R., Moore, F. L., Navarro, M. A., Pittman, J., Raecke, R., Scalone, L., Spolaor, M., Stutz, J., Thornberry, T. D., Tsai, C., Wofsy, S., and Pfeilsticker, K.: Probing the subtropical lowermost stratosphere, tropical upper troposphere, and tropopause layer for inorganic bromine, paper in preparation for Atmos. Chem. Phys. Discuss.
- 1110 Wisher, A., Oram, D. E., Laube, J. C., Mills, G. P., van Velthoven, P., Zahn, A., and Brenninkmeijer, C. A. M.: Very short-lived bromomethanes measured by the CARIBIC observatory over the North Atlantic, Africa and Southeast Asia during 2009–2013, Atmos. Chem. Phys., 14, 3557–3570, doi:10.5194/acp-14-3557-2014, 2014.
- WMO: Scientific Assessment of Ozone Depletion: 2014, Global Ozone Research and Monitoring Project, Report No. 55, World Meteorological Organization, Geneva, Switzerland. , 2014.
- 1115 Wofsy, S. C., Team, H. S., Team, C. M., and Team, S.: HIAPER Pole-to-Pole Observations (HIPPO): fine-grained, global-scale measurements of climatically important atmospheric gases and aerosols, Phil. Trans., 369, 2073–2086, doi:10.1098/rsta.2010.0313, 2011.
- Wolter, K. and Timlin, M. S.: Measuring the strength of ENSO events: How does 1997/98 rank?, Weather, 53, 315–324, doi:10.1002/j.1477-8696.1998.tb06408.x, 1998.
- 1120 Yang, X., Abraham, N. L., Archibald, A. T., Braesicke, P., Keeble, J., Telford, P. J., Warwick, N. J., and Pyle, J. A.: How sensitive is the recovery of stratospheric ozone to changes in concentrations of very short-lived bromocarbons?, Atmos. Chem. Phys., 14, 10 431–10 438, doi:10.5194/acp-14-10431-2014, 2014.
- Zhang, K., Wan, H., Zhang, M., and Wang, B.: Evaluation of the atmospheric transport in a GCM using radon measurements: sensitivity to cumulus convection parameterization, Atmos. Chem. Phys., 8, 2811–2832, doi:10.5194/acp-8-2811-2008, 2008.
- 1125 **Zhang, G. J. and McFarlane, N. A.: Sensitivity of climate simulations to the parameterization of cumulus convection in the Canadian climate centre general circulation model, Atmos. Ocean, 33, 407–446, 1995.**
- 1130 Ziska, F., Quack, B., Abrahamsson, K., Archer, S. D., Atlas, E., Bell, T., Butler, J. H., Carpenter, L. J., Jones, C. E., Harris, N. R. P., Hepach, H., Heumann, K. G., Hughes, C., Kuss, J., Krüger, K., Liss, P., Moore, R. M., Orlikowska, A., Raimund, S., Reeves, C. E., Reifenhäuser, W., Robinson, A. D., Schall, C., Tanhua, T., Tegtmeier, S., Turner, S., Wang, L., Wallace, D., Williams, J., Yamamoto, H., Yvon-Lewis, S., and Yokouchi, Y.: Global sea-to-air flux climatology for bromoform, dibromomethane and methyl iodide, Atmos. Chem. Phys., 13, 8915–8934, doi:10.5194/acp-13-8915-2013, 2013.
- 1135

**Table 1** Summary of the VLS tracers simulated by [participating](#) models, the global total emission flux (Gg VLS yr<sup>-1</sup>) and the rate constant for their reaction with OH (Sander et al., 2011). See text for details of emission inventories.

Tracer #	Species	Tracer name	Ocean emission inventory		Rate constant (VLS + OH reaction)
			Global flux (Gg yr <sup>-1</sup> )	Reference	k(T) (cm <sup>3</sup> molec <sup>-1</sup> s <sup>-1</sup> )
1	Bromoform	CHBr <sub>3</sub> _L	450	Liang et al. (2010)	$1.35 \times 10^{-12} \exp(-600/T)$
2		CHBr <sub>3</sub> _O	530	Ordóñez et al. (2012)	
3		CHBr <sub>3</sub> _Z	216	Ziska et al. (2013)	
4	Dibromomethane	CH <sub>2</sub> Br <sub>2</sub> _L	62	Liang et al. (2010)	$2.00 \times 10^{-12} \exp(-840/T)$
5		CH <sub>2</sub> Br <sub>2</sub> _O	67	Ordóñez et al. (2012)	
6		CH <sub>2</sub> Br <sub>2</sub> _Z	87	Ziska et al. (2013)	

**Table 2** Overview of TransCom-VSLS [participating](#) models and model variants.

#	Model <sup>1</sup>	Institution <sup>2</sup>	Resolution		Meteorology <sup>5</sup>	BL mix.	Convection	Reference
			Horizontal <sup>3</sup>	Vertical <sup>4</sup>				
1	ACTM	JAMSTEC	2.8°×2.8°	67σ	JRA-25	Mellor and Yamada (1974)	Arakawa and Shubert (1974)	Patra et al. (2009)
2	B3DCTM	UoB	3.75°×2.5°	40 σ-θ	ECMWF ERA-Interim	Simple <sup>7</sup>	ERA-Interim, archived <sup>8</sup>	Aschmann et al. (2014)
3	<b>EMAC</b> <sup>6</sup> (_free)	KIT	2.8°×2.8°	39 σ-p	Online, free-running	Jöckel et al. (2006)	Tiedtke (1989) <sup>9</sup>	Jöckel et al. (2006, 2010)
4	<i>EMAC</i> (_nudged)	KIT	2.8°×2.8°	39 σ-p	Nudged to ERA-Interim	Jöckel et al. (2006)	Tiedtke (1989) <sup>9</sup>	Jöckel et al. (2006, 2010)
5	MOZART	EMU	2.5°×1.9°	56 σ-p	MERRA	Holtstlag and Boville (1993)	Note 10	Emmons et al. (2010)
6	NIES-TM	NIES	2.5°×2.5°	32 σ-θ	JCDAS (JRA-25)	Belikov et al. (2013)	Tiedtke (1989)	Belikov et al. (2011, 2013)
7	STAG	AIST	1.125°×1.125°	60 σ-p	ECMWF ERA-Interim	Taguchi et al. (2013)	Taguchi et al. (2013)	Taguchi (1996)
8	TOMCAT	UoL	2.8°×2.8°	60 σ-p	ECMWF ERA-Interim	Holtstlag and Boville (1993)	Tiedtke (1989)	Chipperfield (2009)
9	<i>TOMCAT</i> (_conv)	UoL	2.8°×2.8°	60 σ-p	ECMWF ERA-Interim	Holtstlag and Boville (1993)	ERA-Interim, archived <sup>8</sup>	Chipperfield (2009)
10	<b>UKCA</b> (_low)	UoC/NCAS	3.75°×2.5°	60 σ-z	Online, free-running	Lock et al. (2000)	Gregory and Rowntree (1990)	Morgenstern et al. (2009)
11	<i>UKCA</i> (_high)	UoC/NCAS	1.875°×1.25°	85 σ-z	Online, free-running	Lock et al. (2000)	Gregory and Rowntree (1990)	Morgenstern et al. (2009)

<sup>1</sup> All models are offline CTMs except bold entries which are CCMs. Model variants are shown in italics.

**CCMs ran using prescribed sea surface temperatures from observations.**

<sup>2</sup> JAMSTEC: Japan Agency for Marine-Earth Science and Technology, Japan; UoB: University of Bremen, Germany; KIT: Karlsruhe Institute of Technology, Germany; EMU: Emory University, USA ; NIES: National Institute for Environmental Studies, Japan; AIST: National Institute of Advanced Industrial Science and Technology, Japan; UoL: University of Leeds, UK; UoC: University of Cambridge, UK; NCAS: National Centre for Atmospheric Science, UK.

<sup>3</sup> Longitude×latitude

<sup>4</sup> σ: terrain-following sigma levels (pressure divided by surface pressure); σ-p: hybrid sigma-pressure; σ-θ: hybrid sigma-potential temperature; σ-z: hybrid sigma-height.

<sup>5</sup> MERRA: Modern-era Retrospective Analysis for Research and Applications; JCDAS: Japan Meteorological Agency Climate Data Assimilation System; JRA-25: Japanese 25-year ReAnalysis; ECMWF: European Center for Medium range Weather Forecasting.

<sup>6</sup> ECHAM/MESSy Atmospheric Chemistry (EMAC) model (Roeckner et al., 2006). ECHAM5 version 5.3.02. MESSy version 2.42.

<sup>7</sup> **Simple averaging of tracer mixing ratio below ERA-Interim boundary layer height.**

<sup>8</sup> **Read-in convective massfluxes from ECMWF ERA-Interim. See Aschmann et al. (2011) for B3DCTM implementation and Feng et al. (2011) for TOMCAT implementation.**

<sup>9</sup> **With modifications from Nordeng (1994).**

<sup>10</sup> **Shallow & mid-level convection (Hack , 1994); deep convection (Zhang and McFarlane, 1995).**

---

**Table 3** Summary and location of ground-based surface VSLs measurements used in TransCom-VSLs, arranged from north to south. All sites are part of the NOAA/ESRL global monitoring network, with the exception of TAW, at which measurements were obtained by the University of Cambridge (see main text). \*Stations SUM, MLO and SPO elevated at ~3210m, 3397m and 2810m, respectively.

---

Station	Site Name	Latitude	Longitude
ALT	Alert, NW Territories, Canada	82.5° N	62.3° W
SUM*	Summit, Greenland	72.6° N	38.4° W
BRW	Pt. Barrow, Alaska, USA	71.3° N	156.6° W
MHD	Mace Head, Ireland	53.0° N	10.0° W
LEF	Wisconsin, USA	45.6° N	90.2° W
HFM	Harvard Forest, USA	42.5° N	72.2° W
THD	Trinidad Head, USA	41.0° N	124.0° W
NWR	Niwot Ridge, Colorado, USA	40.1° N	105.6° W
KUM	Cape Kumukahi, Hawaii, USA	19.5° N	154.8° W
MLO*	Mauna Loa, Hawaii, USA	19.5° N	155.6° W
TAW	Tawau, Sabah, Malaysian Borneo	4.2° N	117.9° E
SMO	Cape Matatula, American Samoa	14.3° S	170.6° W
CGO	Cape Grim, Tasmania, Australia	40.7° S	144.8° E
PSA	Palmer Station, Antarctica	64.6° S	64.0° W
SPO*	South Pole	90.0° S	-

---



**Table 4** Correlation coefficient (r) between the observed and simulated climatological monthly mean surface CHBr<sub>3</sub> volume mixing ratio (at ground-based monitoring sites, Table 3). Model output based on CHBr<sub>3</sub>\_L tracer (i.e. using aseasonal emissions inventory of Liang et al. (2010)). Stations in bold denote where virtually all models fail to reproduce phase of the observed CHBr<sub>3</sub> seasonal cycle.

Site	ACTM	B3DCTM	EMAC_F	EMAC_N	MOZART	NIES	STAG	TOMCAT	UKC_LO	UKCA_HI
ALT	0.91	0.90	0.89	0.89	0.95	0.93	0.60	0.94	0.92	0.94
SUM	0.69	0.73	0.71	0.70	0.84	0.71	0.40	0.73	0.75	0.88
BRW	0.96	0.97	0.89	0.91	0.99	0.98	0.73	0.97	0.94	0.97
<b>MHD</b>	-0.89	-0.89	-0.93	-0.89	-0.85	-0.89	-0.79	-0.90	-0.91	-0.73
LEF	0.84	0.72	0.74	0.78	0.83	0.74	0.35	0.43	0.78	0.88
HFM	0.64	0.61	0.66	0.69	0.79	0.46	0.08	0.58	0.40	0.81
<b>THD</b>	-0.87	-0.65	-0.58	-0.42	0.26	-0.65	-0.63	-0.51	-0.48	-0.12
NWR	0.92	0.91	0.91	0.93	0.98	0.94	0.74	0.94	0.92	0.93
KUM	0.74	0.74	0.72	0.73	0.78	0.70	0.57	0.74	0.74	0.69
MLO	0.94	0.97	0.99	0.98	0.98	0.95	0.95	0.99	0.95	0.93
TAW	-0.27	-0.08	0.17	-0.05	-0.34	-0.07	-0.15	0.23	0.13	0.22
SMO	0.56	0.45	0.43	0.72	0.32	0.23	0.04	0.72	0.59	-0.19
CGO	-0.64	0.72	-0.22	-0.18	-0.53	0.31	0.85	-0.71	-0.72	-0.35
PSA	0.13	0.24	0.60	0.44	0.40	-0.39	0.16	0.14	0.09	0.62
SPO	0.90	0.91	0.85	0.89	0.94	0.41	0.71	0.92	0.93	0.88

---

**Table 5** As Table 4 but for CH<sub>2</sub>Br<sub>2</sub>.

---

---

Site	ACTM	B3DCTM	EMAC_F	EMAC_N	MOZART	NIES	STAG	TOMCAT	UKCA_LO	UKCA_HI
ALT	0.90	0.97	0.79	0.82	0.96	0.98	0.77	0.94	0.85	0.96
SUM	0.71	0.93	0.75	0.76	0.92	0.91	0.87	0.77	0.79	0.96
BRW	0.87	0.92	0.82	0.85	0.93	0.91	0.90	0.88	0.93	0.93
<b>MHD</b>	-0.65	-0.73	-0.72	-0.69	-0.76	-0.75	-0.64	-0.72	-0.71	-0.76
LEF	0.87	0.73	0.84	0.84	0.94	0.94	0.47	0.62	0.88	0.96
HFM	0.82	0.79	0.83	0.84	0.95	0.90	-0.02	0.75	0.72	0.92
THD	0.54	0.80	0.73	0.79	0.78	0.84	0.04	0.69	0.66	0.75
NWR	0.90	0.88	0.91	0.89	0.99	0.97	0.86	0.91	0.92	0.97
KUM	0.90	0.89	0.90	0.91	0.99	0.91	0.74	0.90	0.92	0.98
MLO	0.90	0.89	0.94	0.91	0.96	0.90	0.30	0.91	0.93	0.97
TAW	-0.83	-0.80	-0.78	-0.75	-0.39	-0.47	-0.12	0.15	0.20	-0.16
SMO	-0.08	0.67	-0.14	0.59	0.38	-0.12	0.34	0.97	0.74	0.00
CGO	0.59	-0.43	0.45	0.30	0.64	-0.06	-0.42	0.80	0.80	0.41
PSA	0.17	0.71	0.52	0.68	0.75	0.08	0.62	0.72	0.65	0.68
SPO	0.88	0.91	0.82	0.86	0.95	-0.04	0.97	0.90	0.94	0.88

---

# TransCom-VSLS

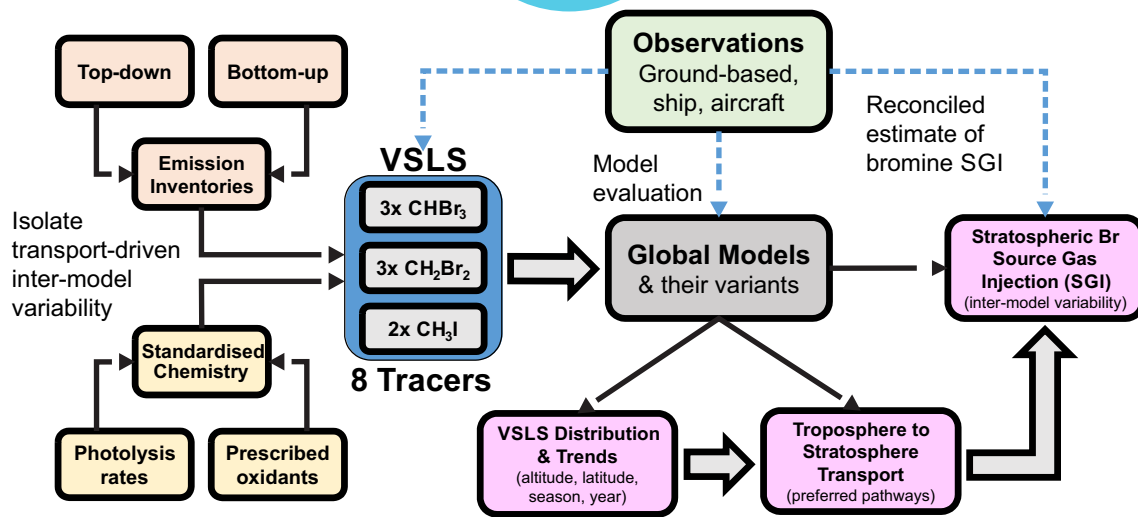


Figure 1. Schematic of the the TransCom-VSLS project approach.

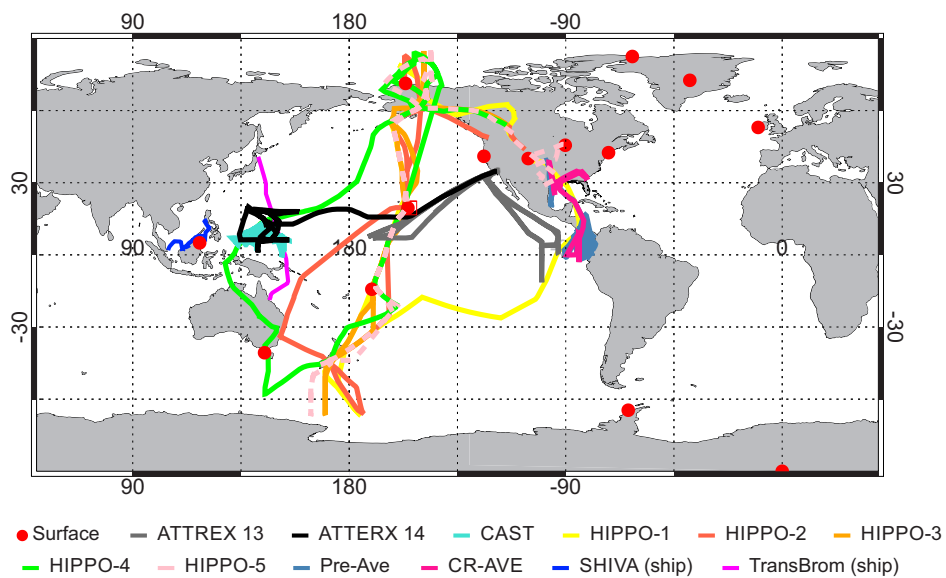
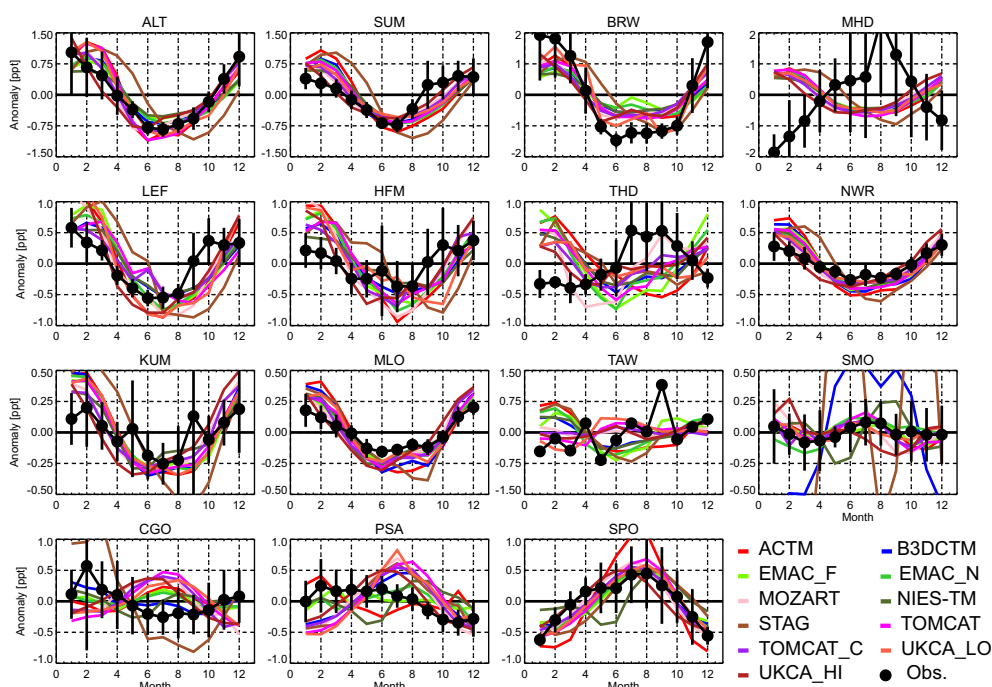


Figure 2. Summary of ground-based and campaign data used in TransCom-VSLS. See main text for details.



**Figure 3.** Comparison of the observed and simulated seasonal cycle of surface  $\text{CHBr}_3$  at ground-based measurement sites (see Table 3). The seasonal cycle is shown here as climatological (1998-2011) monthly mean anomalies, calculated by subtracting the climatological monthly mean  $\text{CHBr}_3$  mole fraction (ppt) from the climatological annual mean, in both the observed (black points) and model (coloured lines, see legend) data sets. The location of the surface sites is summarised in Table 3. Model output based on  $\text{CHBr}_3$ \_L tracer (i.e. using aseasonal emissions inventory of Liang et al. (2010)). Horizontal bars denote  $\pm 1\sigma$ .

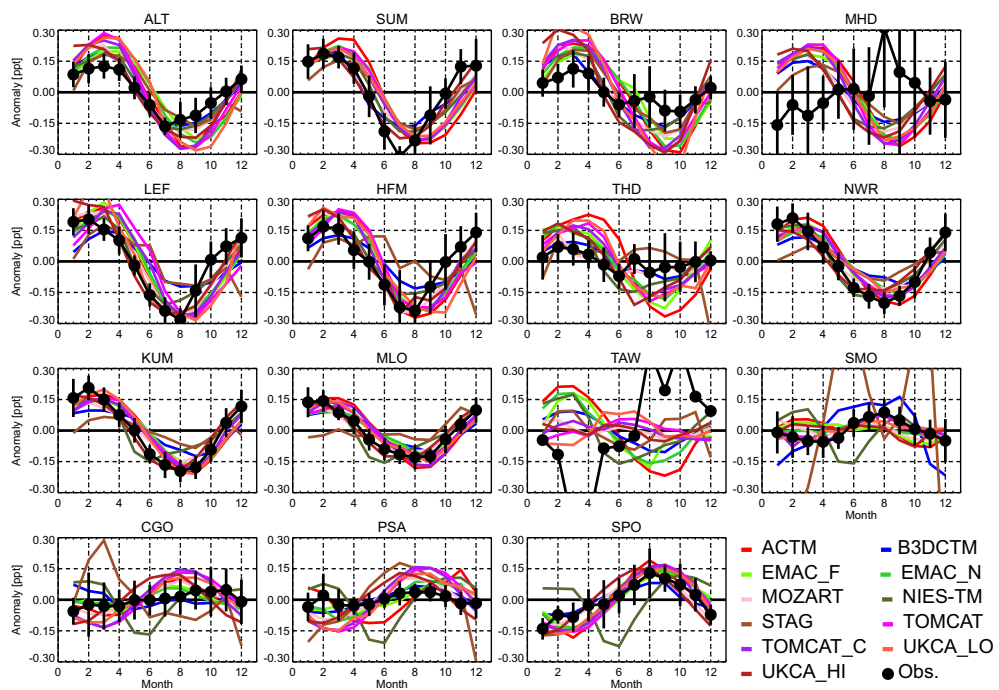
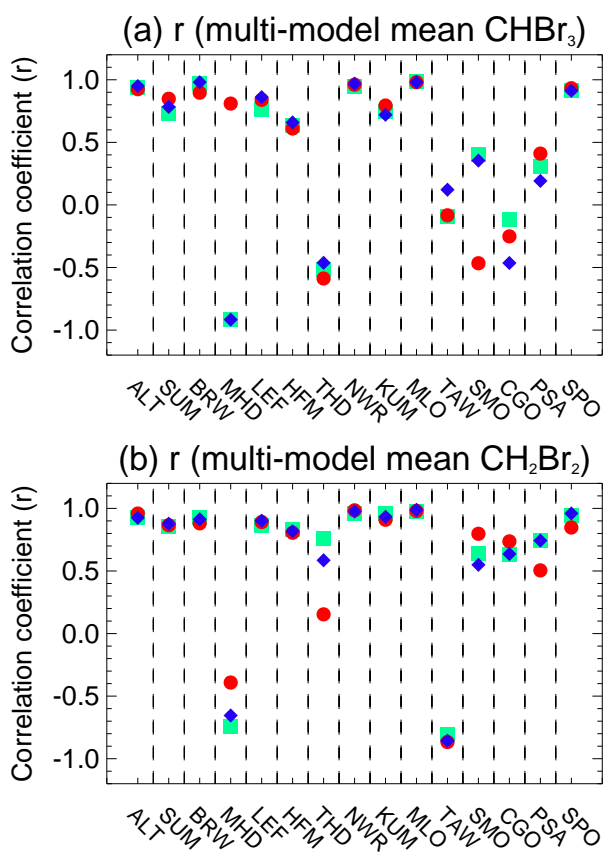
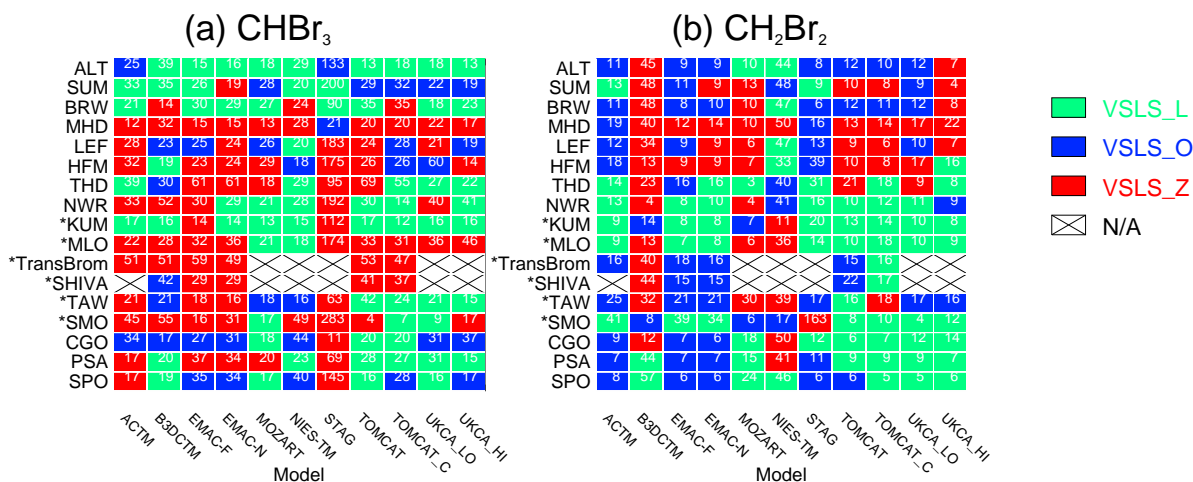


Figure 4. As Figure 3 but for  $\text{CH}_2\text{Br}_2$ .



**Figure 5.** Correlation coefficient ( $r$ ) between observed and multi-model mean (a)  $\text{CHBr}_3$  and (b)  $\text{CH}_2\text{Br}_2$ , at ground-based monitoring sites. The correlation here represents the mean annual seasonal variation. At each site,  $3 \times r$  values are given, reflecting the 3 different model  $\text{CHBr}_3$  tracers; green squares denote the  $\text{CHBr}_3\text{-L}$  tracer (top-down derived Liang et al. (2010) emissions), blue diamonds denote the  $\text{CHBr}_3\text{-O}$  tracer (top-down Ordóñez et al. (2012) emissions) and red circles denote the  $\text{CHBr}_3\text{-Z}$  tracer (bottom-up Ziska et al. (2013) emissions).



**Figure 6.** Summary of agreement between model (a) CHBr<sub>3</sub> and (b) CH<sub>2</sub>Br<sub>2</sub> tracers and corresponding surface observations (ground-based, see Table 3, and TransBrom/SHIVA ship cruises). The fill colour of each cell (see legend) indicates the tracer giving the best agreement for that model, i.e. the lowest mean absolute percentage error (MAPE, see main text for details), and the numbers within the cells give the MAPE value (%), for each model compared to the observations. CHBr<sub>3</sub>\_L tracer used the Liang et al. (2010) emissions inventory, CHBr<sub>3</sub>\_O tracer used Ordóñez et al. (2012) and CHBr<sub>3</sub>\_Z tracer used Ziska et al. (2013). Sites marked with \* are tropical locations. Certain model-measurement comparisons are not available (N/A).

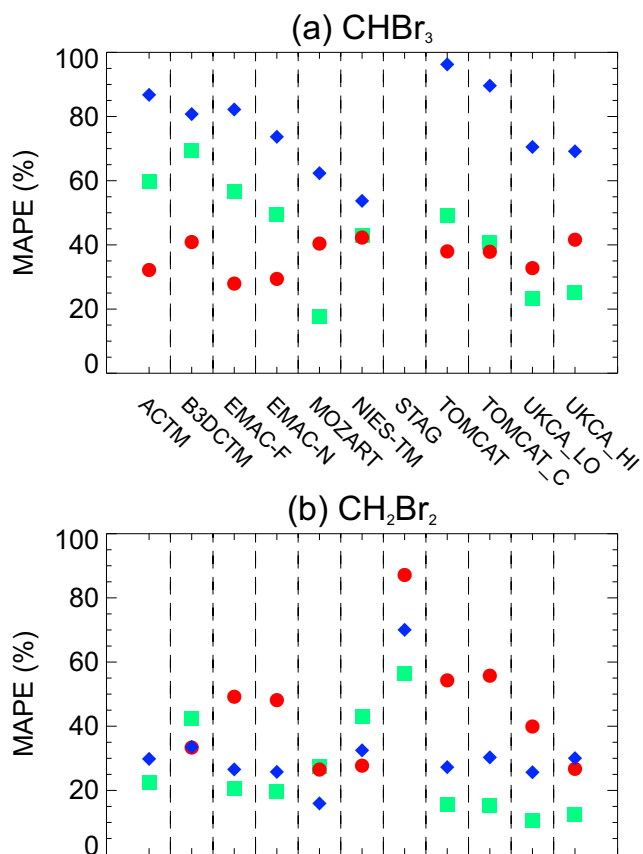


**Figure 7.** Overall mean absolute percentage error (MAPE) between model (a)  $\text{CHBr}_3$  and (b)  $\text{CH}_2\text{Br}_2$  tracers and corresponding surface observations, within the tropics only (i.e. sites KUM, MLO, TAW, SMO and the TransBrom and SHIVA ship cruises). Note, the scale is capped at 100%. A small number of data points fall outside of this range. Green squares denote the  $\text{CHBr}_3_{\text{L}}$  tracer, blue diamonds denote the  $\text{CHBr}_3_{\text{O}}$  tracer and red circles denote the  $\text{CHBr}_3_{\text{Z}}$  tracer.



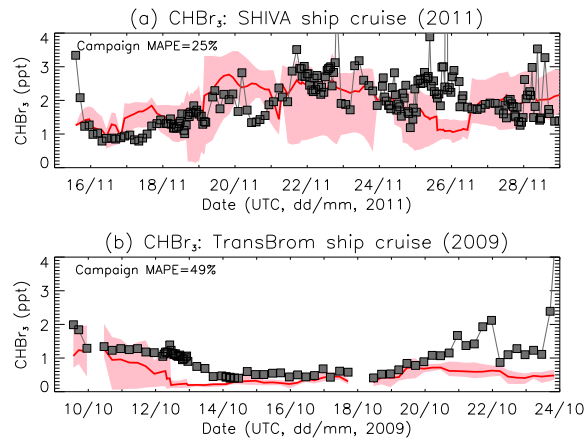


**Figure 8.** Comparison of modelled versus observed CHBr<sub>3</sub> surface volume mixing ratio (ppt) during (a) SHIVA (2011) and (b) TransBrom (2009) ship cruises. The multi-model mean is shown and the shaded region is the model spread. The mean absolute percentage error (MAPE) over each campaign is annotated.

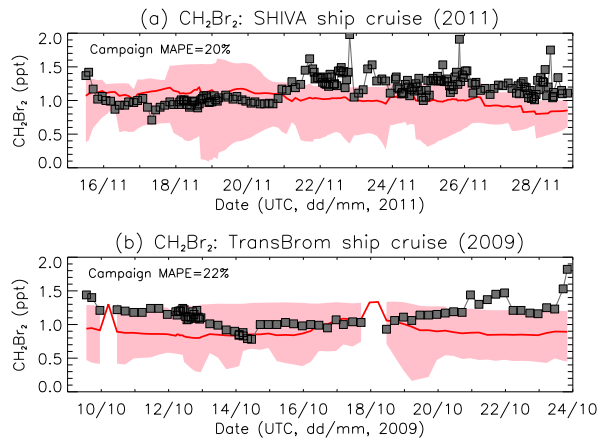


**Figure 9.** As Figure 8 but for CH<sub>2</sub>Br<sub>2</sub>.

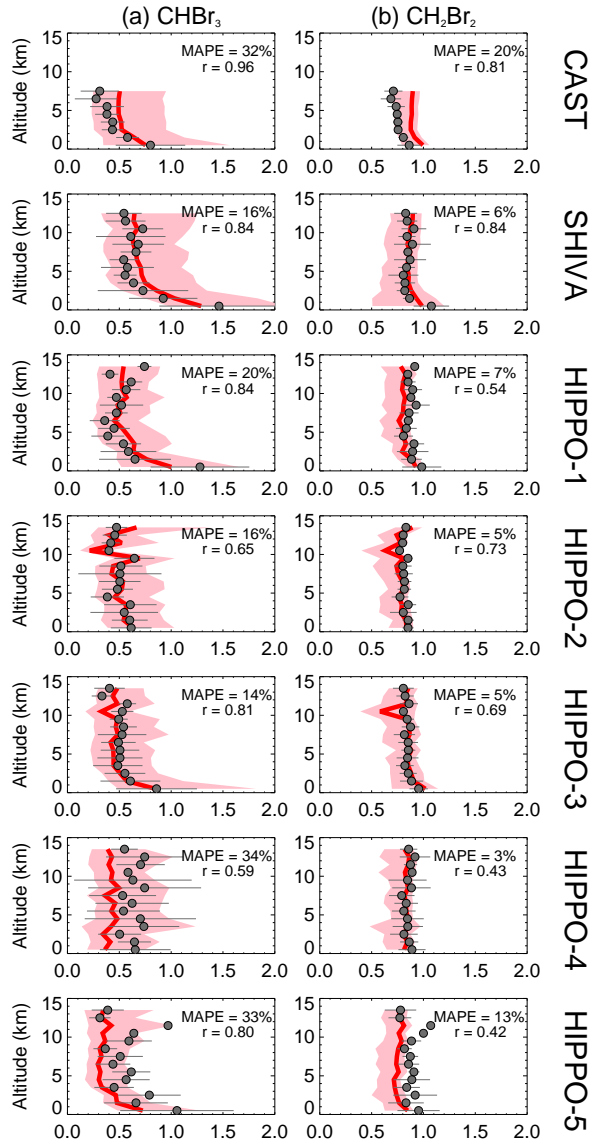


**Figure 10.** Compilation of modelled versus observed tropical profiles of (a) CHBr<sub>3</sub> and (b) CH<sub>2</sub>Br<sub>2</sub> mixing ratio (ppt) from recent aircraft campaigns. Details of campaigns given in Section 2.4. Campaign mean observed profiles derived from tropical measurements only and averaged in 1 km vertical bins (filled circles). The horizontal bars denote  $\pm 1\sigma$  from the observed mean. Shown is the corresponding multi-model mean profile (red) and model spread (shading). All participating models were included in the MMM with the exception of STAG (see Section 3.1.2). Models were sampled in the same space/time as the observed values, though for the comparison to CAST data, a climatological model profile is shown. The model-measurement correlation coefficient ( $r$ ) and the mean absolute percentage error (MAPE, see main text) between the two are indicated in each panel.

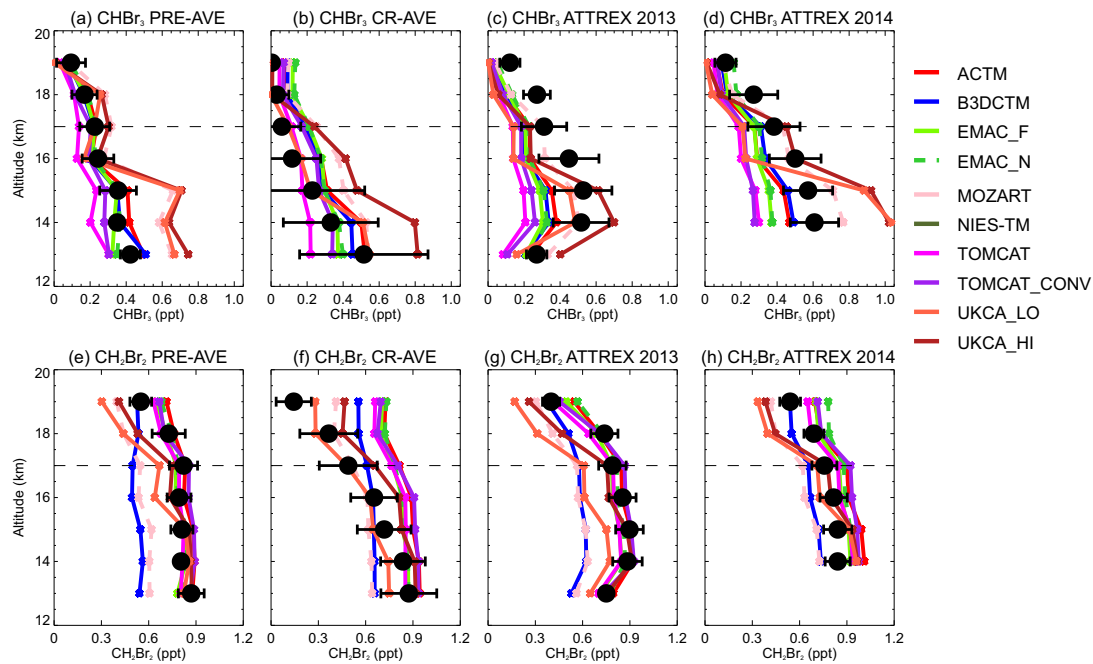


**Figure 11.** Comparison of modelled versus observed volume mixing ratio (ppt) of  $\text{CHBr}_3$  (panels a-d) and  $\text{CH}_2\text{Br}_2$  (panels e-h) from aircraft campaigns in the tropics (see main text for campaign details). The observed values (filled circles) are averages in 1 km altitude bins and the error bars denote  $\pm 1\sigma$ . The dashed line denotes the approximate cold point tropopause for reference.

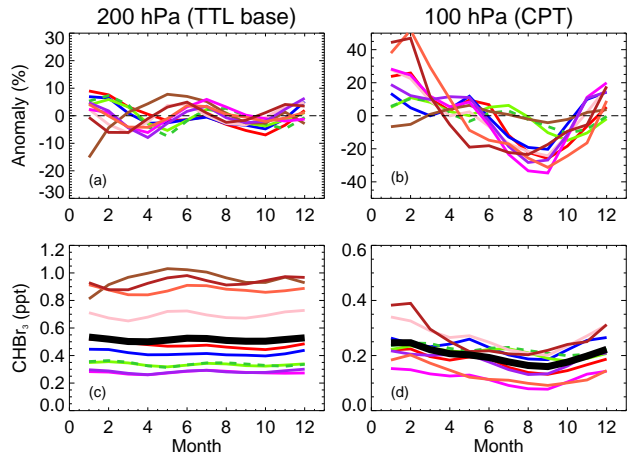


**Figure 12.** Simulated monthly mean anomalies of CHBr<sub>3</sub> volume mixing ratio (vmr), expressed as a percentage with respect to the annual mean, for (a) 200 hPa, the approximate base of the tropical tropopause layer (TTL) and (b) 100 hPa, the cold point tropopause (CPT). Panels (c) and (d) show the CHBr<sub>3</sub> vmr (ppt) at these levels. All panels show tropical ( $\pm 20^\circ$  latitude) averages over the full simulation period (1993-2012). See Figure 3 for legend. Thick black line denotes multi-model mean.

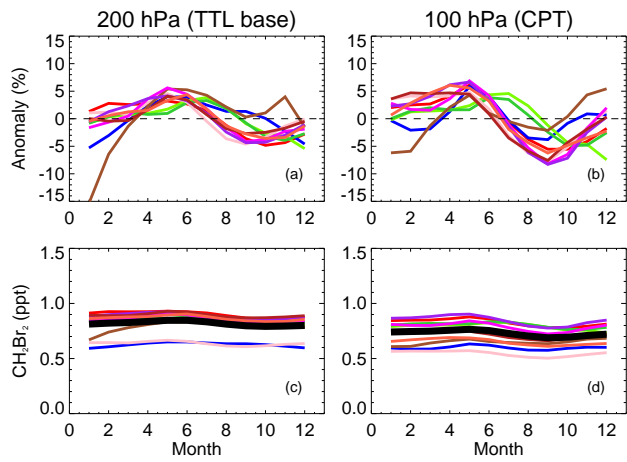


**Figure 13.** As Figure 12 but for CH<sub>2</sub>Br<sub>2</sub>.

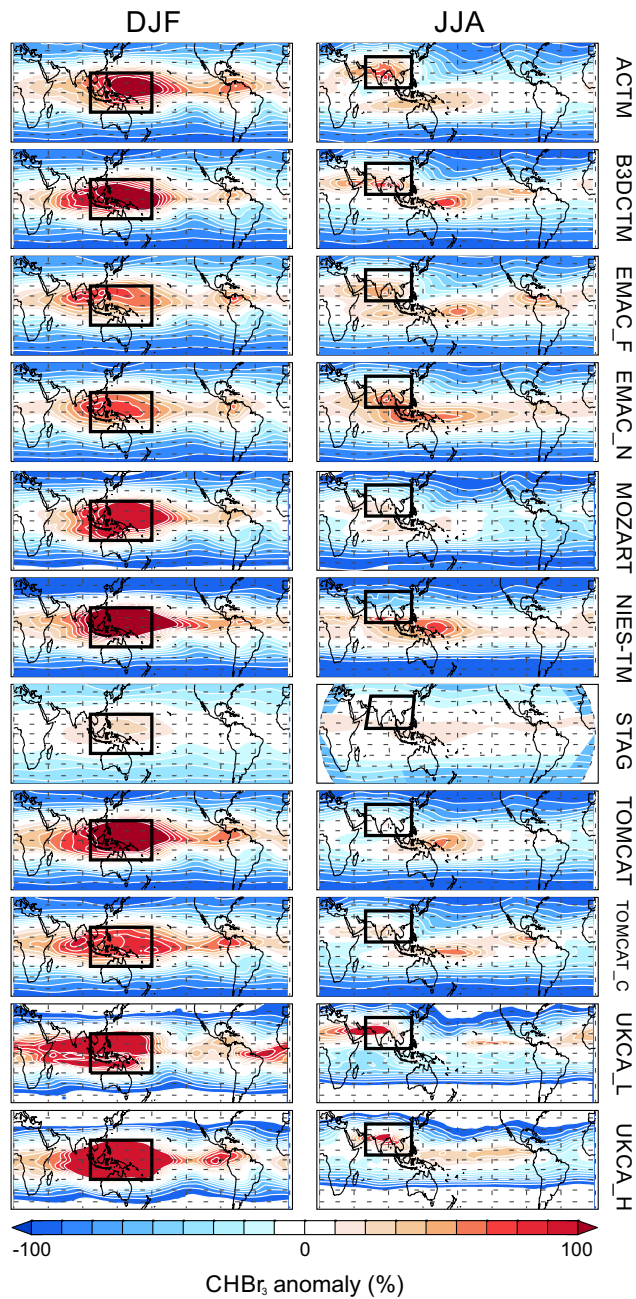


**Figure 14.** Simulated anomalies of the CHBr<sub>3</sub> volume mixing ratio with respect to the tropical ( $\pm 30^\circ$  latitude) mean (expressed in %) at 100 hPa for (a) boreal winter (DJF) and (b) boreal summer (JJA). The boxes highlight the tropical West Pacific and location of the Asian Monsoon - regions experiencing strong convection.

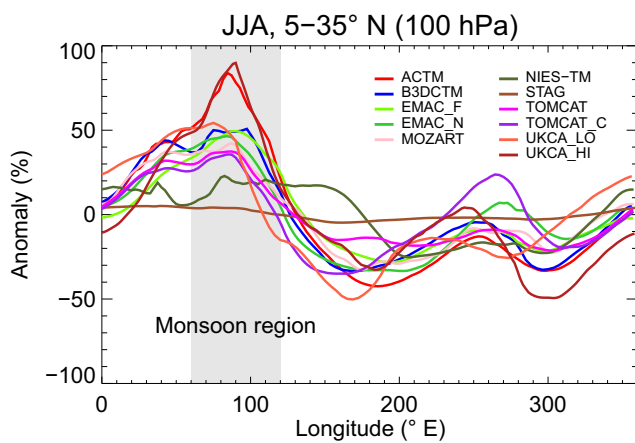


**Figure 15.** Simulated anomalies of the  $\text{CHBr}_3$  volume mixing ratio at 100 hPa, as a function of longitude. Expressed as a percentage (%) departure from the mean within the latitude range of the Asian Monsoon ( $5^\circ\text{N}$ - $35^\circ\text{N}$ ), during boreal summer (JJA).

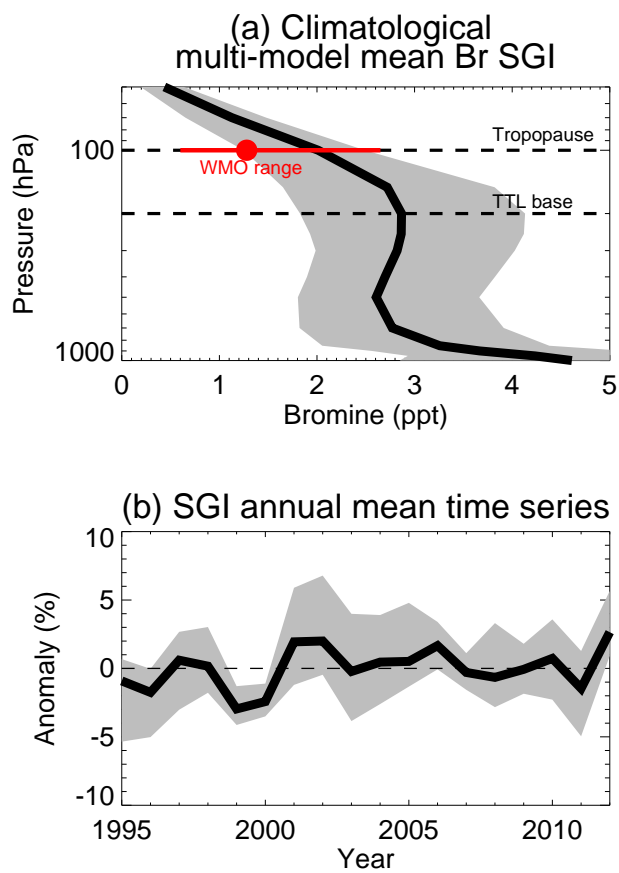


**Figure 16.** (a) climatological multi-model mean source gas injection of bromine (ppt) from  $\text{CHBr}_3$  and  $\text{CH}_2\text{Br}_2$  (i.e.  $[3 \times \text{CHBr}_3] + [2 \times \text{CH}_2\text{Br}_2]$  mixing ratio). The shaded region denotes the model spread. Also shown is the best estimate (red circle) and SGI range from these gases (based on observations) reported in the most recent WMO  $\text{O}_3$  Assessment Report (Carpenter and Reimann, 2014). (b) time series of multi-model mean stratospheric bromine SGI anomalies. Anomalies are calculated as the departure of the annual mean from the climatological mean (%).

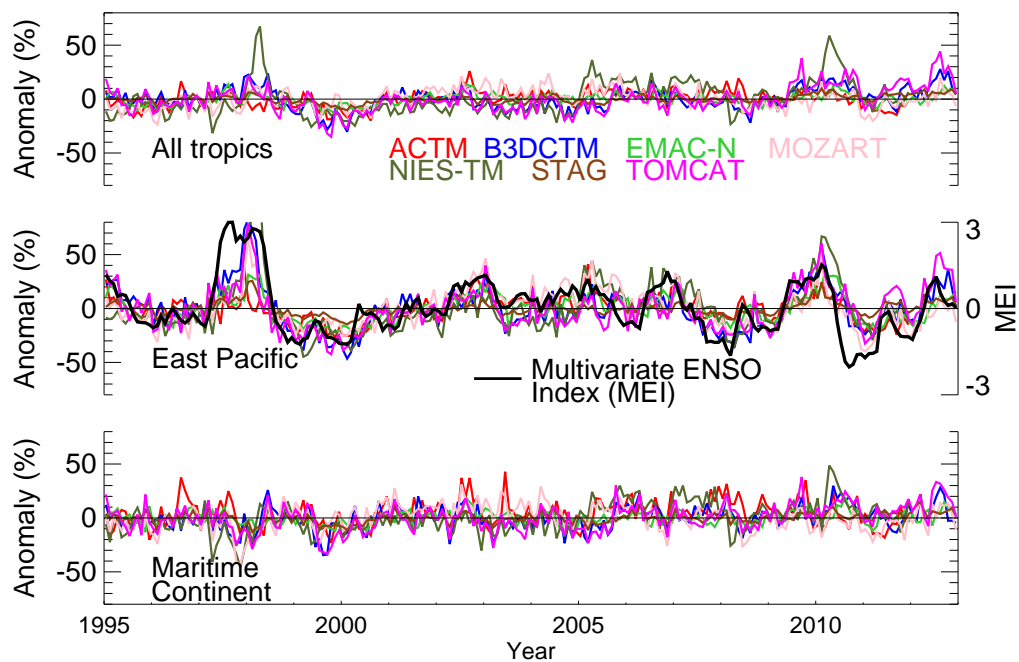


**Figure 17.** Monthly mean anomalies of  $\text{CHBr}_3$  volume mixing ratio at 100 hPa, expressed as departures from the climatological monthly mean (%) over (a) tropical latitudes ( $\pm 20^\circ$ ), (b) the tropical East Pacific ( $\pm 20^\circ$  latitude,  $180^\circ$ - $250^\circ\text{E}$  longitude) and (c) the Maritime Continent ( $\pm 20^\circ$  latitude,  $100^\circ$ - $150^\circ\text{E}$  longitude). For the East Pacific region, the Multivariate ENSO Index (MEI) is also shown (see text). Note anomalies from free-running models not shown.



Supplement of:

**A multi-model intercomparison of halogenated very short-lived substances (TransCom-VLS): linking oceanic emissions and tropospheric transport for a reconciled estimate of the stratospheric source gas injection of bromine**

R. Hossaini et al.

Correspondence to: Ryan Hossaini (r.hossaini@leeds.ac.uk)

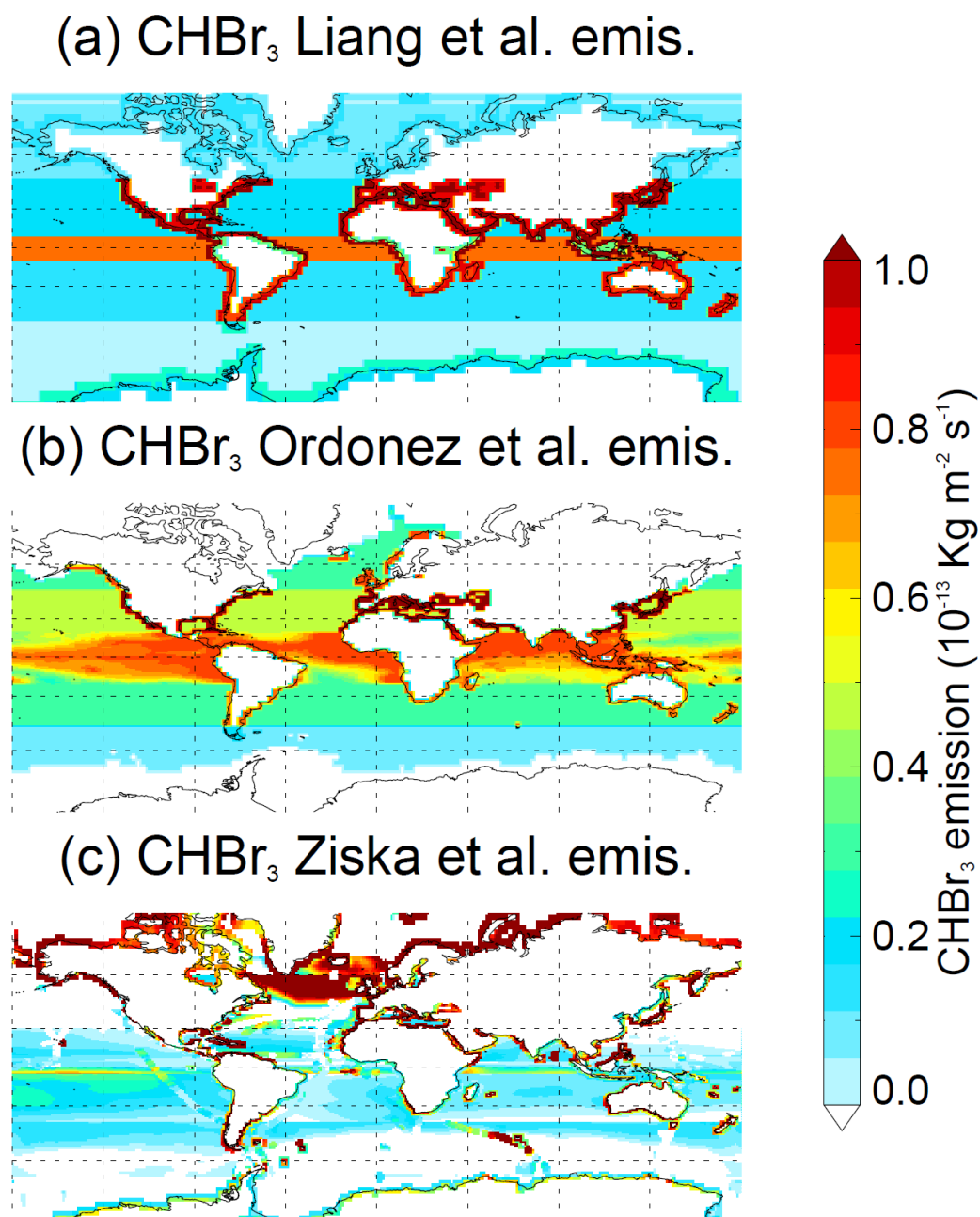
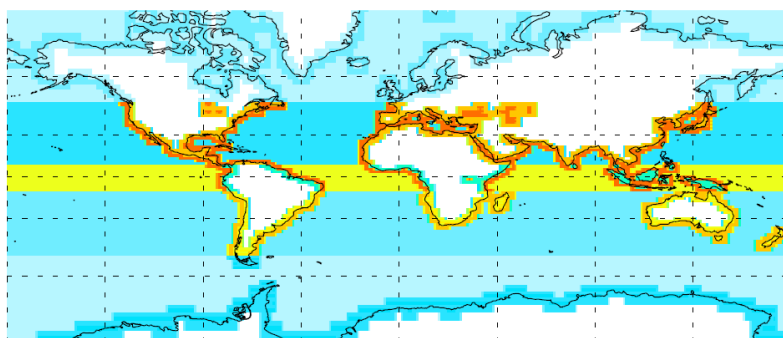
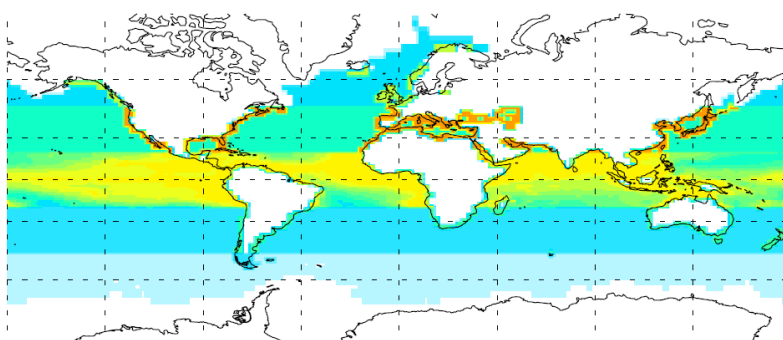


**Figure S1:** Bromoform ( $\text{CHBr}_3$ ) surface emission field ( $10^{-13} \text{ kg m}^{-2} \text{ s}^{-1}$ ) on  $1^\circ \times 1^\circ$  grid from the (a) Liang et al. (2010), (b) Ordóñez et al. (2012) and (c) Ziska et al. (2013) inventories.

(a) CH<sub>2</sub>Br<sub>2</sub> Liang et al. emis.



(b) CH<sub>2</sub>Br<sub>2</sub> Ordóñez et al. emis.



(c) CH<sub>2</sub>Br<sub>2</sub> Ziska et al. emis.

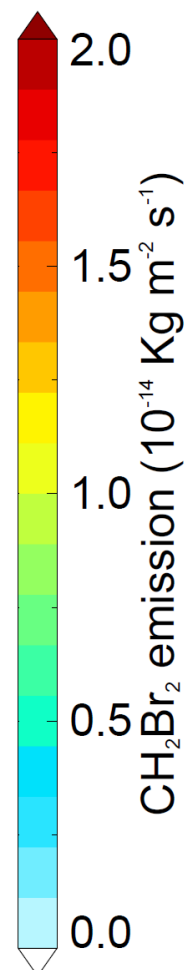
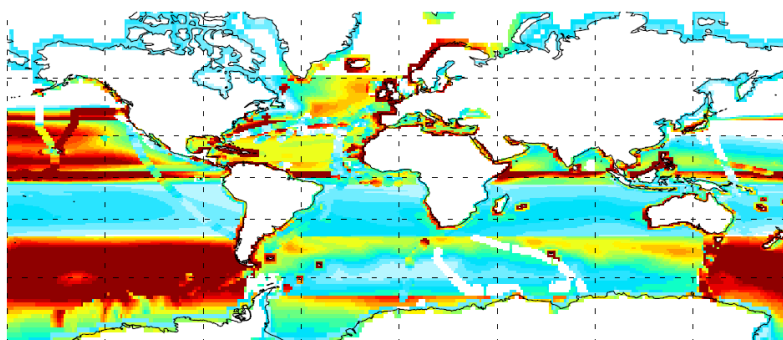


**Figure S2:** Dibromomethane (CH<sub>2</sub>Br<sub>2</sub>) surface emission field ( $10^{-14}$  kg m<sup>-2</sup> s<sup>-1</sup>) on  $1^\circ \times 1^\circ$  grid from the (a) Liang et al. (2010), (b) Ordóñez et al. (2012) and (c) Ziska et al. (2013) inventories.

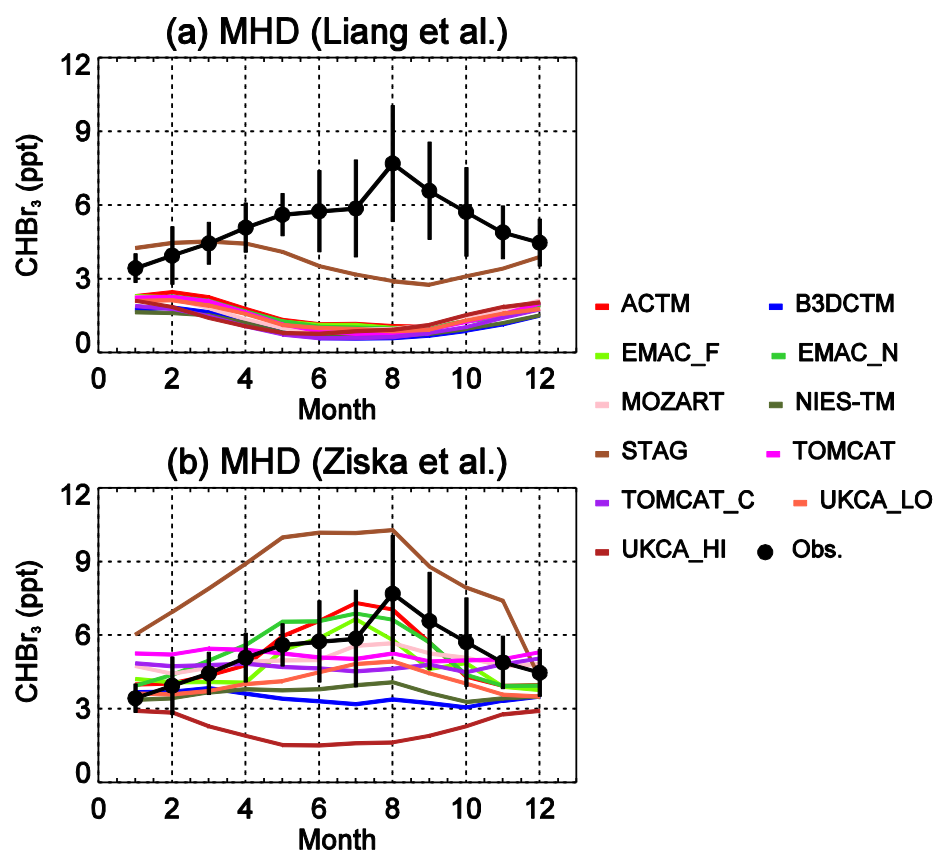


**Figure S3:** Comparison of observed  $\text{CHBr}_3$  surface mixing ratio (ppt) at Mace Head (MHD) to models using (a) Liang et al. (2010) emissions inventory and (b) Ziska et al. (2013) emissions inventory. The data show climatological monthly averages. Vertical bars denote  $\pm 1$  standard deviation from the monthly mean.

Model	r
ACTM	0.79
B3DCTM	-0.64
EMAC-F	0.66
EMAC-N	0.73
MOZART	0.87
NIES-TM	0.66
STAG	0.73
TOMCAT	-0.37
TOMCAT_C	-0.52
UKCA_LO	0.87
UKCA_HI	-0.77

**Table S1:** Correlation coefficient (r) between the observed and simulated climatological monthly mean  $\text{CHBr}_3$  volume mixing ratio (ppt) at Mace Head. Model output based on  $\text{CHBr}_3_Z$  tracer (i.e. using aseasonal emissions inventory of Ziska et al. 2013). See main text also.